DTU Mechanical Engineering
Department of Mechanical Engineering

Humidity control inside electronic enclosures:

Developing design principles based on empirical understanding

Salil Joshy

PhD Thesis

Humidity control inside electronic enclosures:
Developing design principles based on empirical understanding

PhD Thesis
by
Salil Joshy

October 2018

Supervisors :
Professor Rajan Ambat
Senior Researcher Morten Stendahl Jellesen

Section of Materials and surface engineering
Department of Mechanical Engineering
Technical university of Denmark (DTU)
Kgs. Lyngby 2800

Preface

This thesis is submitted in candidacy for a PhD degree from the Technical University of Denmark. The work titled "Humidity control inside electronic enclosures : Developing design principles based on empirical understanding" has been carried out at the department of Mechanical Engineering, section of materials and surface engineering, under the supervision of Professor Rajan Ambat and Senior researcher Morten Stendahl Jellesen. The PhD project was supported by Innovation Fund Denmark through the IN-SPE project (Innovation consortium for sustained performance of electronics). The duration of the PhD programme was January 2015 to October 2018.

Acknowledgements

I would like to acknowledge my supervisors Rajan Ambat and Morten Stendahl Jellesen for their guidance, continuous support, and invaluable advice throughout the study. I appreciate their dedication to the project, the time spent for fruitful discussions and the freedom given to me to explore different approaches.

IN-SPE member companies Danfoss A/S, Grundfos A/S, Vestas Wind Systems A/S, and Eltek are acknowledged for the funding and overall support of the PhD program. Special thanks to Annemette Riis, Jens Peter Krog, John B. Jacobsen, Kirsten Stentoft-Hansen, Dorthe Johansen, Niels Martin Henriksen, Øystein Larsen, Willy Høydal for all the fruitful discussions and advice in connection with the PhD studies.

I am thankful to my colleagues from the research group, the section of Materials and Surface Engineering and the section of Manufacturing engineering. Thanks to Marianne Burggraf for her help in the lab and Lars Pedersen for help with the experimental setups. Special thanks to Vadimas Verdingovas, Helene Conseil, Kamila Piotrowska, Zygimantas Staliulionis, Parizad Shojaee and Sankhya Mohanty for their help and contributions to the project.

I would also like to thank my family and friends for their support and encouragement during the study.

Abstract

This PhD work was supported by Innovation fund Denmark and was part of IN-SPE (Innovation consortium for sustained performance of electronics) project. The aim of this PhD work was to understand the humidity build-up inside electronic enclosures and study suitable humidity control methods to improve climatic reliability of electronics. In this regard, the main focus of the work was the effect of enclosure design and packaging related parameters on humidity build up and humidity control.

The use of electronic control units and devices in wide variety of applications and also in different climatic regions has led to more and more humidity related failures in electronics. Currently, the enclosure design for electronics are based on experience gained over the years at major electronic manufacturers, rather than based on scientific knowledge. This work aims to contribute to the scientific understanding of humidity build up and humidity control techniques at enclosure level.

Chapter 1 introduces the background to humidity related reliability issues in electronics. Also explained are the objectives of the current work and structure of this thesis. Chapter 2 reviews literature on water layer formation on printed circuit board assemblies (PCBA), humidity related failures and mechanisms of humidity transport into electronic enclosures. Chapter 3 reviews the methods currently used to prevent humidity related failures and suitable humidity control techniques in electronics. Chapter 4 summarises the materials and experimental methods used in this work. Results of the PhD work were appended with this thesis as individual research papers in chapters 5, 7, 9 and as non-manuscript form in chapters 6 and 8.

Paper-1 studied forced condensation as a humidity control method in electronic applications. The effect of enclosure related parameters like opening sizes, enclosure volumes, cooler surface area and cooling temperature on relative humidity (RH) were studied. Paper-2 studied the effect of enclosure related parameters like opening size, inter-PCB spacing, heat capacity and power dissipation on humidity accumulation, condensation and degradation of surface insulation resistance (SIR) in an electronic enclosure with parallel arrangement of PCBs. The work in chapter 6 was done to answer fundamental questions on humidity transfer from warm to cold. The parameters studied were warm temperature, cold temperature and connecting hole size. Chapter 8 studied humidity and temperature inside an electronic enclosure with retained water.

The investigations have demonstrated humidity transfer from warm to cold and have shown that preferential condensation based humidity control techniques were suitable for electronic applications. By suitable sizing of various enclosure openings and cooling temperature the RH inside the electronic enclosure can be reduced to prevent humidity related failures. Electronic enclosure related parameters like opening size, PCB spacing and heat capacity were found to affect humidity related reliability of electronics.

Paper-3 studied a methodology to predict humidity and contamination related failures in common electronic circuits using experimental data of SIR. The methodology was also used to identify more reliable circuit topologies.

Resume

Dette ph.d. arbejde blev støttet af Innovationsfonden og indgik i IN-SPE (Innovationskonsortium for pålidelig elektronik). Formålet med dette ph.d. arbejde var at forstå opbygningen af fugt inde i kabinetter til elektronik og undersøge metoder til styring af fugt og derved opnå øget pålidelighed af elektronik. Fokus har været på effekten af kabinetdesign og parametre relevante for fugt opbygning og fugt styring.

Brugen af elektronik i mange forskellige applikationer og også under forskellige klimatiske påvirkninger har ført til flere fugt relaterede fejl. Typisk er kabinet design til elektronik baseret på erfaringer hos elektronik producenter. Dette arbejde sigter mod at bidrage til den fundamentale forståelse af fugt opbygning og luftfugtighedskontrolteknikker.

Kapitel 1 introducerer baggrunden for fugtrelateret pålidelighed af elektronik, samt målene med det nuværende arbejde og struktur af denne afhandling. Kapitel 2 gennemgår litteratur om dannelse af vandlag på printkort, fugtighedsrelaterede fejl og mekanismer for fugttransport i kabinetter til elektronik. Kapitel 3 gennemgår de metoder, der i øjeblikket bruges til at forhindre fugt relaterede fejl og passende fugt styringsteknikker i elektronik. Kapitel 4 opsummerer de eksperimentelle metoder, der anvendes i dette arbejde.

Resultaterne af ph.d.-arbejdet er vedlagt denne opgave som individuelle forskningspublikationer i kapitel 5, 7, 8 og desuden i kapitel 6 og 8.

Artikel 1 omhandler kondensation som en fugt kontrolmetode i elektronik. Effekten af indkapslingsrelaterede parametre som åbningsstørrelser, indkapslingsvolumener, køligere overfladeareal og køletemperatur på relativ fugtighed blev undersøgt. Artikel 2 undersøger effekten af indkapslingsrelaterede parametre som åbningsstørrelse, printkort afstand, varmekapacitet og effekttab på fugt akkumulering, kondensering og effekten på overfladeisoleringsmodstand i et elektronisk kabinet med parallelt arrangerede printkort. Kapitel 6 beskriver fundamentale spørgsmål om fugt overførsel fra varme til kolde områder. Effekten af temperatur og hul størrelse er undersøgt. Kapitel 8 undersøgte fugt og temperatur i et kabinet med vand på væskeform.

Undersøgelserne demonstrerede mulig fugt overførsel fra varme til kolde områder og derved at fugt styring kan bruges til elektronik applikationer. Ved passende dimensionering af forskellige indkapslingsåbninger og afkølingstemperatur kan fugten i indkapslingen reduceres og være med til at forhindre fugtighedsrelaterede fejl. Kabinet relaterede parametre som åbningsstørrelse, printkort afstand og varmekapacitet viste sig at påvirke den fugtrelaterede pålidelighed af elektronik.

Artikel 3 undersøgte en metode til at forudse fugt- og forureningsrelaterede fejl i elektroniske kredsløb ved brug af eksperimentelle data. Metoden blev også brugt til at identificere mere pålidelige kredsløb.

List of abbreviations

ABS	Acronitrile butadiene styrene
AH	Absolute humidity
BET	Brunauer-Emmett-Teller
BGA	Ball grid array
CFD	Computational fluid dynamics
COP	Coefficient of performance
DRH	Deliquescence relative humidity
ECM	Electrochemical migration
ECU	Electronic control unit
EMI	Electromagnetic interference
HASL	Hot air solder levelling
HVAC	Heating, ventilation, and air conditioning
IGBT	Insulated-gate bipolar transistor
IP	Ingress protection
IPC	Association Connecting Electronics Industries
MOSFET	Metal-oxide-semiconductor field-effect transistor
NFF	No fault found
PC	Polycarbonate
PCB	Printed circuit board
PCBA	Printed circuit board assembly
QFN	Quad flat no-lead
RC	Resistor-capacitor
RH	Relative humidity
RTD	Resistance temperature detector
SIR	Surface insulation resistance
SST	Solid state transformer
TEC	Thermoelectric cooler
WOA	Weak organic acid

List of publications

The following articles constitute a part of the thesis

1. **S. Joshy**, R. Ambat, "Humidity control in electronic enclosures by forced condensation", draft to be submitted

2. **S. Joshy**, R. Ambat, "Humidity accumulation and condensation in electronic enclosures", submitted to Microelectronics Reliability.

3. **S. Joshy**, V. Verdingovas, M. S. Jellesen, R. Ambat, "Circuit analysis to predict humidity related failures in electronics - Methodology and recommendations", Microelectronics Reliability, Vol. 93, pp. 81-88, Feb. 2019

The following articles have been published during the course of the PhD, but do not constitute a part of thesis.

Journal articles

1. V. Verdingovas, **S. Joshy**, M. S. Jellesen, R. Ambat, "Analysis of surface insulation resistance related failures in electronics by circuit simulation," Circuit World, Vol. 43, Issue 2, pp. 45–55, 2017.

Conference proceedings / oral presentations

1. **S. Joshy**, V. Verdingovas, M. Jellesen, R. Ambat, "Simulation of electronic circuit sensitivity towards humidity using electrochemical data on water layer", 17th Electronics Packaging Technology Conference (EPTC), pp. 1-5, 2015.

2. Z. Staliulionis, **S. Joshy**, M. Jabbari, S. Mohanty, R. Ambat and J. H. Hattel, "Analysis of moisture transport between connected enclosures under a forced thermal gradient," 18th Electronics Packaging Technology Conference (EPTC), pp. 320–324, 2016.

3. **S. Joshy**, M. S. Jellesen, R. Ambat, "Effect of interior geometry on local climate inside an electronic device enclosure", 16th IEEE Intersociety Conference on Thermal and Thermomechanical Phenomena in Electronic Systems (ITherm), pp. 779-783, 2017.

4. **S. Joshy**, M. S. Jellesen, R. Ambat, "Reliability of electronics to humidity-related failures", Book of Abstracts Sustain 2017, Technical University of Denmark, 2017.

5. **S. Joshy**, M. S. Jellesen, R. Ambat, "Effect of internal heating and packaging parameters on humidity profile and corrosion reliability inside an electronic enclosure", 17th Nordic corrosion congress, 2018

Contents

Chapter 1

Introduction

1.1 Background

Electronic devices are used in different climatic conditions around the world. Some examples are offshore wind turbines, solar microinverters, automobile electronic control units (ECU), wearable electronics like smart watches, household appliances etc. Offshore wind turbines are exposed to high humidity and salt containing aerosols. Electronics used in photovoltaic applications are exposed to varying intensity of radiation from the sun, humidity etc. Automobiles use a wide variety of ECUs for engine control, power steering, anti-lock braking, electronic braking distribution, stability control to name a few. Some of these ECUs are in the controlled climate of the passenger compartment, but, others are exposed to uncontrolled ambient climate. Wearable devices like smart watches and health monitoring gadgets are exposed to corrosive sweat from the human body.

The 2008 Paris climate agreement envisages limiting the rise in average global atmospheric temperature to less than 2^oC. This has resulted in a drive towards renewable energy production like solar, wind, tidal etc in favour of coal and other fossil fuel based energy power plants. The generated unregulated power from these renewable sources needs to be processed and fed to the existing power grids. The emissions from automobiles are also being reduced globally through legislation. This has led the automobile industry from internal combustion engine based propulsion to hybrid-electric and fully electric power trains. All these entail more wide spread use of electronics in power production, power transmission, and transportation segments in the future. An example of this is the solid-state transformer (SST) concept for power transmission. An SST can provide voltage regulation, reactive power compensation, dc-sourced renewable integration and communication capabilities in addition to the traditional step-up/step-down functionality of a transformer[1].

1.1.1 Humidity and contamination related failures

Figure 1.1 shows the different sources for failures in electronics[2]. Humidity and contamination related failures make up 25% of failures in electronics[2][3]. High humidity can cause formation of water layer on printed circuit board assembly (PCBA) due to deliquescence or condensation. Presence of the water layer leads to failures like high leakage currents and short-circuits due to electro chemical migration (ECM)[4][5][6][7]. Failures and faults in electronics due to humidity can be

temporary or permanent. The temporary nature of faults can be due to the water layer evaporating away or a short-circuiting dendrite being vaporised due to the high current flowing through it. These transient failures lead to occurrence of no fault found (NFF) failure in electronic equipment[8]. The permanent failures are the result of corrosion processes under way. Presence of hygroscopic contamination on PCBA increases the risk of humidity related failures by reducing the critical relative humidity (RH) at which water layer is formed. The main sources of contamination on PCBA are PCB manufacturing, component assembly process and atmospheric particulates.

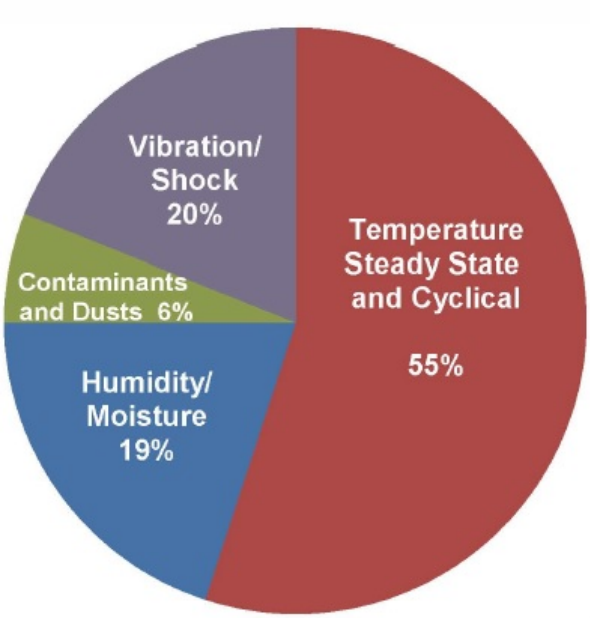

Figure 1.1: Source of failures in electronics (Wang et al., 2013 [2])

1.1.2 Humidity accumulation inside electronic enclosures

Electronics is usually placed in an enclosure to protect from ambient climate, atmospheric particulate contamination, for better heat transfer to the ambient, shielding from electromagnetic interference (EMI) etc. Electronic enclosures can prevent ingress of liquid water or entry of particulate matter to a certain extent by use of diffusion plugs[9]. But, diffusion plugs allow free movement of humidity between ambient and enclosure. An electronic enclosure with openings can delay, but, cannot fully prevent ingress of humidity from the ambient by mass transport mechanisms like diffusion and convection[10][11][12]. Prevention of humidity ingress from the ambient is possible only with hermetically sealed enclosures, which are not practical since, openings are required on an enclosure for connection of external wiring harness, pressure equalisation with ambient and as drain holes for condensed water accumulated inside the enclosure. Humidity can also accumulate by diffusion through the walls of a polymer enclosure. High humidity can result from the release of absorbed and adsorbed humidity from the walls of an enclosure. So, a passive electronic enclosure cannot always protect the electronics from high humidity conditions. This necessitates use of humidity control techniques in electronic enclosures to prevent humidity related failures.

1.1.3 Humidity control techniques

The most widely used method to protect electronics from high humidity is to coat the surface of PCBA with a conformal coating. A conformal coating prevents water layer formation on PCBA surface by acting as a barrier between humid air and PCBA. But, the effectiveness of conformal coating as a method to prevent humidity related failures decreases in the presence of ionic residue from no-clean solder fluxes used in component assembly process. Also, conformal coatings show failures like blistering, delamination, bubbles, pinholes and cracking under cycling temperatures and pressures.

Another technique to prevent high humidity inside electronic enclosures is by the use of desiccants. Desiccants have been used for humidity control in heating, ventilation, and air conditioning (HVAC) applications[13][14]. When the desiccant becomes saturated with adsorbed moisture, it either needs to be replaced or regenerated. Replacement is feasible only in repairable electronic systems where as, regeneration requires built-in mechanically actuated devices to expose the desiccant to ambient air. This severely limits the use of desiccants for humidity control in electronic devices to just storage and shipping.

1.2 Objectives of the work

The main focus of this work is to experimentally study humidity control inside electronic enclosures by forced condensation. Another focus of the work is to study the effect of power dissipation and different geometric parameters of an electronic enclosure on humidity accumulation under cyclic ambient temperature. Feasibility of internal heating for humidity control was also investigated. The electronic enclosure was modelled after a real electronic control unit with parallel PCB arrangement. This work also suggests a methodology to model performance of electronic circuits under different conditions of humidity and contamination. The simulation methodology would help predict humidity related failures in electronics by using leakage current data from standard SIR patterns. The following are the major investigations done in this work:

- Effect of geometrical parameters like controlled opening sizes, enclosure volumes and cold surface temperature on steady state and transient characteristics of preferential condensation based humidity control.
- Effect of enclosure geometric parameters like inter-PCB spacing, heat capacity, controlled opening sizes on humidity accumulation under cycling ambient temperature conditions and feasibility of utilising internal heating for humidity control.
- Investigation of a simulation methodology to predict humidity related failures under different conditions of humidity and contamination.

1.3 Structure of the thesis

Figure 1.2 shows the overall structure of the thesis. Chapters 1, 2, 3 and 4 introduce the background, literature on the topics and materials and experimental methods. Chapter 5 is a study of humidity control by forced condensation. Chapter 6 studies the transfer of humidity from warm to cold using glass enclosures to answer fundamental questions on using condensation for humidity control. Chapter 7 investigates humidity accumulation in electronic enclosures due to cycling ambient temperature and internal heating. Chapter 8 studies humidity and temperature profiles in an electronic enclosure with retained water inside. Chapter 9 introduces a simulation methodology to predict humidity failures in electronic circuits. The overall discussion and conclusions are presented in chapters 10 and 11.

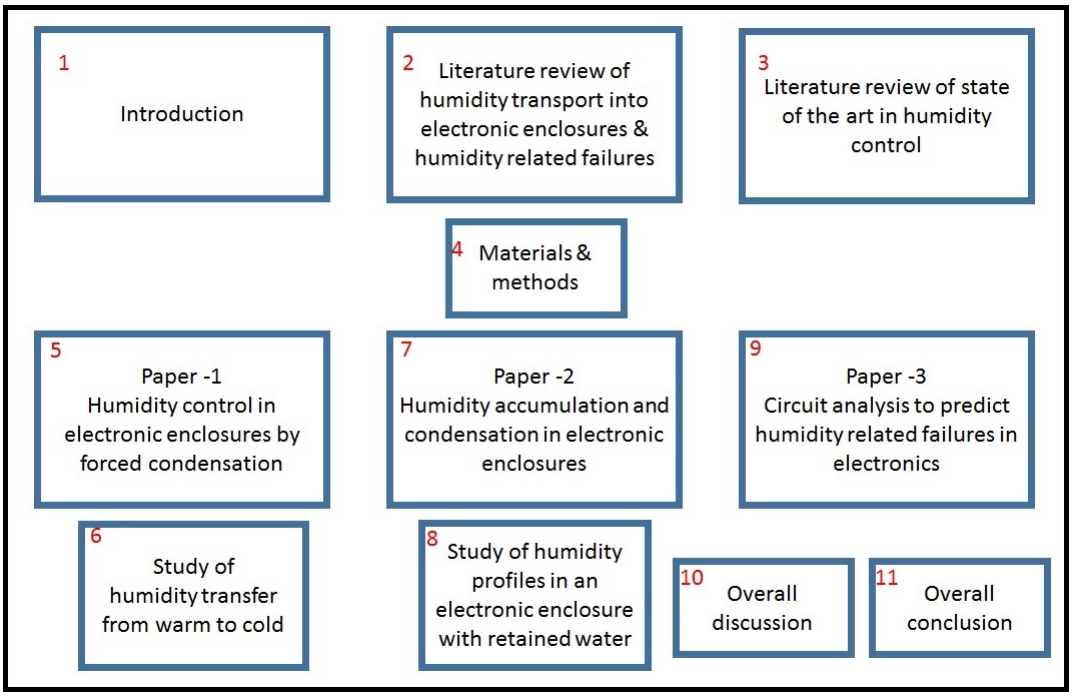

Figure 1.2: Structure of the PhD thesis showing literature reviewed and different investigations

Bibliography

[1] K. Mainali, A. Tripathi, S. Madhusoodhanan, A. Kadavelugu, D. Patel, S. Hazra, K. Hatua, S. Bhattacharya, "A Transformerless Intelligent Power Substation: A three-phase SST enabled by a 15-kV SiC IGBT", IEEE Power Electronics Magazine, vol. 2, Issue 3, pp. 31-43, 2015.

[2] H. Wang, M. Liserre, F. Blaabjerg, "Toward reliable power electronics: challenges design tools and opportunities", IEEE Ind. Electron. Mag., vol. 7, no. 2, pp. 17-26, 2013.

[3] C. Sintamarean, F. Blaabjerg, H. Wang, Y. Yang, "Real field mission profile oriented design of a SiC-based PV-inverter application", IEEE Transactions on Industry Applications, Vol. 50, Issue 6, pp. 4082-4089, 2014

[4] D. Minzari, M. S. Jellesen, P. Moller and R. Ambat, " On the electrochemical migration of tin in electronics," Corrosion science, Vol. 53, Issue 10, pp. 3366–3379, 2011.

[5] D. Minzari, M.S. Jellesen, P.R. Møller et al., "Electrochemical migration on electronic chip resistors in chloride environments", IEEE Trans. Device Mater. Reliab., vol. 9, no. 3, pp. 392-402, 2009.

[6] V. Verdingovas, M.S. Jellesen, R. Ambat, "Influence of sodium chloride and weak organic acids (flux residues) on electrochemical migration of tin on surface mount chip components", Corrosion Engineering science and technology, vol. 48, Issue 6, pp. 426-435, 2013.

[7] V. Verdingovas, M. S. Jellesen and R. Ambat, "Solder Flux Residues and Humidity-Related Failures in Electronics: Relative Effects of Weak Organic Acids Used in No-Clean Flux Systems," Journal of Electronic Materials, Vol. 44, Issue 4, pp. 1116–1127, 2015.

[8] J. Jones, J. Hayes, "Investigation of the occurrence of no-faults-found in electronics", IEEE Transactions on Reliability, vol. 50, no. 3, pp. 289-292, 2001.

[9] M. Tencer, J-S. Moss, "Humidity Management of Outdoor Electronic Equipment: Methods Pitfalls and Recommendations", IEEE Trans. Components and Packaging Tech., vol. 25, no. 1, pp. 66-72, 2002.

[10] M. Tencer, "Moisture Ingress into Non hermetic Enclosures and Packages.A Quasi-Steady State Model for Diffusion and Attenuation of Ambient Humidity Variations", Electronic components and technology conference, pp. 196–209, 1994.

[11] H. Conseil-Gudla, Z. Staliulionis, M. S. Jellesen, M. Jabbari, J. H. Hattel, R. Ambat, " Humidity build-up in electronic enclosures exposed to constant conditions," IEEE transactions on components packaging and manufacturing technology, vol.7, Issue 3, pp. 412–423, 2017.

[12] H. Conseil, V. C. Gudla, M. S. Jellesen, R. Ambat, Humidity build-up in a typical electronic enclosure exposed to cycling conditions and effect on corrosion reliability, IEEE Transactions on Components, Packaging and Manufacturing Technology, vol. 6, Issue 9, pp. 1379–1388, 2016.

[13] M. M. Rafique, P. Gandhidasan, H. M. S. Bahaidarah, " Liquid desiccant materials and dehumidifiers – A review," Renewable and Sustainable Energy Reviews, Vol. 56, pp. 179–195, 2016.

[14] M. Sultan, I. I. El-Sharkawy, T. Miyazaki, B. B. Saha, S. Koyama, " An overview of solid desiccant dehumidification and air conditioning systems," Renewable and Sustainable Energy Reviews, Vol. 46, pp. 16–29, 2015.

Chapter 2

Humidity accumulation and failures in Electronics

2.1 Climatic reliability of electronics

Use of electronic products in uncontrolled application environments has led to failures due to temperature and humidity. Failure or malfunction of an electronic equipment can lead to loss of property, loss of life, customer dissatisfaction and loss of brand value for the manufacturer. Wang et. al. [1] has shown that humidity and contamination related failures account for 25% of failures in power electronic systems. Humidity and contamination related failures are the result of local electrochemical corrosion on PCBA surface. Electrochemical corrosion can occur on PCBA due to presence of a) metals/alloys b) potential bias and c) humid environment. PCBA surface also has hygroscopic and ionic residues from the manufacturing and component assembly process. Hygroscopic nature of the contamination causes a thicker water layer to form on PCBA even at lower RH values. The ionic nature of the residues increases the conductivity of the water layer formed. This leads to increased leakage currents and electrochemical migration (ECM)[2]. In this regard, cleanliness of PCBA and accumulation of high humidity in electronic enclosures become important aspects concerning reliability of electronic equipment during its life time. Figure 2.1 illustrates the factors causing electrochemical corrosion in electronic applications.

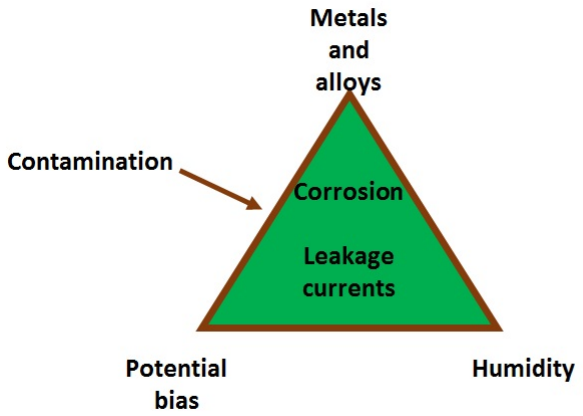

Figure 2.1: Factors causing corrosion in electronics under humid conditions

This chapter reviews the literature on humidity related failures in electronics and various factors that contribute to it. These include enhancement of water layer thickness due to the presence of contamination and different ways in which high humidity accumulates in an electronic enclosure. Also discussed are the fundamental mass transport mechanisms, which contribute to humidity accumulation and different matrices for quantifying humidity.

2.2 Water layer formation on PCBA

A surface exposed to humid air develops a thin microscopic layer of water. The number of monolayers of water present on a surface in the presence of humid air can be calculated according to Brunauer-Emmett-Teller (BET) theory[3] by:

$$N = \frac{cx}{(1-x)(1+(c-1)x)} \tag{2.1}$$

where,

$$c = e^{\frac{E_0 - E}{RT}}$$

and,

$$x = \frac{P}{P_0}$$

is the relative humidity (RH).

As observed from equation 2.1 the thickness of the water layer is dependent on the RH of the ambient air, with the water layer thickness increasing with higher values of RH. For $\alpha-$ aluminium surfaces the number of monolayers is one at 35% RH and five at 70% RH[4]. The conductivity of water layer increase with larger number of monolayers[4]. The number of monolayers required for ionic conductivity leading to failure varies from three to ten in literature[5]. Water can condense on surface of a PCBA when the temperature of the surface decreases below dew point temperature of the ambient air. Dew point temperature has been described in section 2.5.2. A thicker water layer can also form on surface of PCBA due to presence of hygroscopic and ionic contamination. At lower RH values the surface insulation resistance of PCBA remain high. When the RH exceeds deliquescence RH (DRH) of the contamination on the PCBA surface, a thin film of saturated solution develops on the contamination particle[6]. Thus, a thicker water layer can form even at lower RH values due to presence of hygroscopic contamination. The presence of a conductive water layer on PCBA surface decreases the surface insulation resistance leading to unacceptable leakage currents.

2.3 Contamination

The main sources of contamination on PCBA are from PCB manufacturing, component assembly process and application environment[6]. The PCB manufacturing related contamination present on PCBA are curing agents, flame retardants, etching chemicals etc. Human handling of the PCBA during production can result in chlorides, organic acids, oils etc being present on the PCBA[2]. Contamination from application environment consist of dust, aerosols and other particulate matter

containing ionic and hygroscopic materials. Figure 2.2 shows the different sources of contamination on PCBA[6]. The most common cause of leakage currents and SIR reduction related faults in electronics is caused by solder flux residues from component assembly process on PCBA[6].

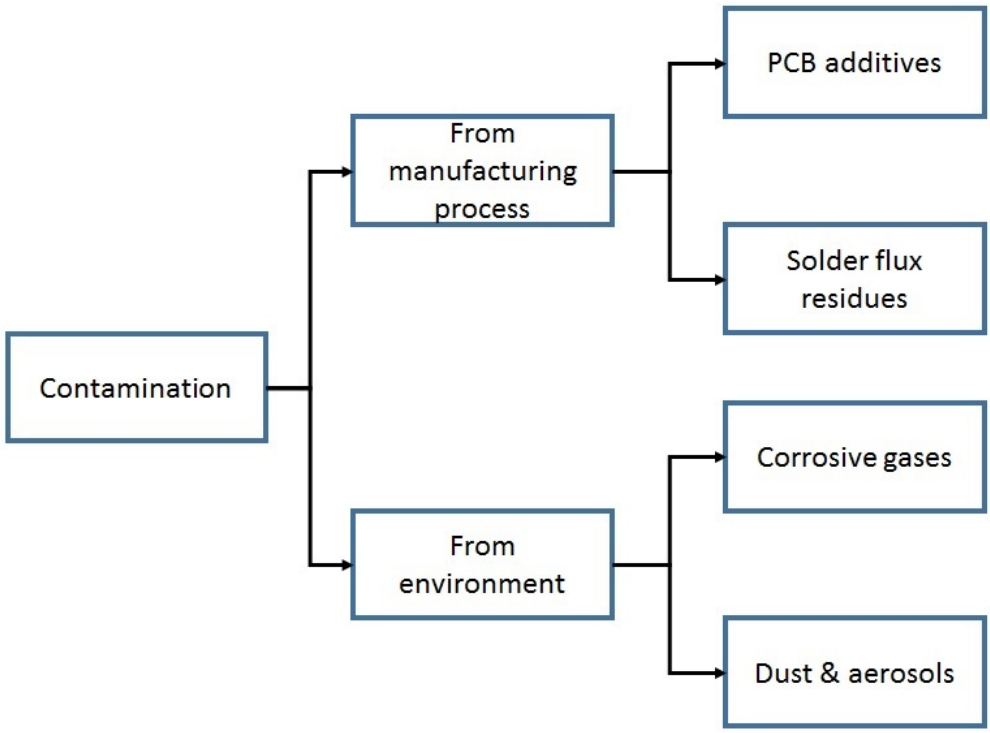

Figure 2.2: Source of contamination in electronics(Verdingovas, 2015 [6])

2.3.1 Solder flux residues

No-clean solder fluxes are widely used for soldering electronic components to PCB. It is assumed that no-clean solder fluxes decompose during the soldering process and leave behind minimal benign residues on the PCBA. But, it has been found that soldering with no-clean fluxes leave behind considerable amounts of residues[7][8]. The main failure causing constituent of no-clean fluxes is the activator component of the flux which is commonly a weak organic acid (WOA). Many of these WOAs are hygroscopic and ionic in nature leading to water layer formation due to deliquescence and subsequent reduction in SIR. Table 2.1 gives a list of commonly used WOAs in solder fluxes and their properties.

In reflow soldering process for surface mount components, the solder flux paste is applied to the contact pads, components are temporarily attached and the entire assembly is introduced into a reflow oven. During this process the flux around component pads will spread away and gets trapped under components like ball grid arrays (BGA), quad flat no-lead (QFN) and other surface-mount components. The flux residues remain even after the reflow soldering process, which could lead to failures over time[9]. For through hole components, flux is sprayed on the bottom side of the PCB where the solder-wave makes contact. The low surface tension of the liquid flux causes it to flow and get trapped in the space between bottom side

Table 2.1: Properties of WOAs in no-clean solder fluxes

WOA.	DRH(%)	Solubility(g/1Kg water)
Adipic	>98	15_{15^oC}
Succinic	>98	83.5_{25^oC}
Glutaric	83-89	1400_{25^oC}
DL-Malic	75-84	1440_{26^oC}
Palmitic	-	0.007_{20^oC}

of PCB and pallet[8][9]. The area between pallet and bottom side of PCB experience less temperature during preheating and wave soldering causing incomplete decomposition of the flux leading to presence of residues on PCBA[9].

2.3.2 Contamination from user environment

Contamination from user environment causing corrosion in electronics can be classified as corrosive gases and particulate contamination. Corrosive gases like SO_x, H_2S etc can react with the metallisation on the PCB causing corrosion[10][11]. Minzari et. al. [10] has shown the formation of silver dendrites on silicone encapsulated hybrid circuits in the presence of sulphurous gases. It is observed that permeation of sulphur gases and humidity through the silicone coating resulted in uniform corrosion, formation of Ag_2S and migration of silver[10].

Particulate contamination found in atmosphere contain nitrate, sulphate, chloride, ammonium etc[12]. They are hygroscopic and when deposited on PCBA, aid in water layer formation causing failures. Dust and aerosols get drawn into electronic enclosures through openings in the enclosure and due to forced air convection cooling. Tencer[13] describes the different mechanisms of deposition of aerosols in electronics which include brownian diffusion, gravitational settling, thermophoresis, electrophoresis etc. When the RH inside the electronic enclosure increases beyond the deliquescence RH of the particulate contamination deposited on PCBA, a conductive water layer is formed. Another important factor required for SIR degradation on PCBA due to atmospheric particulates is connectivity, which is the bridging from particle to particle[13].

2.4 Important humidity related failures

2.4.1 Leakage currents/SIR degradation

Leakage currents are unintended currents flowing between two nodes of an electronic circuit on a PCBA. As related to humidity related failures, leakage currents occur because of a conducting water layer formation between two nodes as explained in section 2.2. The flow of leakage currents can affect the normal functionality of an electronic circuit leading to equipment malfunction or failure. A reduction of SIR is the result of flow of leakage currents. Kinner[14] shows the different pathways a leakage current could take on a PCBA in presence of water layer and ionic contamination. Zou and Hunt[15] has studied methods to characterise conduction

mechanisms on a PCBA using a.c impedance. Under low RH conditions, the bulk of the SIR measured is due to the high resistivity of the substrate. But, under humid conditions and presence of ionic contamination a conducting water layer forms on the surface of the substrate. The conducting water layer can form a parallel path of higher conductivity compared to the substrate. This leads to considerable leakage currents between two nodes of a circuit through the water layer compared to the substrate. The current is carried by ions in the water layer.

Leakage currents/SIR reduction on PCBA under humid conditions and presence of contamination can be found in literature[16][17][18][19][20]. From literature, it can be seen that solder flux residues are the most frequent cause for leakage currents/SIR degradation. Use of surface insulation resistance (SIR) patterns is an electrical method to quantify contamination and predict the propensity for leakage currents on a PCBA [14][15]. A method to prevent considerable leakage current on PCBA is to have a cleaning step in the production process after component assembly to remove the no-clean solder flux residues.

2.4.2 Electrochemical migration

Electrochemical migration (ECM) occurs when the metal ions from the anode part of the micro-electrochemical cells formed on PCBA deposit themselves on the cathode by transport through the conductive water layer in presence of a electric potential difference. The deposition of the positive metal ions causes a dendrite to grow from cathode to anode, eventually causing a short circuit between the anode and cathode. The dendrite might disappear due to the heat generated by the short circuit current. ECM can happen in the presence of a thick water layer formed due to deliquescence and condensation or in the presence of monolayers of water molecules in humid conditions[21]. The ECM that happens commonly in electronics applications is due to formation of a thick water layer in condensing conditions and presence of hygroscopic contamination. Minzari has studied ECM of tin in electronic applications[22][23]. The solder fluxes used in electronic component plays an important role in ECM on PCBA[24][16][17].

2.5 Humidity accumulation in electronic enclosures

2.5.1 Enclosures for electronics

The function of an electronic enclosure is to:

- Protect the electronics from aggressive ambient climate
- provide a suitable path for excess heat dissipated in the electronics to be removed to the ambient
- shield the electronics from external electromagnetic interference (EMI)
- shield the EMI generated by the electronics, and
- aesthetic reasons.

Electronic enclosures come in all shapes and sizes. Enclosures are normally made of aluminium or a polymeric material. Common polymer materials used to make enclosures are Polycarbonate (PC), acronitrile butadiene styrene (ABS) etc. Aluminium enclosures are preferred in applications with higher heat dissipation due to the high thermal conductivity of aluminium and also its lower cost compared to copper. Enclosures could also be made of combination of metal and polymer with metal parts serving to dissipate heat more efficiently to the ambient.

Figure 2.3 shows a typical parallel arrangement of aluminium plates simulating PCBs inside an enclosure. In power electronic applications, higher power carrying circuits could be located on a separate PCB called a 'power PCB'. The logic circuits can be located on another PCB called a 'control or logic PCB'. This is done to minimise conducted emissions caused by high frequency switching power circuits from interfering with the operation of the logic circuits.

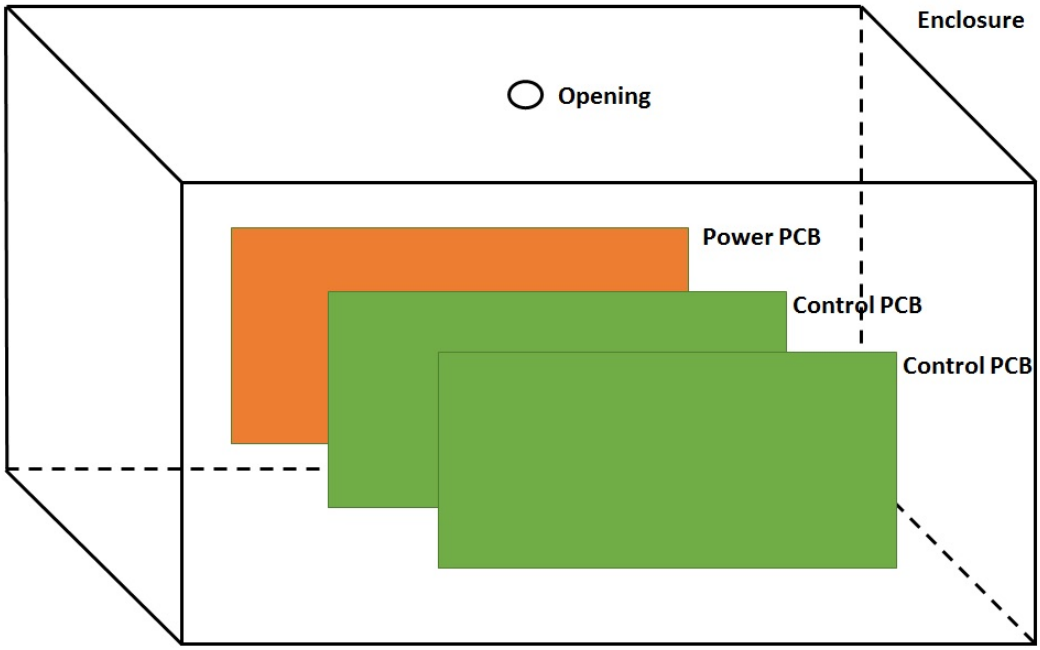

Figure 2.3: Typical internal view of enclosures used in electronics

Figure 2.3 also shows openings in enclosures used in electronics. Openings in electronic enclosures could be intentional or unintended openings. Openings in electronics could be:

- To aid in forced convective transfer of heat from the electronics to ambient
- A path for retained liquid water to flow out of the enclosure
- Space between wires in an unsealed signal connector
- Cracks in the enclosure body

2.5.2 Quantification of humidity

Humidity is water vapour present in air. The amount of water vapour present in air can be expressed using various quantities like mass fraction, absolute humidity,

relative humidity, dew point temperature etc. The amount of water vapour present in a volume of air 'V' can be expressed using the ideal gas law :

$$P_v.V = m \cdot R_v \cdot T \tag{2.2}$$

where P_v is the partial pressure of water vapour in air, 'm' is the mass of water vapour, R_v is the gas constant for water vapour and 'T' is the absolute temperature. The following sections explain each of the methods of quantification.

Absolute humidity

Absolute humidity (AH) is the total mass of water vapour present in a unit volume of air. AH is the value m/V in equation 2.2. The common units of AH are g/m^3 and kg/m^3. The amount of water vapour a volume of air can hold varies with the temperature of the air. When a volume of humid air at a particular AH and temperature is cooled, the excess water vapour starts to condense out in the form of liquid water. Absolute humidity can be calculated according to the approximate formula:

$$AH = \frac{2.16 \times (RH/100) \times 288.68 \times (1.098 + T/100)^{8.02}}{273 + T} \tag{2.3}$$

where 'T' is the temperature in degree Celsius and RH is the relative humidity as percent. Figure 2.4 shows the maximum amount of AH air can hold at different temperatures.

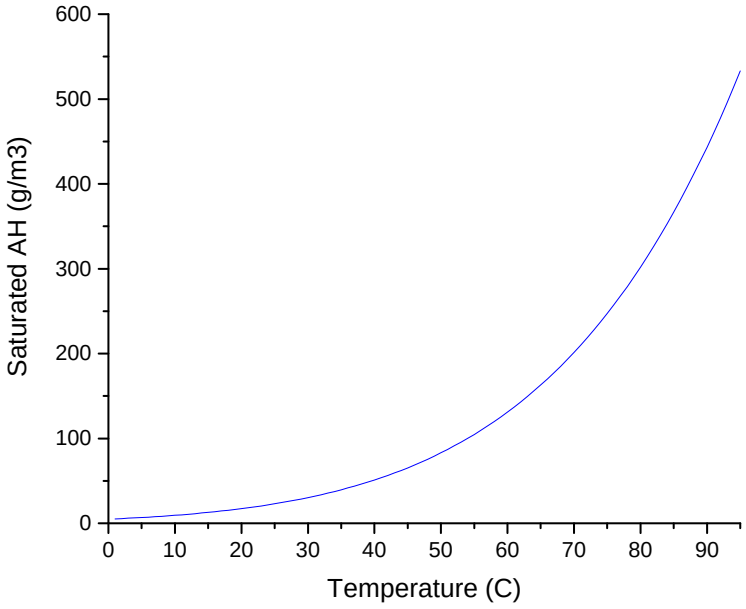

Figure 2.4: Variation of saturated AH with temperature

Relative humidity

Relative humidity(RH) is the fraction of partial pressure of water vapour of a volume of air to its saturated vapour pressure at a given temperature. 100% RH signifies the air is saturated with water vapour. RH is expressed in percent as:

$$RH(\%) = \frac{P_v}{P_{vsat}} \cdot 100 \tag{2.4}$$

Dew point

Dew-point temperature is the temperature air should be cooled to raise its RH to 100%. Dew-point temperature can be approximated using the Magnus formula[25] as :

$$T_{dew} = \frac{a \cdot [ln(RH/100) + \frac{b \cdot T}{a+T}]}{b - [ln(RH/100) + \frac{b \cdot T}{a+T}]} \tag{2.5}$$

where 'a' is 243.12, 'b' is 17.62, 'RH' is the relative humidity in percent and 'T' is the temperature in celsius. The importance of dew-point temperature is that air with a particular RH would condense on a surface having a temperature less than or equal to the dew-point temperature of the air.

2.5.3 Humidity transport into electronic enclosures

Humidity can enter an electronic enclosure through intended or unintended openings in the enclosure. Humidity accumulation occurs when the ambient AH is higher than the AH inside the enclosure. The main transport modes for humidity between ambient and the enclosure are:

- Diffusion - isothermal and non-isothermal
- Convection - forced and natural

Figure 2.5 depicts the different modes of humidity transfer between ambient and electronic enclosures[26].

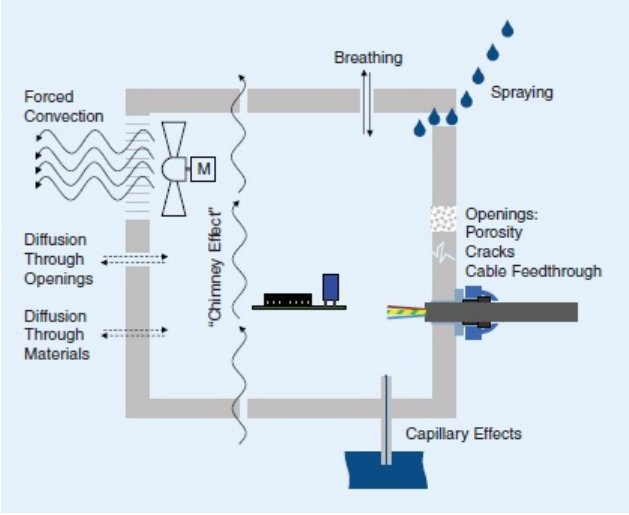

Figure 2.5: Moisture transport in an electronic enclosure (Jacobsen et al., 2014 [26])

Humidity can diffuse through intended or unintended openings and also through polymer walls of an enclosure. Forced and natural convection are used in electronics for cooling purposes, giving rise to exchange of humid air between the enclosure and ambient. Natural convection between the electronic enclosure and ambient also occurs due to ambient temperature and pressure changes.

At any time, an electronic enclosure could be exchanging humidity with surroundings under all combinations of humidity transport modes. Conseil et. al. details humidity accumulation in electronic enclosures under conditions of diffusion[27] and convection[28] with the ambient. The following subsections introduce diffusion and convective modes of transport.

Diffusion

Diffusion is the process by which matter is transported from one part of a system to another as a result of random molecular motions[29]. The net movement of a species is from a region of higher concentration to regions of lower concentration. The driving force behind diffusion is the gradient in concentration. For isotropic materials the rate of transfer of diffusing substance through unit area of a section is proportional to the concentration gradient measured normal to the section[29]. For a one-dimension system this becomes:

$$F = -D\frac{\delta C}{\delta x} \tag{2.6}$$

where, 'D' is the diffusion constant of the material. Equation 2.12 is called the Fick's first law of diffusion after Adolf Fick. Fick's second law of diffusion relates the time differential of concentration at a location in space to differential of concentration with respect to position. For a one-dimensional system this becomes[29] :

$$\frac{\delta C}{\delta t} = D\frac{\delta^2 C}{\delta x^2} \tag{2.7}$$

Tencer[30] has shown that for an enclosure as in figure 2.6 with opening dimensions much larger than the enclosure wall thickness, isothermal diffusion of humidity can be modelled mathematically like the charging of an electrical capacitor through a resistance.

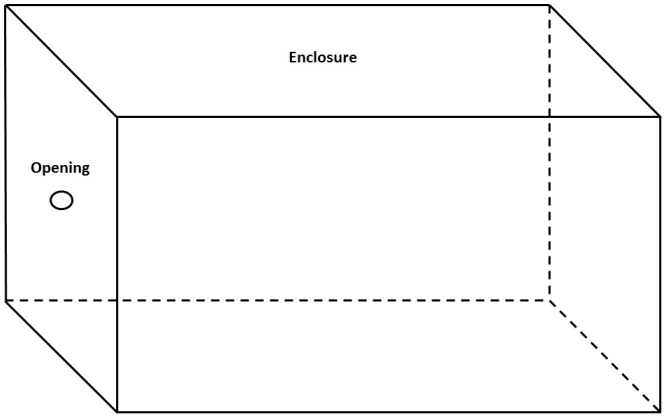

Figure 2.6: Schematic of an electronic enclosure with an opening

The time constant for charging is given by:

$$\tau = \frac{VL}{AD} \tag{2.8}$$

where 'V' is the volume of the enclosure, 'L' is the thickness of the enclosure wall, 'A' is the area of the opening and 'D' is the diffusion coefficient for water vapour in air, $0.24cm^2/s$. If volume 'V' is considered as hygric capacitance then the equivalent resistance becomes :

$$R = \frac{L}{AD} \tag{2.9}$$

Humidity can also diffuse into an electronic enclosure with no openings through polymer walls of the enclosure. This involves combined sorption of water molecules by the polymer and diffusion. The dissolution of water vapour in a solvent can be described by Henry's law. Henry's law states that the concentration of a dissolved gas is proportional to the partial pressure of the gas in contact with the solution.

$$C = kp \tag{2.10}$$

where, 'C' is the concentration of the gas, 'k' is the solubility coefficient and 'p' is the partial pressure of the gas. The diffusion coefficient can be combined with the solubility coefficient to give permeability.

$$P = kD \tag{2.11}$$

When including effect of solubility, Ficks first law becomes:

$$F = -P\frac{\delta p}{\delta x} \tag{2.12}$$

where 'P' is the permeability and 'p' is the partial pressure of water vapour.

Convection

Convection is the transport of mass, heat or momentum along with the bulk motion of a fluid. An example is transport of water vapour due to flow of humid air. Convection can be classified broadly as natural or forced. Natural convection occurs due to interaction of gravity with a fluid having a density gradient. The density gradient could be because of a temperature gradient or a concentration gradient. Natural convection of air in electronic enclosures occur because of temperature gradient caused due to heat dissipation by electronic components. Forced convection occurs in electronic enclosures because of the operation of fans used for cooling. Convection results in exchange of humid air between the electronic enclosure and the ambient. This could result in humidity accumulation inside the enclosure if the ambient absolute humidity is higher than the humidity inside the enclosure.

Convective heat transfer is described by Newton's law of cooling. For a vertical flat plate of area 'A' and surface temperature T_s the heat transferred from the plate to the fluid around it is given by:

$$Q = hA(T_s - T_\infty) \tag{2.13}$$

where T_∞ is the temperature of the bulk fluid and 'h' is the convective heat transfer coefficient. The non-dimensional convective heat transfer coefficient called Nusselt number is given by the formula:

$$N_u = \frac{hL}{K} \tag{2.14}$$

where 'L' is the length of the flat plate and 'K' is the conductivity of the fluid around the plate. The significance of the Nusselt number is that it is the factor by which heat or mass transfer gets amplified compared to when the only transport mode is conduction or diffusion for heat or mass, respectively. Due to the similarities in the differential equations used for transport of heat and mass, equations 2.13 and 2.14 can be used to describe mass transport also.

Convective transfer from a surface leads to the formation of boundary layers. A boundary layer is the region of fluid surrounding the flat plate where the variable of interest like temperature, velocity, concentration has a value different from the bulk of the fluid. Figure 2.7 shows the formation of a velocity boundary layer on a heated flat plate[31]. The thickness of the boundary layer in figure 2.7 at any location along the surface is defined as the distance from the surface at which the difference between the surface and bulk values reach 99%.

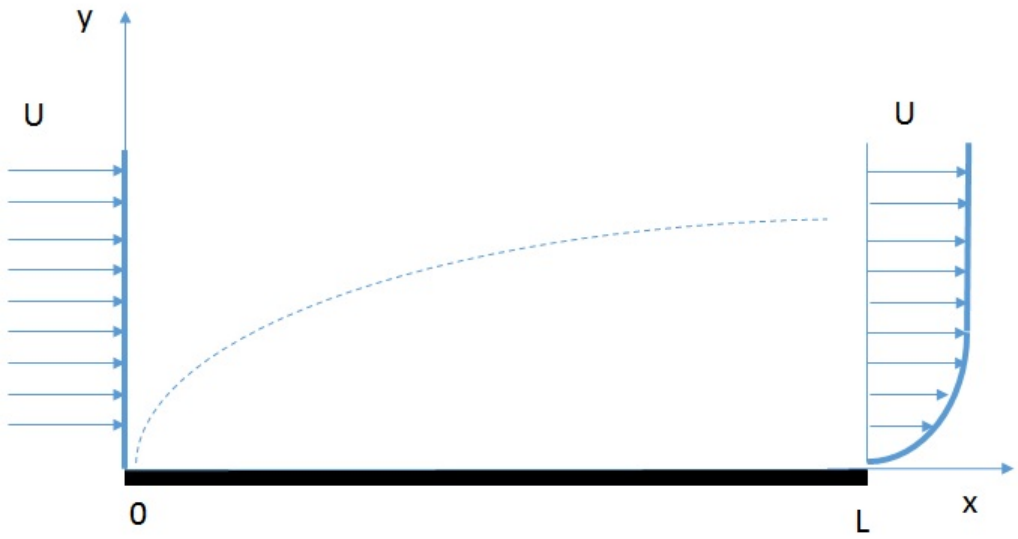

Figure 2.7: Boundary layer on a heated plate (White, 2009 [31])

The convection problem is solved by finding the solution to the equations of conservation of mass, momentum and energy. For a two dimensional system the equations are:

$$\frac{\partial u}{\partial x} + \frac{\partial v}{\partial y} = 0 \tag{2.15}$$

$$u\frac{\partial u}{\partial x} + v\frac{\partial v}{\partial y} = v\frac{\partial^2 u}{\partial y^2} \tag{2.16}$$

$$u\frac{\partial T}{\partial x} + v\frac{\partial T}{\partial y} = \alpha\frac{\partial^2 T}{\partial y^2} \tag{2.17}$$

The equations 2.15, 2.16 and 2.17 are non-linear partial differential equations therefore, solution to the above equations in a practical application need the use of a computer.

Bibliography

[1] H. Wang, M. Liserre, F. Blaabjerg, "Toward reliable power electronics: challenges design tools and opportunities", IEEE Ind. Electron. Mag., vol. 7, no. 2, pp. 17-26, 2013.

[2] R. Ambat, "Perspectives on climatic reliability of electronic devices and components", Imaps 2008, Rhode Island, USA, Nov. 2008.

[3] A. W. Adamson, A. P. Gast, Physical chemistry of surfaces, John wiley and sons Inc., 1997.

[4] B.-D. Yan, S.L. Meilink, G.W. Warren et al., "Water adsorption and surface conductivity measurements on alpha-alumina substrates", IEEE Trans. Compon. Hybrids Manuf. Technol., vol. 10, no. 2, pp. 247-251, 1987.

[5] M. Tencer, J-S. Moss, "Humidity Management of Outdoor Electronic Equipment: Methods Pitfalls and Recommendations", IEEE Trans. Components and Packaging Tech., vol. 25, no. 1, pp. 66-72, 2002.

[6] V. Verdingovas, " Climatic reliability of electronics - Early prediction and control of contamination and humidity effects", PhD thesis, Technical university of Denmark, Kgs. Lyngby, March 2015.

[7] M. S. Jellesen, D. Minzari, U. Rathinavelu, P. Moller and R. Ambat, "Corrosion failure due to flux residues in an electronic add-on device", Engineering failure analysis, vol. 17, Issue 6, pp. 1263-1272, 2010.

[8] H. Conseil-Gudla, M. S. Jellesen, R. Ambat, " Contamination profile on typical printed circuit board assemblies vs soldering process," Soldering and surface mount technology, Vol. 26, Issue 4, pp. 194-202, 2014.

[9] P. Isaacs, T. Munson, "What Makes No-Clean Flux Residue Benign", SMTA Pan Pacific Conference 2016 Proceedings.

[10] D. Minzari, M. S. Jellesen, P. Moller and R. Ambat, "Morphological study of silver corrosion in highly aggressive sulfur environments," Engineering failure analysis, vol. 18, Issue 8, pp. 2126 – 2136, 2011.

[11] C. Hillman, J. Arnold, S. Binfield, and J. Seppi, "Silver and Sulfur: Case Studies, Physics, and Possible Solutions," SMTA International Conference, 2007.

[12] J. D. Sinclair, L. A. Psota-Kelty, C. J. Weschler and H. C. Shields, " Deposition of Airborne Sulfate, Nitrate, and Chloride Salts as It Relates to Corrosion of Electronics," Journal of electrochemical society, Vol. 137, Issue 4, pp. 1200–1206, 1990.

[13] M. Tencer, "Deposition of aerosol ("hygroscopic dust") on electronics – Mechanism and risk," Microelectronics reliability, vol. 48, Issue 8, pp. 584–593, 2008.

[14] P. Kinner, "The principle of surface insulation resistance (SIR) testing and its role in establishing the electrochemical reliability of a printed circuit board," Proceedings of 2004 International Conference on the Business of Electronic Product Reliability and Liability, 2014.

[15] L. C. Zou; C. Hunt, "Characterization of the Conduction Mechanisms in Adsorbed Electrolyte Layers on Electronic Boards Using AC Impedance," Journal of the Electrochemical Society, Vol. 156, Issue 1, pp. C8–C15, 2009.

[16] V. Verdingovas, M. S. Jellesen and R. Ambat, "Relative effect of solder flux chemistry on the humidity related failures in electronics," Soldering and Surface Mount Technology, Vol. 27, Issue 4, pp. 146–156, 2015.

[17] V. Verdingovas, M. S. Jellesen and R. Ambat, "Solder Flux Residues and Humidity-Related Failures in Electronics: Relative Effects of Weak Organic Acids Used in No-Clean Flux Systems," Journal of Electronic Materials, Vol. 44, Issue 4, pp. 1116–1127, 2015.

[18] V. Verdingovas, M.S. Jellesen, R. Ambat, "Influence of sodium chloride and weak organic acids (flux residues) on electrochemical migration of tin on surface mount chip components", Corrosion Engineering science and technology, vol. 48, Issue 6, pp. 426-435, 2013.

[19] V. Verdingovas, M. S. Jellesen, and R. Ambat, "Impact of NaCl Contamination and Climatic Conditions on the Reliability of Printed Circuit Board Assemblies", IEEE Trans. Device Mater. Reliab., vol. 14, no. 1, pp. 42-51, 2014.

[20] J. E. Sohn, U. Ray, "Weak organic acids and surface insulation resistance ", Circuit world, vol. 21, Issue 4, pp. 22-26, 1995.

[21] S. J. Krumbein, "Tutorial: Electrolytic models for metallic electromigration failure mechanisms", IEEE Trans. Rel., vol. 44, no. 4, pp. 539-549, Dec. 1995.

[22] D. Minzari, " Investigation of electronic corrosion mechanisms", PhD thesis, Technical university of Denmark, Kgs. Lyngby, June 2010.

[23] D. Minzari, M. S. Jellesen, P. Moller and R. Ambat, " On the electrochemical migration of tin in electronics," Corrosion science, Vol. 53, Issue 10, pp. 3366–3379, 2011.

[24] D. Q. Yu, W. Jillek, E. Schmitt, " Electrochemical migration of lead free solder joints," Corrosion science, Vol. 17, Issue 3, pp. 229–241, 2006.

[25] Sensirion, Application Note Dew-point calculation, pp.1-3, Available : http://irtfweb.ifa.hawaii.edu/~tcs3/tcs3/Misc/Dewpoint_Calculation_Humidity_Sensor_E.pdf [Accessed : 03-April-2019]

[26] J. B. Jacobsen, J. P. Krog, A. H. Holm, L. Rimestad, "Climate-Protective Packaging: Using Basic Physics to Solve Climatic Challenges for Electronics in Demanding Applications", IEEE Ind. Electron. Mag., vol. 8, no. 3, pp. 51-59, 2014.

[27] H. Conseil-Gudla, Z. Staliulionis, M. S. Jellesen, M. Jabbari, J. H. Hattel, R. Ambat, " Humidity build-up in electronic enclosures exposed to constant conditions," IEEE transactions on components packaging and manufacturing technology, vol.7, Issue 3, pp. 412–423, 2017.

[28] H. Conseil, V. C. Gudla, M. S. Jellesen, R. Ambat, Humidity build-up in a typical electronic enclosure exposed to cycling conditions and effect on corrosion reliability, IEEE Transactions on Components, Packaging and Manufacturing Technology, vol. 6, Issue 9, pp. 1379–1388, 2016.

[29] J. Crank, "The mathematics of diffusion", Oxford university press, 1975.

[30] M. Tencer, Moisture Ingress into Non hermetic Enclosures and Packages.A Quasi-Steady State Model for Diffusion and Attenuation of Ambient Humidity Variations, Electronic components and technology conference, pp. 196–209, 1994.

[31] F. M. White, "Fluid Mechanics", McGraw-Hill, 2009.

Chapter 3

Methods to prevent humidity failures in electronics

This chapter reviews the methods to prevent SIR degradation and humidity related failures. Broadly, one method to prevent humidity related failure is to increase the intrinsic humidity robustness of the PCBA by proper design and cleanliness. Another method is to avoid contact with humidity or reduce the humidity level in contact with the PCBA surface. Second method include reducing the humidity inside the electronic enclosure or by preventing the humidity from forming a water layer on PCBA surface by application of a barrier. The most widely used method is by applying conformal coatings or by the use of potting material. Coatings and potting provide protection by preventing humidity from forming a conductive water layer. Heating, desiccants, and forced condensation are humidity control techniques, which provide protection by reducing the humidity inside the electronic enclosure. Heating reduces RH inside the enclosure, where as desiccants and condensation reduces the absolute content of water vapour in the air inside the electronic enclosure.

3.1 Conformal coatings

Conformal coatings are thin layers of synthetic resins or plastics that are applied to PCBs and conform to the contours of the assembly[1]. Conformal coatings are used in all types of electronics - automotive, industrial, military, aerospace and medical where protection is required from engine fluids, chemicals, dust, abrasion, pressurisation/depressurisation, fluid/moisture resistance etc. According to the Association Connecting Electronics Industries (IPC), the functions of a conformal coating as regards to humidity are: to inhibit current leakage and short circuit due to humidity and contamination from service environment and inhibit corrosion[2]. Additional functionalities include protection from physical abuse, such as handling, abrasion, temperature extremes, and radiation[3]. The common materials used for conformal coatings are acrylics, epoxies and silicones. Conformal coating type is selected for an application based on its moisture absorption and permeation properties. The basic requirement for a conformal coating acting as a barrier to moisture penetration is excellent adhesion to the surface where it is applied. Lack of adhesion causes voids where moisture can permeate from the ambient causing water layer formation on the surface in the voids. The adhesion to the surface depends on many factors like material properties of the coating, application process, wettability of the coating on the

surface, presence of impurities on the surface etc. PCBA manufacturing process and component assembly leaves behind hygroscopic and ionic contamination, which if not removed before application of a conformal coating can lead to improper adhesion with PCBA. So, the use of conformal coatings requires a cleaning step in the production of PCBA. Other requirements for a conformal coating include low moisture vapour transmission rate, low out-gassing, low stress etc[3]. The desirable electrical properties of a coating include high insulation resistance, high dielectric breakdown voltage, low dielectric constant and dissipation factor. A standard used for testing the performance, quality and consistency of a conformal coating is IPC-CC-830B[2].

3.1.1 Conformal coating failures

Good performance of a conformal coating requires the PCBA to be clean before applying the coating. Presence of contamination under the coating leads to blistering, delamination, leakage currents and corrosion. Blistering can occur due to a mismatch in the surface energies of the coating and surface. Blistering can also happen if the coating allows humidity to permeate in to the interface between the surface and the coating. Bubbles and pin holes occur in coatings due to premature drying, quick application of the coating and entrapment of air. Uneven thickness of the coating is another problem occurring due to capillary effects, gravity etc. Too thin coating leads to inadequate protection where as too thick a coating leads to problems like bubbles, cracking and delamination. One of the main disadvantages of using conformal coating is that an extra cleaning step is required in the PCBA manufacturing process. Also, conformal coatings cannot be expected to work reliably in ECUs subjected to high cycling temperatures and pressures due to delamination and cracking of the coating.

3.2 Potting

In contrast to conformal coatings which were thin coatings of polymer applied to the surface of a PCBA, potting involves filling the enclosed volume of PCBA with a special curable liquid compound. The liquid compound is allowed to solidify inside the electronic enclosure, preventing exposure of the PCBA to moisture and corrosive compounds. Common potting materials used are epoxy, polyurethane, silicone etc[4]. Potting helps prevent failures due to humidity, contamination, corrosive gases and also reduces effects of vibration on electronic components.

3.3 Desiccants

Desiccants are hygroscopic materials which can absorb water vapour from air thus, buffering the humidity levels inside an electronic enclosure. Use of desiccants is a method of absolute humidity control, where the concentration of water vapour in the air is controlled[5]. Solid and liquid desiccants are commonly used in HVAC as part of dehumidifying the process air[6][7].

When a desiccant gets saturated, humidity absorption capability decreases. A saturated desiccant has to be either replaced or regenerated. Regeneration is commonly accomplished by heating the desiccant. Heating causes the desiccant to loose

the adsorbed moisture to the ambient air due to higher vapour pressure generated inside. When used for humidity control in electronics, desiccants need to be exposed to ambient air during regeneration by using mechanisms like a rotating desiccant bed. Other wise, the released humidity would condense on the PCBA. The presence of moving components in desiccant based humidity control makes their use less attractive in most electronics applications. Desiccant based humidity control techniques are suitable for electronics equipment, which undergo periodic repair or maintenance, where the saturated desiccant can be replaced. A good desiccant should have large humidity storage capability and low regeneration temperature. It should also be non-volatile, non-corrosive and stable[6]. In electronics, desiccants are widely used during storage and shipping. Common desiccants used in electronics are silica gel, activated alumina, zeolite etc.

3.4 Heating

The principle of heating as a method of humidity control is to keep the electronics warm enough so that the RH near the critical surfaces are below a certain safe limit say, 60%. AH_{sat} depends strongly on temperature and can be given by[5]

$$AH_{sat} = const \cdot exp(\frac{-E}{kT}) \tag{3.1}$$

where 'E' is the energy of evaporation, 'k' is the Boltzmann constant, 'T' is absolute temperature and AH is expressed as concentration. As the temperature of a parcel of humid air is increased, value of AH_{sat} increases according to equation 3.1. Since RH is the ratio of AH to AH_{sat}, RH decreases with increasing temperature. Therefore, humidity related failures in electronics can be prevented by maintaining the RH inside an electronic enclosure below a safe limit by heating. Maximum value of RH to prevent formation of a water layer (on a clean surface) thick enough for ionic conductivity is 60%[5][8]. If the RH near PCBA surfaces can be maintained below 60% by heating, humidity related failures can be prevented. The value of ΔT required to keep the RH below 60% is shown to be between $8 - 10^oC$[5]. However, the required humidity level can be higher depending on the cleanliness of the PCBA based on the flux chemistry used for the soldering process and the residue level on the board.

3.4.1 Heat production for humidity control

Heat to raise the temperature of PCBA surfaces can be generated by convective and radiative methods. In convective methods[9][10] the heat produced by a heating element is transported to the intended surface of PCBA by convection of warm air. In radiative heating, the heated element produces electromagnetic radiation which when absorbed by a surface causes heating of the surface. Radiative heating even though used widely for heating of building interiors[11][12], it is still not practical to be used for electronic applications due to the large size of the radiation producing elements.

Heat is also produced in an electronic unit by power dissipation from the electronic components. The principal power dissipating components in electronics are power resistors, inductors, transformers and semiconductors like diodes, metal oxide

semiconductor field effect transistor (MOSFETS) and insulated gate bipolar transistor (IGBT). In resistors, power dissipation occurs because of joule heating due to current flow. In inductors and transformers heat is produced due to copper losses (joule heating) in the coils and core losses in the magnetic core due to fluctuations in the magnetic field. Semiconductor devices like diodes, MOSFETs and IGBTs dissipate heat due to ohmic losses (joule heating) and also due to switching losses when the switches change states from ON to OFF and vice versa. The heat dissipated by the electronic components could be preserved inside the electronic enclosure by suitable insulation and used to keep the critical surfaces of the PCBA warm to prevent humidity related failures, depending on the application.

3.5 Condensation

Humidity in a volume of air can be reduced by condensing the water vapour in the air by forced condensation. Condensation occurs when a volume of humid air is cooled below its dew point temperature. The formula for dew point temperature is given by equation[13]:

$$T_{dew} = \frac{a \cdot [ln(RH/100) + \frac{b \cdot T}{a+T}]}{b - [ln(RH/100) + \frac{b \cdot T}{a+T}]} \tag{3.2}$$

where 'a' is 243.12, 'b' is 17.62, 'RH' is the relative humidity in percent and 'T' is the temperature in celsius. The process of condensation is an exothermic process with release of heat energy to the surface where condensation occurs. For water, the enthalpy of condensation is 40.66kJ/mol at normal pressure and 373^oC.

There are two main types of condensation - film and dropwise condensation[14][15]. In film condensation, the condensate wets the surface and forms a liquid film on the surface that slides down under the influence of gravity. The thickness of the liquid film increases in the flow direction as more vapour condenses on the film. In dropwise condensation, the condensed vapour forms droplets on the surface instead of a continuous film, and the surface is covered by countless droplets of varying diameters [14]. Drop condensation is the most common type of condensation found in nature. Figure 3.1 shows the two main types of condensation.

Figure 3.1: Types of condensation on a surface (Stephan, 1992 [15])

In film condensation, the heat released has to be transported from the surface of the liquid film through the liquid to the cold surface. The film of already condensed liquid acts as a resistance to heat transfer. In drop condensation, the condensed

drops slide down under the influence of gravity, creating new locations for condensation to happen. Hence, the heat transfer rates are much higher with drop condensation than film condensation. Therefore, drop condensation is preferred to film condensation when higher condensing rates are required. Film condensation can be described theoretically by Nusselt film condensation theory[15].

3.5.1 Thermoelectric coolers

Thermoelectric coolers(TECs) are well suited for forced condensation based dehumidification in electronic enclosures. TECs work on the principle of peltier effect. When a voltage difference is applied to a thermoelectric device a temperature difference is produced. Peltier effect has been applied for cooling[16][17], dehumidification[18][19], atmospheric water generation[20][21] etc.

A basic thermoelectric cooler (TEC) consists of a thermocouple, which consists of a n-type and p-type semiconductor. A typical TEC consists of many thermocouples connected electrically in series and thermally in parallel to each other. The thermocouples are sandwiched between thermally conducting plates. Figure 3.2 shows the construction of a TEC[22].

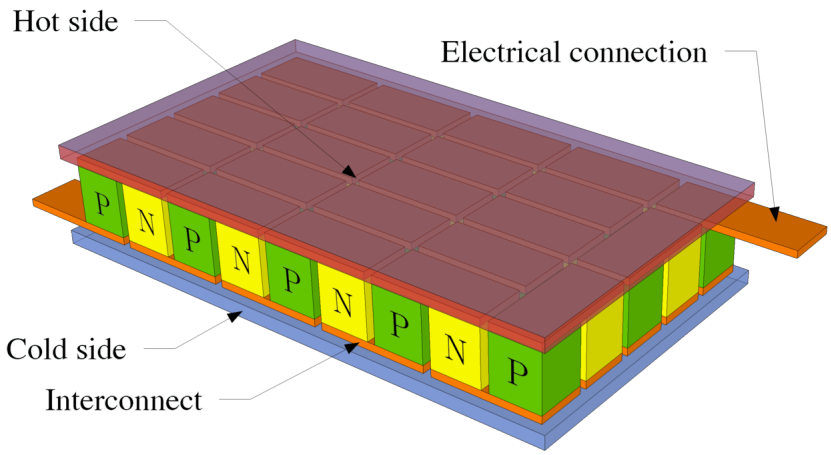

Figure 3.2: TEC construction (Wikipedia [22])

When d.c current is passed through the TEC, one side of the device is cooled and the other side gets heated due to peltier effect. The amount of cooling achieved by the cold side is proportional to the current passing through the TEC. The advantage of using TEC for cooling are lack of moving parts, reliability, small size, low noise, electrical control of cooling etc.

3.6 Humidity control

Control of humidity has been used widely in HVAC[23][24] and in special applications like museums, historic buildings and artefacts[25][26]. HVAC applications control humidity to improve the comfort of the occupants in houses, offices etc. Humidity control in HVAC applications is commonly done by passing the process air over a cooling coil to dehumidify the air. Cooling coils are operated normally by vapour compression refrigeration systems. Hybrid systems which incorporate desiccants

have shown to give better humidity control[27]. Use of desiccants in humidity control also need moving mechanisms like rotating desiccant beds for regeneration of the desiccants[28][29]. All the above applications use considerable amount of energy for their operation and also feature moving components which makes them less attractive for electronic applications.

Kim et al. [30] has compared different humidity control techniques like heating, fan, forced condensation and desiccants for a light emitting diode application. Forced condensation based humidity control was found to be the most suitable. Narayanaswamy[31] has studied the need for humidity control in subsea electrical enclosures and suggests heating and use of desiccants. The above mentioned literature does not take into account factors like enclosure and packaging related parameters to optimise the humidity control process by heating or forced condensation.

TEC based forced condensation humidity control is used in HVAC[18][19], water production[20][21] etc. In the above mentioned applications, the design is done to draw in as much air as possible into the enclosure using fans to increase the rate of dehumidification where as, forced condensation humidity control in electronics should work at comparatively low ingress rates through openings in the enclosure[5]. Although many applications of condensation based dehumidification use a TEC, some special electronic applications like pumps for circulating cold water inherently provide a cold and condensing surface which can be used for dehumidification by suitably interfacing with the electronic enclosure[32][33].

Bibliography

[1] S. Zhan, M. H. Azarian, and M. G. Pecht,"Surface Insulation Resistance of Conformally Coated Printed Circuit Boards Processed With No-Clean Flux", IEEE transactions on electronics packaging manufacturing, vol. 9, no. 3, pp. 217–223, 2006.

[2] IPC-HDBK-830,"Guidelines for design, selection and application of conformal coatings", 2002.

[3] J. J. Licari, Coating Materials for Electronic Applications, 1st ed. Norwich, NY: Noyes Publications, 2003, pp. 2.

[4] electrolube.com, 'Resins for potting and encapsulation in the electronics and electrical industries', Available: https://www.electrolube.com/technical-articles/resins-for-potting-and-encapsulation/ [Accessed: 25-July-2018]

[5] M. Tencer, J-S. Moss, "Humidity Management of Outdoor Electronic Equipment: Methods Pitfalls and Recommendations", IEEE Trans. Components and Packaging Tech., vol. 25, no. 1, pp. 66-72, 2002.

[6] M. M. Rafique, P. Gandhidasan, H. M. S. Bahaidarah, "Liquid desiccant materials and dehumidifiers – A review", Renewable and sustainable energy reviews, vol. 56, pp. 179-195, 2016.

[7] M. Sultan, I. I. El-Sharkawy, T. Miyazaki, B. B. Saha, S. Koyama, " An overview of solid desiccant dehumidification and air conditioning systems," Renewable and Sustainable Energy Reviews, Vol. 46, pp. 16–29, 2015.

[8] M. Tencer, "Moisture Ingress into Non hermetic Enclosures and Packages.A Quasi-Steady State Model for Diffusion and Attenuation of Ambient Humidity Variations", Electronic components and technology conference, pp. 196–209, 1994.

[9] I. Belov, J. Ryden, J. Lindeblom, Y. Zhang, T. Hansson, F. Bergner, and P. Leisner, "Application of CFD Modelling for Energy Efficient Humidity Management of an Electronics Enclosure in Storage under Severe Climatic Conditions," EuroSimE, p. 1-8, 21-23 April 2008.

[10] I. Belov, M. Lindgren, J. Ryden, Z. Alavizadeh, P. Leisner, "CFD assisted design evaluation and experimental verification of a logic controlled local PCB heater for humidity management in electronics enclosure," 11th International Thermal, Mechanical and Multi-Physics Simulation, and Experiments in Microelectronics and Microsystems (EuroSimE), 2010.

[11] D. Anastaselos, I. Theodoridou, A. M. Papadopoulos, M. Hegger, "Integrated evaluation of radiative heating systems for residential buildings", Energy, vol. 6, no. 7, pp. 4207-4215, July 2011.

[12] B. W. Olesen, "Comparative Experimental Study of Performance of Radiant Floor-Heating Systems and a Wall Panel Heating System Under Dynamic Conditions", Transactions-American society of heating refrigerating and air-conditioning engineers, vol. 100, no. 1, pp. 1011-1023, 1994.

[13] Sensirion, Application Note Dew-point calculation, pp.1-3, Available : http://irtfweb.ifa.hawaii.edu/~tcs3/tcs3/Misc/Dewpoint_Calculation_Humidity_Sensor_E.pdf [Accessed : 03-April-2019]

[14] Y. A. Cengel, A. J. Ghajar, "Heat and Mass Transfer: Fundamentals and Applications", McGraw-Hill, 2015.

[15] K. Stephan, "Heat Transfer in condensation and boiling", Springer-Verlag Berlin Heidelberg, 1992.

[16] B.J Huang, C.J. Chin, C.L. Duang, "A design method of thermoelectric cooler", International Journal of Refrigeration-revue Internationale Du Froid, vol. 23, no. 3, pp. 208-218, 2000.

[17] K. Chen, S.B. Gwilliam, "An analysis of the heat transfer rate and efficiency of TE (thermoelectric) cooling systems", International Journal of energy research, vol. 20, no. 5, pp. 399-417, 1996.

[18] J.G. Vian, D. Astrain, M. Dominguez, "Numerical modelling and a design of a thermoelectric dehumidifier", Applied thermal engineering, vol. 22, no. 4, pp. 407-422, 2002.

[19] Y. Yao, Y. Sun, D. Sun, C. Sang, M. Sun, L. Shen, H. Chen, "Optimization design and experimental study of thermoelectric dehumidifier", Applied thermal engineering, vol. 123, pp. 820-829, 2017.

[20] B. Gido, E. Friedler, D.M. Broday, "Assessment of atmospheric moisture harvesting by direct cooling", Applied thermal engineering, vol. 182, pp. 156-162, 2016.

[21] D. Milani, A. Abbas, A. Vassallo, M. Chiesa, D.A. Bakri, "Evaluation of using thermoelectric coolers in a dehumidification system to generate freshwater from ambient air", Chemical engineering sciences, vol. 66, no. 12, pp. 2491-2501, 2011.

[22] wikipedia.org, 'Thermoelectric cooling', By michbich - own creation, CC BY 3.0, Available: https://commons.wikimedia.org/w/index.php?curid=9076557 [Accessed: 8-August-2018]

[23] V. Vakiloroaya, B. Samali, A. Fakhar, "A review of different strategies for HVAC energy saving", Energy conversion and management, Vol. 77, pp. 738-754, 2014

[24] L. Z. Zhang, "Energy performance of independent air dehumidification systems with energy recovery measures", Energy, Vol. 31, pp. 8-9, 2006

[25] C. Sease, "The Development of the Humidity Control Module at Field Museum", Journal of the American institute for conservation, Vol. 30, Issue 2, pp. 187-196, 1991.

[26] X. J. Zhang, C. V. Yu, S. Li, Y. M. Zheng, F. Xiao, "A museum storeroom air-conditioning system employing the temperature and humidity independent control device in the cooling coil", Applied thermal engineering, Vol. 31, Issue 17-18, pp. 3653-3657, 2011.

[27] P. Mazzei, F. Minichiello, D. Palma, "HVAC dehumidification systems for thermal comfort: a critical review", Applied thermal engineering, Vol. 25, issue 5-6, pp. 677-707, 2005

[28] G. Angrisani, A. Capozzoli, F. Minichiello, "Desiccant wheel regenerated by thermal energy from a microcogenerator: Experimental assessment of the performances", Applied energy, Vol. 88, issue 4, pp. 1354-1365, 2011

[29] P. Stabat, D. Marchio, "Heat-and-mass transfers modelled for rotary desiccant dehumidifiers", Applied energy, Vol. 85, issue 2-3, pp. 128-142, 2008

[30] C. S. Kim, J. G. Lee, J. H. Cho, D. Y. Kim, T. B. Seo, "Experimental study of humidity control methods in a light-emitting diode (LED) lighting device", Journal of mechanical science and technology, Vol. 29, issue 6, pp. 2501-2508, 2015

[31] V. Narayanaswamy, "A review of thermal and humidity management needs and feasible solutions for next generation subsea electric systems", Underwater technology, Vol. 32, issue 2, pp. 129-143, 2014

[32] grundfos.com, 'UPM3 OEM circulator pump for HVAC systems', Available: https://www.grundfos.com/products/find-product/upm3.html#brochures. [Accessed: 19-July-2018]

[33] wilo.com, 'Wilo-Stratos PICO', Available:http://productfinder.wilo.com/com/en/c00000016000391ce00020023/product.html#tab=3. [Accessed: 19-July-2018]

Chapter 4

Materials and methods

4.1 Materials in electronics

This sections describes the materials, test boards, enclosures and experimental methods used for investigations presented in the appended papers. More detailed discussion on specific materials and methods for each investigation can be found in the appended papers.

4.1.1 Hygroscopic contamination-Sodium chloride

Sodium chloride at $15.6\mu g/cm^2$ was used as contamination in the investigation of impedance change during humidity accumulation in chapter. As per IPC J-STD-001D standard, the maximum allowable surface contamination level is $1.56\mu g/cm^2$ sodium chloride equivalent for soldered electrical and electronic assemblies. A ten times higher contamination level was used for better sensitivity of the measurements.

4.1.2 SIR PCBs

The SIR PCBs used to study degradation of impedance due to humidity accumulation in chapter 7 is shown in figure 4.1. The FR-4 board was made in accordance with IPC-4101/21. The thickness of the PCB was 1.6mm. The SIR pattern had a hot-air solder levelled (HASL) finish (Sn/Ag/Cu) solder alloy. The dimensions of the SIR pattern were 25mm x 13mm with a pitch distance of 0.3mm. The comb pattern had 21 pairs of electrodes with an overlap of 10.8mm each.

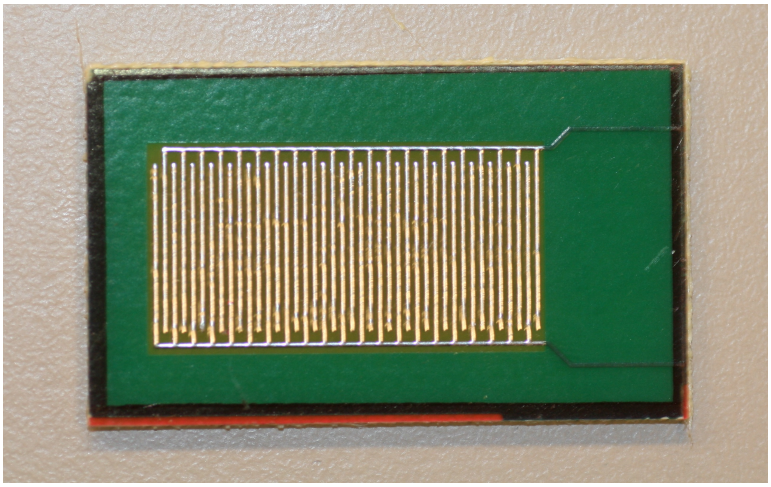

Figure 4.1: SIR PCB used to study impedance degradation with humidity

4.1.3 Electronic enclosures

The enclosures used for the experiments in chapter 5 were made of polycarbonate. Each of the enclosures had dimensions of 170mm x 140mm x 95mm and thickness of 3.3mm. The ingress protection (IP) rating of the enclosures was IP 66/67. The experimental set-up was made by joining two similar enclosures back to back.

The enclosures used for experiments described in chapter 7 were made of aluminium. The external dimensions of the enclosure was 263mm x 162mm x 91mm. Thickness of the walls of the enclosure was 4mm. The enclosures had an ingress protection rating of IP 66/67/68.

4.2 Climatic testing

The experimental works described in chapters 5 and 7 were conducted in controlled climate inside an ESPEC SH-641 environment chamber. The operational range for temperature and humidity were $-40^oCto150^oC$ and 30% to 95% RH, respectively. The accuracy for temperature and humidity control were $\pm 0.5^oC$ and $\pm 3.0\%$ RH, respectively.

Temperature and humidity sensors were placed at different locations inside the environment chamber and enclosures. The temperature sensors used were PT1000 type resistance temperature detectors (RTD) with an accuracy of $\pm 0.6^oC$. The humidity sensors used were HIH 4021 from Honeywell with an accuracy of 3.5% RH. The sensed temperature and humidity were logged using Keithley Model 2700 data acquisition system. The sampling rate of the data varied for different experiments but, the maximum sampling interval used was 2 min.

4.3 Software packages used

The circuit simulations in chapter 9 were done using Cadence Orcad Capture version 16.6. The CFD simulations in chapter 5 were done using COMSOL Multiphysics version 5.3.

4.4 Impedance measurements

Impedance measurements of the contaminated SIR PCBs in chapters 7 and 8 were done using a Biologic VSP series instrument. The impedance measurements were made at a fixed frequency of 20KHz. The instrument had a 20V compliance voltage with adjustable range (upper limits -20V and +20V). The current resolution of the instrument was 760pA.

Chapter 5

Humidity control in electronic enclosures by forced condensation

Abstract

The purpose of this work is to study humidity control by forced condensation in electronic enclosures. Humidity control using thermoelectric dehumidifiers has attracted lot of attention. There is no literature on application of condensation based dehumidifiers for electronics applications. In this paper, a two-chamber design with warm and cold chambers was used as a model system to investigate the condensation effects. Both chambers were connected by an opening and a cooling element was placed in the cold chamber. The two chambers also had openings to the ambient. The two-chamber setup helped to control outflow and ingress for each chamber separately by changing the size of respective openings. The experimental setup also simulated a situation where the warm chamber was assumed to house electronics and cold chamber contained a condensing surface. The size of chamber-to-chamber, chamber-to-ambient openings and cooling temperature are varied to study their effects on RH inside both chambers. A computational fluid dynamics (CFD) model of the experimental set-up was made and used to study the effect of cooler surface area and volume of the chambers on natural convection between the enclosures and between enclosures and ambient. The RH inside the two chambers was found to depend on the combination of openings used between the chambers and their respective openings to the ambient.

Keywords: Humidity, Electronic enclosure, Reliability, Condensation, Dehumidification.

To be submitted as: **S. Joshy**, R. Ambat, "Humidity control in electronic enclosures by forced condensation".

5.1 Introduction

The application of electronics in high humidity environments has made more frequent failures due to humidity. Electronics are used in high humidity environments like offshore wind turbines, wearable devices etc and uncontrolled environments like automobiles. Trend towards miniaturisation and development of high efficiency, low-power dissipating electronics has added to the complexity of the problem of humidity related failures in electronics. Advent of low $R_{DS(on)}$ and low switching charge MOSFETs based on SiC and GaN would reduce the overall heat dissipated in power electronics, thus favouring lower temperatures and high humidity inside power converters which use these technologies.

The main failure modes in electronics due to humidity are high leakage currents and electrochemical migration(ECM)[1]. High humidity can result in electronic enclosures due to diffusion, release of absorbed humidity from the walls of the enclosure[2] and under cycling conditions of ambient temperature and power dissipation[3]. High humidity can condense to form liquid water on the printed circuit board assembly (PCBA) when the temperature of the surface equals dew point temperature. Presence of ionic contamination from PCBA manufacturing process and atmospheric dust causes the water layer formed to be conductive leading to leakage currents and ECM. The residues on PCBA due to manufacturing process and atmospheric dust[4] could also be hygroscopic, leading to water layer formation at RH significantly below the saturated level. No-clean fluxes commonly used for electronic component assembly contain weak-organic acids (WOA) as activators which are hygroscopic and ionic[5].

The most commonly used technique to prevent humidity-related failures in electronics is by application of a conformal coating. According to the Association Connecting Electronics Industries (IPC), the functions of a conformal coating as regards to humidity are: to inhibit current leakage and short circuit due to humidity and contamination from service environment and inhibit corrosion[6]. There are various types of conformal coatings available in the market like acrylic, epoxy, silicone, polyurethane, paralyne etc. Literature shows that use of conformal coatings improve reliability if the level of contamination on PCB before coating is minimised [7]. Conformal coatings prevent humidity-related failures by delaying the diffusive transport of water molecules to the PCB surface[7] and also by preventing the formation of a conductive water layer[8]. No-clean solder fluxes leave behind ionic contamination which degrade the performance of conformal coatings [7][9]. Therefore, a cleaning step is necessary in the PCBA manufacturing process to limit the degradation of conformal coating performance.

Another way to prevent humidity-related problems in electronics is to keep the relative humidity (RH) inside the enclosure below a safe limit such as 60%. Industrial technologies for dehumidification can be broadly classified as desiccant based and cooling based. In the former type, the excess humidity is removed by absorption and adsorption into specific materials called desiccants. Desiccants could be in liquid [10] or solid [11] state as applied for heating, ventilation, and air-conditioning application. Desiccant based dehumidification systems need rotary devices to expose the desiccants to process and regeneration air-streams alternatively. If desiccants are used for humidity control in ECUs, it would require the use of rotating components which would lower the overall reliability of the electronic system, when

the main intent was reliability improvement. Cooling can be achieved either by vapour-compression cycle or by thermoelectric coolers(TEC). TECs are particularly advantageous for electronic applications due to their direct use of electric power for cooling, small size, quite operation, lack of moving parts and low power consumption. TECs are employed for cooling of electronics, but there is a lack of literature on the use of TEC based dehumidifiers for electronic applications. In certain specialised applications like motors with integrated drive electronics for pumping cold water, condensing surfaces are inherently present which can be utilised for dehumidification of the electronics by connecting the electronic enclosure with the suitable surface through openings. The two-chamber setup presented in this work also simulates an application like a pump used to circulate cold water where motor electronics is housed in a separate chamber compared to the impeller which pumps the water.

This study used a two chamber experimental setup to study condensation based humidity control in electronic enclosures. The chambers were connected to each other and to ambient by openings. The two-chamber setup with openings helped to achieve different transient mass transport rates for water vapour into and out of each chamber controlled by the size of the respective opening, thus enabling to study the effect of opening sizes on humidity profiles inside an electronic enclosure. The two-chamber setup also helped to isolate the net flows into and out of each chamber to specific openings. The cold chamber was assumed to house the condensing surface and warm chamber, the electronics. The size of the openings on the chambers was varied to study their effect on RH inside both chambers. Effect of cooling element temperature on RH inside both the chambers was studied. A CFD model of the two chamber setup was made and a parametric study of cooler surface area and chamber volumes were performed. The RH inside the chambers was observed to depend on the combination of opening sizes used.

5.2 Materials and methods

The two-chamber setup consists of two polycarbonate enclosures of dimensions 170mm X 140mm X 95mm connected back to back. Each of the enclosures are IP 66/67 rated. Openings were made on the common wall of the enclosures and also to the ambient. Figure 5.1 and 5.2 shows a block diagram and picture of the two-chamber experimental setup.

The experimental setup was placed inside an ESPEC SH-641 environment chamber. The chamber RH and temperature were 97% and 25^oC respectively. The cold chamber had a metal surface of circular cross section through which cold water was circulated. This cold surface was the condensing and dehumidifying element. Cold water at 10^oC was circulated using a thermostat. A pair of temperature and RH sensors were placed in air at the centre of each chamber. The temperature sensors used were of PT1000 type resistive temperature sensors. The RH sensor used was HIH-4021 made by Honeywell. The data from the sensors were logged using a Keithley 2700 data acquisition system.

The experimental setup was allowed to equilibrate in RH and temperature to the environment chamber climate. The experiment starts when the RH inside the chambers reach 90% and water at 10^oC was circulated through the metal plate inside the cold chamber. The RH inside the cold and warm chambers reduced until steady state conditions are achieved. The experiment was done for different values of the

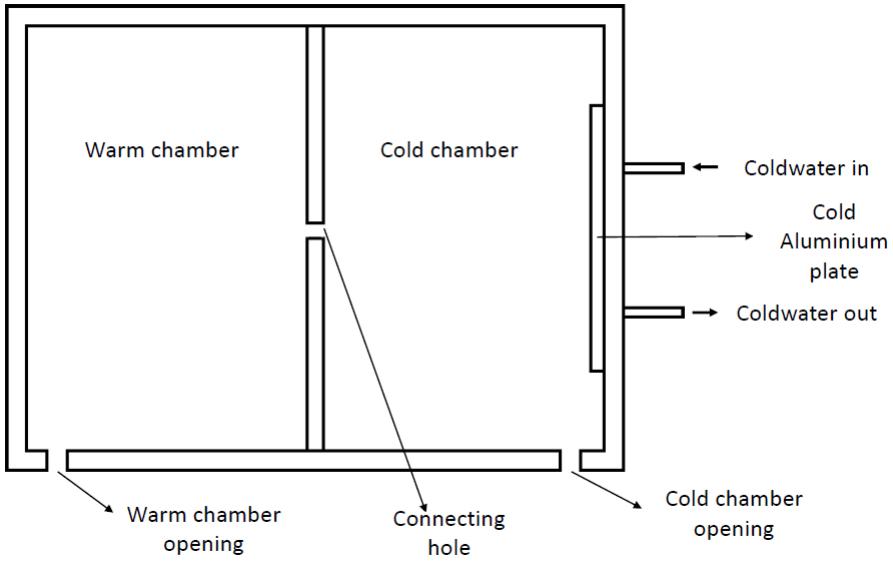

Figure 5.1: Block diagram of the experimental set-up

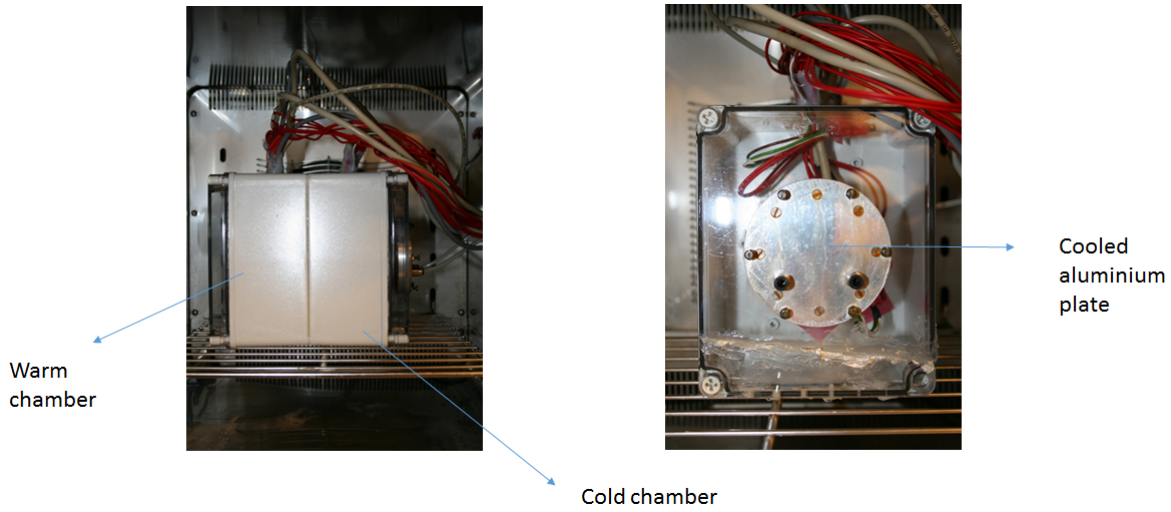

Figure 5.2: Experimental set-up placed inside the climatic chamber with required sensor connections

openings and cooling temperature. The opening sizes used were 1mm, 2mm, 3mm, 4mm, 5mm and 6mm. The cooling temperatures studied were such that the ambient dew-point temperature was always greater than the cold surface temperatures. This ensured that condensation occurred on the cold plate. Table 5.1 gives the values of cooling temperatures studied. COMSOL Multiphysics version 5.3 was used to make the CFD model.

5.3 Results

Cooling of the cold plate results in natural convection inside the cold and warm chambers. Figure 5.3 shows a CFD simulation of velocity field and the directions of flow of air through the openings of the chambers during steady state using a 2-D

Table 5.1: Cooling temperatures studied

No.	Cold water temperature(^oC)
1	2.5
2	5
3	7.5
4	10
5	12.5
6	15

model. The velocity profile is for a slice that passes through the centre of all the three openings. It was observed that the net flow in the experimental set-up entered through the warm chamber opening, then through the connecting hole to the cold chamber and exited through the cold chamber opening. Steady state concentrations are achieved in the chambers when the net mass transfer of water vapour into and out of each of the chambers is zero.

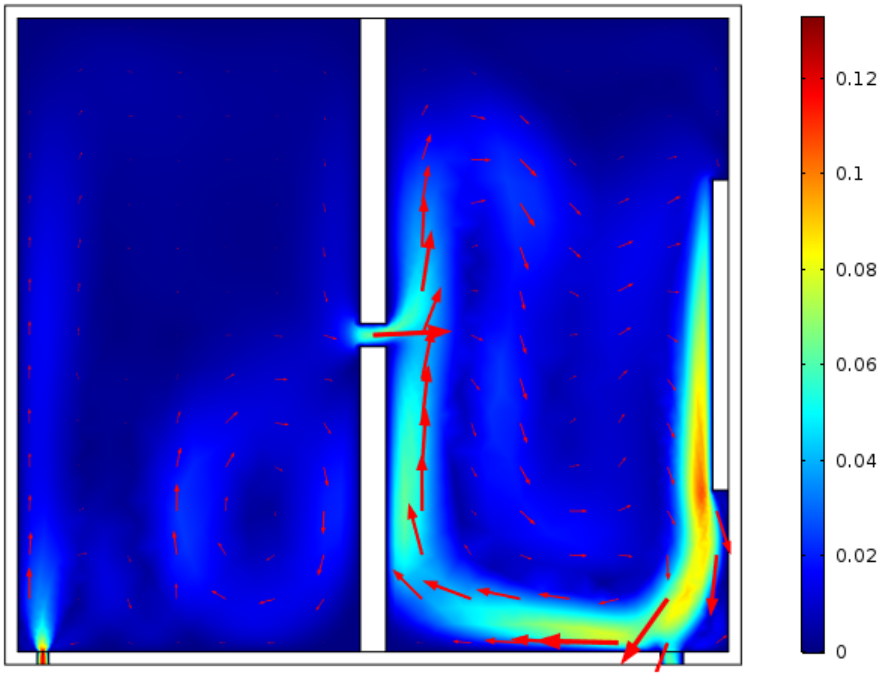

Figure 5.3: Steady state air velocity inside the chambers in m/s

Figures 5.4 shows the typical RH, AH and temperature variations inside the chambers when cold water at 10^oC was circulated inside the cooling plate. The profiles in figure 5.4 are for a hole combination of 6mm each for warm chamber opening, connecting hole and cold chamber openings respectively. Due to the condensing conditions on the cold plate the AH and RH inside the cold chamber decreased below the ambient level to $14.5g/m^3$ and 66% respectively. The warm chamber also experienced a delayed decrease in humidity to AH and RH values of $15.4g/m^3$ and 65% respectively. The temperature inside the cold chamber measured by the sensor decreased by 2^oC due to the effect of cold water circulation, but, the temperature

inside the warm chamber remained the same as the ambient at 25^oC. The temperature measured on the cooling plate was 15^oC. The humidity profiles showed a transient time during which the humidity in both chambers decreased. A flat area in the humidity profiles was observed when mass balance was achieved in both chambers. After this point, the humidity increased over time when the condensing plate surface area was saturated with water droplets. The humidity values presented in the following sections correspond to the flat area of the humidity profiles.

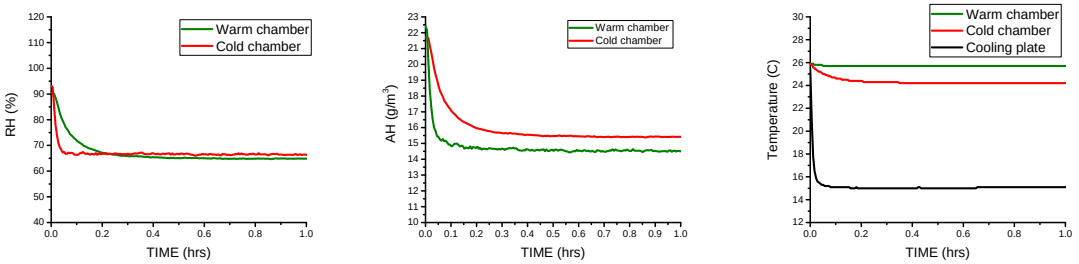

(a) RH profile (b) AH profile (c) Temperature profile

Figure 5.4: RH and AH inside the cold and warm chambers

It was also observed from figure 5.3 that there were two distinct flows observed in both chambers - humidity controlling flow which reduced the RH in each chamber and ingress of humidity whose effect was to increase the RH. In the warm chamber the humidity controlling flow was from the warm to cold chamber through the connecting hole while the ingress was from the ambient through the warm chamber opening. In the cold chamber, the humidity controlling flow was from the bulk of the cold chamber volume to the cold plate. The humidity ingress into the cold chamber was both from ambient through the cold chamber opening and also from warm chamber through the connecting hole.

The following sections analyse the humidity profiles inside both chambers due to the effects of warm chamber opening, connecting hole, cold chamber opening, cooling temperature, cooler area and the chamber volumes.

5.3.1 Effect of cooling temperature

The effect of cooling temperature on humidity profiles in warm and cold chambers is studied for a hole combination of warm chamber opening, connecting hole and cold chamber opening with a size of 6mm. Figure 5.5 shows the steady-state temperatures measured on the cold plate for the different values of circulated cold water temperatures. The cold plate temperatures were higher than the circulated water temperature due to heat loss to the air by convection.

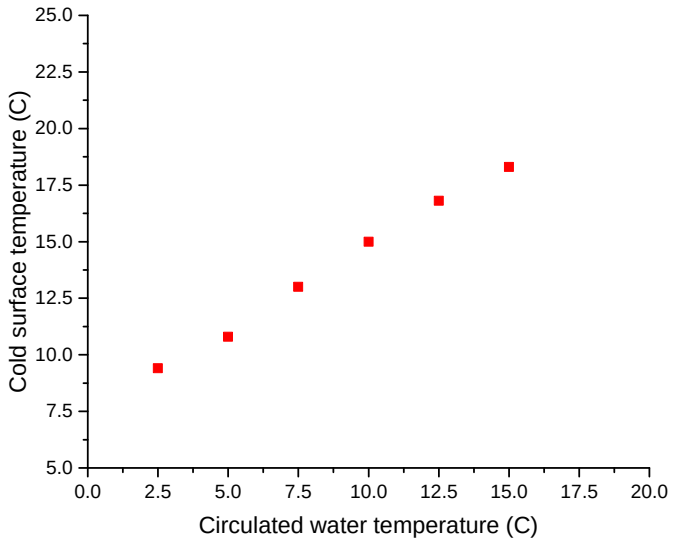

Figure 5.5: Measured cold surface temperature for different temperatures of circulated water

Figure 5.6 shows the results of CFD simulation for airflow from warm to cold chamber with different cold surface temperatures. The cold surface temperatures used as input to the CFD simulation were the experimentally determined values shown in figure 5.5. When the temperature on the cold surface decreases, the natural convection flow from warm to cold chamber increased as shown in figure 5.6.

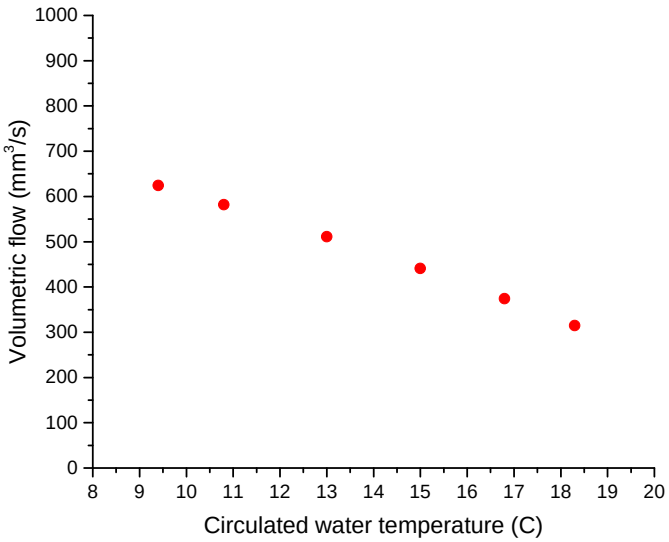

Figure 5.6: CFD simulation results of steady state volumetric flow of air from warm to cold chamber for different cold surface temperatures

Figure 5.7 shows the RH and AH inside the warm and cold chambers for different temperatures of circulated cold water.

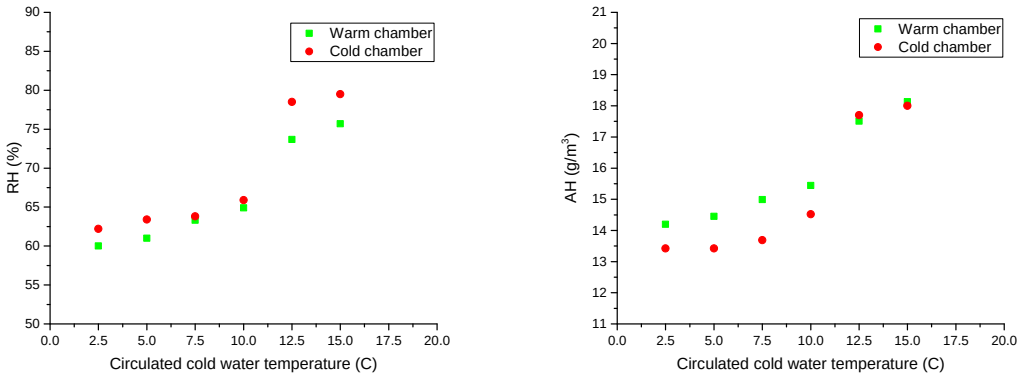

(a) RH profile

(b) AH profile

Figure 5.7: RH and AH inside the cold and warm chambers for different temperatures of circulated cold water

For a cold plate temperature of 9.4^oC the RH in the cold and warm chambers were 62.2% and 60% respectively. The RH in the cold chamber was higher than in the warm chamber for this temperature. But, the AH in the warm chamber was higher than the cold chamber signifying transport of humidity from warm to cold chamber. The RH in the cold and warm chamber increased to 79.5% and 75.7% with increase in cold surface temperature from 9.4^oC to 18.3^oC. The RH in the cold and warm chambers showed a jump of 10% and 11.4% respectively for change in cold plate temperature of 15^oC to 16.8^oC. For other temperatures the change in RH in both chambers were much less.

5.3.2 Effect of cold chamber opening

The effect of cold chamber opening on humidity profile inside the chambers is studied by varying the cold chamber opening diameter from 1mm to 6mm in intervals of 1mm. The warm chamber opening and the connecting hole are fixed at 6mm diameter. Figure 5.8 shows the experimentally measured RH and AH values.

It was observed from figure 5.8a that the RH in the cold chamber was 51.4% for 1mm diameter opening and it increased to 67.1% for 6mm diameter opening. Similar increase was found for cold chamber AH. The volumetric flow of air through the connecting hole for different cold chamber opening sizes is shown in figure 5.9. It was observed that humid airflow rates into cold chamber from the warm chamber increased with higher cold chamber opening sizes. The increase in cold chamber humidity with increasing opening size was due to the higher ingress of humidity from the warm chamber to cold chamber due to higher flow rates.

It was observed from figure 5.9 that the volumetric flow rate of air from the warm to cold chamber increases with larger diameter of the cold chamber opening. Since the warm chamber AH is higher than cold chamber AH, this flow from the warm chamber into the cold chamber contributes to increasing the AH in cold chamber. This also explained why the RH and AH in the warm chamber decreased with increasing cold chamber opening diameters. For 1mm diameter opening on the cold chamber the volumetric flow from warm to cold chamber was almost negligible at 1.38 mm^3/s. This resulted in steady state RH in the warm chamber at 85%.

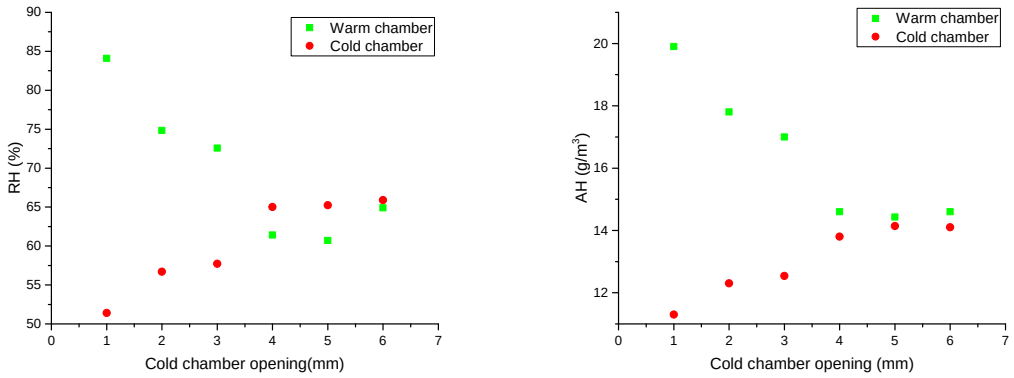

(a) RH profile

(b) AH profile

Figure 5.8: RH and AH inside the cold and warm chambers for different cold chamber openings

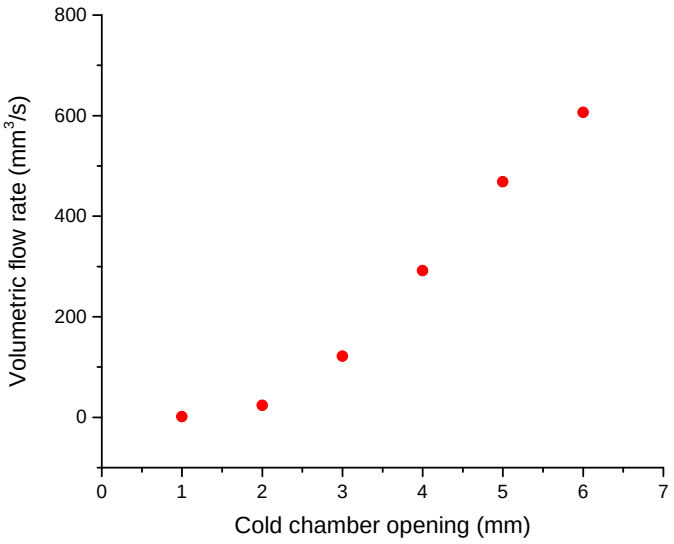

Figure 5.9: Steady state volumetric flow of air from warm to cold chamber for different sizes of cold chamber opening

With increase in the cold chamber opening diameter and higher volumetric flow through the connecting hole, the humidity in the warm chamber reduced due to more humidity removal from warm to cold chamber. The steady state RH in the warm chamber was found to be 61.5% for 6mm diameter cold chamber opening. It was also observed that the cold and warm chamber humidities did not vary for cold chamber opening sizes greater than 4mm.

5.3.3 Effect of connecting hole

The effect of connecting hole on humidity profile inside the chambers is studied by varying the connecting hole diameter from 1mm to 6mm in intervals of 1mm. The warm chamber opening and the cold chamber opening are fixed at 6mm diameter.

Figure 5.10 shows the experimentally measured RH and AH values.

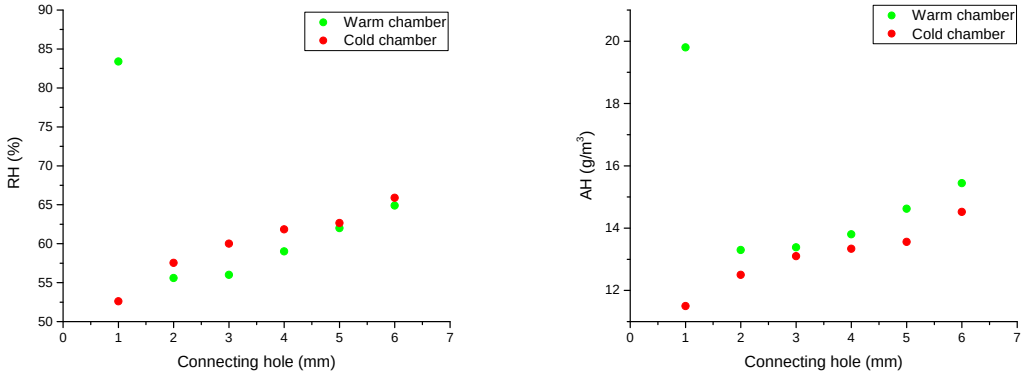

(a) RH profile (b) AH profile

Figure 5.10: RH and AH inside the cold and warm chambers for different sizes of connecting hole

Figure 5.11 shows the volumetric flow rate of air through the connecting hole at steady state. It was observed that the flow rate shows an increase from $0.65mm^3/s$ to $606mm^3/s$ for a change in connecting hole diameter from 1mm to 6mm.

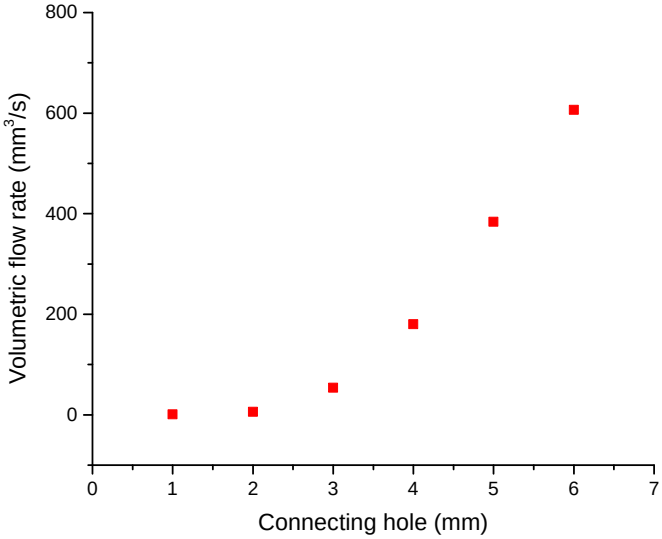

Figure 5.11: Steady state volumetric flow of air from warm to cold chamber for different sizes of connecting hole

It was observed from figure 5.10a that humidity inside the warm chamber did not reduce much from the ambient RH for connecting hole size of 1mm, even though the cold chamber RH is low at 52.6%. With increase in connecting hole size, the steady state humidity in the warm chamber increased from 55.6% to 65% for hole size variation from 2mm to 6mm. The increase in connecting hole size from 1mm to 6mm also caused an increase in cold chamber RH from 52.6% to 66% as shown by figure 5.11.

5.3.4 Effect of Warm chamber opening

To study the effect of warm chamber opening on the humidity profiles inside the chambers, the cold chamber opening and connecting hole sizes are kept fixed at 6mm. The warm chamber opening diameter is varied from 1mm to 6mm with intervals of 1mm. Figure 5.12 shows the RH and AH profiles in the warm and cold chambers for different diameterss of the warm chamber opening. It was observed that the RH and AH levels in both chambers increased with increasing size of the warm chamber opening.

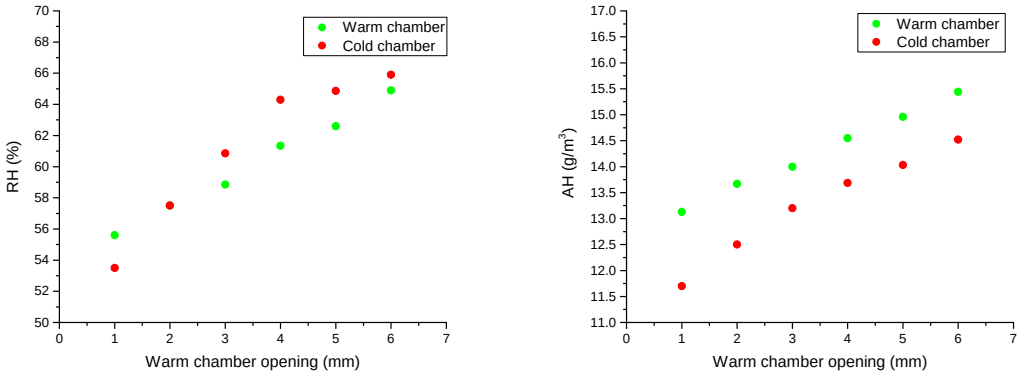

(a) RH profile

(b) AH profile

Figure 5.12: RH and AH inside the cold and warm chambers for different sizes of warm chamber opening

The warm chamber RH showed an increase from 55.6% to 66% where as the cold chamber RH increased from 53.5% to 66% for change in warm chamber opening from 1mm to 6mm. It was also observed that humidity control still occurred in the warm chamber for warm chamber opening size of 1mm in contrast to the results with cold chamber opening and connecting hole of 1mm. The corresponding increase in volumetric flow rate from warm to cold chamber for change in warm chamber opening size from 1mm to 6mm was $1.23mm^3/s$ to $606mm^3/s$ as shown in figure 5.13. In spite of this increase in volumetric flow from warm to cold chamber, the humidity inside the warm chamber increased with higher warm chamber opening size.

5.3.5 Effect of opening sizes on transient times

Transient time is defined as the time from the start of applying cooling to the instant when the RH inside the warm chamber approaches within 3.5% of the final steady state value. Figures 5.14a, 5.14b and 5.14c show the transient times for humidity control in the warm chamber for different sizes of cold chamber opening, connecting hole and warm chamber opening. It was observed that transient times reduced with increasing opening sizes due to higher volumetric flow rates as shown before in figures 5.9, 5.11 and 5.13. The lower values of transient times for cold chamber opening and connecting hole for 1mm opening size was due to absence of humidity control for this opening size. Where as, for warm chamber opening size of 1mm showed a transient time of 10hrs.

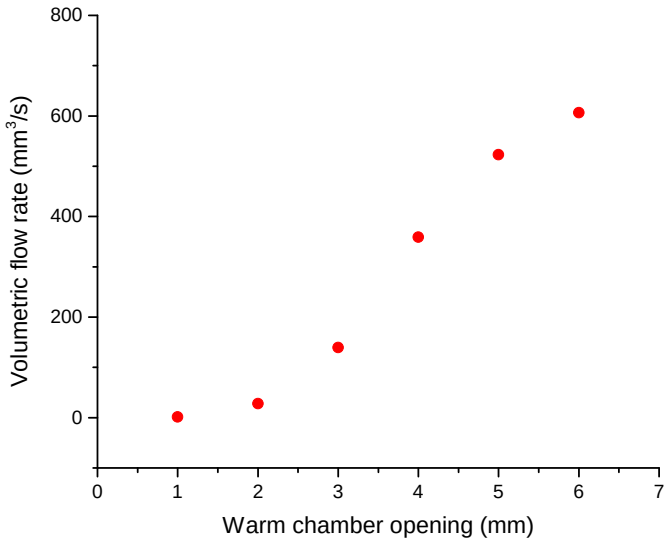

Figure 5.13: Steady state volumetric flow of air from warm to cold chamber for different sizes of warm chamber opening

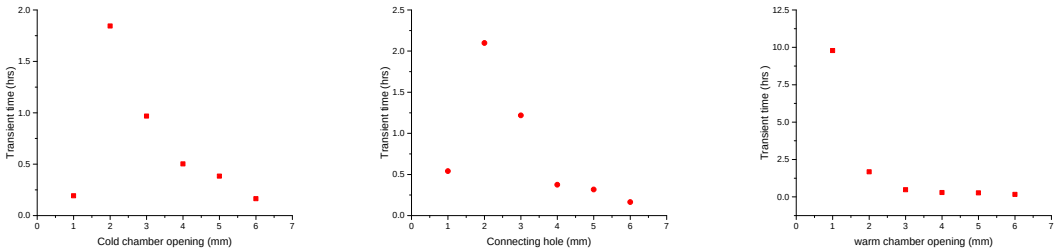

(a) Transient time for cold chamber opening sizes

(b) Transient time for connecting hole sizes

(c) Transient time for warm chamber opening sizes

Figure 5.14: Transient time for RH inside warm chamber for different opening sizes

5.3.6 Effects of cooler surface area and cold chamber volume

A parametric study of steady state airflow velocity from the warm to cold chamber was done to find the effect of cooling surface area and cold chamaber volume on condensation humidity control. The cooling surface radius was varied from 10mm to 50mm. The cold chamber volume was varied by using different lengths of the cold chamber keeping other dimensions fixed. Figure 5.15a shows the effect of cooling surface radius and figure 5.15b shows the effect of cold chamber volume on the airflow velocity from warm to cold chamber.

Figure 5.15a showed that airflow rate into the cold chamber increased with higher cooler surface area. Also figure 5.15b showed that volumetric flow rate into the cold chamber increased for a smaller size. The results also suggest that a higher airflow velocity into the cold chamber can be achieved not just by increasing the opening sizes but also by a higher condensing surface area and also by a smaller cold chamber volume. It would also be preferable to use a smaller opening size at the expense of

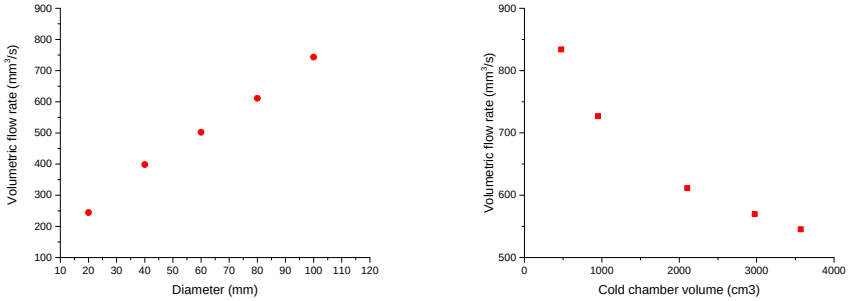

(a) Effect of cooling surface area

(b) Effect of cold chamber volume

Figure 5.15: Simulation of variation in volumetric flow rate from warm to cold chamber due to cooling surface area and cold chamber volume

higher condensing surface area to minimise the ingress of humid ambient air into both the chambers.

5.3.7 Discussion

The RH values in the warm and cold chambers decreased with lower cold plate temperatures due to lower values of saturated humidity at colder temperatures. Lower cold plate temperatures causes more humidity to condense on the cold plate thus lowering the AH and RH inside the cold chamber as shown in figure 5.7. A lower cold plate temperature also increased the air flow rate from the warm to cold chamber as shown in figure 5.6. This lead to a lower steady state RH and AH in warm chamber for lower cold plate temperature.

It was observed that the effect of opening sizes was to control the airflow rates and thus affect the steady state humidity and transient times. The dominant effect of cold chamber opening was to control the warm chamber to cold chamber flow. With increase in the cold chamber opening diameter and consequently higher volumetric flow through the connecting hole as shown in figure 5.9, the humidity in the warm chamber reduced due to higher humidity removal from warm to cold chamber. But, the cold chamber RH increased due to higher ingress into the cold chamber from the warm chamber. For 1mm opening size for cold chamber opening, humidity control in warm chamber was totally absent due to the low humidity control flow into the cold chamber compared to the high ingress from ambient through the 6mm warm chamber opening.

Similar to the case of 1mm cold chamber opening, 1mm connecting hole caused minimal decrease in warm chamber RH compared to ambient. This was because the humidity controlling flow through the connecting hole into the cold chamber is very low with 1mm connecting hole as shown in figure 11. The ingress from the ambient through the 6mm warm chamber hole was high compared to the humidity flow rate from warm to cold chamber through the 1mm hole. The high ingress flow rates compared to the humidity controlling flow results in high humidity in the warm chamber for 1mm connecting hole. The steady state RH in warm chamber decreased for larger sizes of the connecting hole because of the higher humidity control flow into the cold chamber. As the connecting hole size increases, the higher humidity

control flow also caused a corresponding increase in the ingress rates into the warm chamber. This increased the steady state humidity in the warm chamber as shown in figure 5.10a. The increase in connecting hole size from 1mm to 6mm also caused an increase in cold chamber RH due to the higher humid air ingress into the cold chamber from the warm chamber as shown by figure 5.10a.

The primary effect of warm chamber opening was to control the ingress of humidity from ambient to warm chamber as observed from figure 5.12a. The steady state values of RH in warm chamber increased with larger warm chamber openings due to higher ingress from ambient. The cold chamber humidity showed a corresponding increase due to the higher transport of humidity from warm to cold chamber with higher hole sizes as signified by the volumetric flow rates shown in figure 5.13. In contrast to the cold chamber opening and connecting hole, 1mm warm chamber opening still allowed the humidity in warm chamber to reduce but at a lower rate as shown in figure 5.14c.

To achieve low steady state RH in the warm chamber the preferable sizes for the openings would be small size for both warm chamber opening and connecting hole and larger sizes for cold chamber opening as observed from figures 5.12a, 5.10a and 5.8a respectively. The size of the openings would also be determined by considerations for energy spent in keeping the cold plate at a specific temperature. As more water condenses on the cold plate due to ingress from the ambient, more energy would have to be spent in keeping the plate cool and hence, humidity control. This becomes critical for battery operated electronics using peltier elements for humidity control[12] where conserving the battery for the primary functionality would be critical than auxiliary considerations like humidity control.

Transient times for RH reduction in warm chamber was in the order of hours to few minutes for different sizes of the three openings investigated. From figures 5.14a, 5.14b and 5.14c it was seen that the transient times decreased with increasing opening sizes for cold chamber opening, connecting hole and warm chamber opening respectively. This agrees with the simulation results of volumetric flow rates with different diameters of the three openings where, the flow rates increased with increasing hole sizes. The higher flow rates with larger opening sizes caused the transient times to be lower. It was also shown by simulation that cold plate surface area and cold chamber volume influenced the steady state RH and transient times by affecting the volumetric flow rates of air from warm to cold chamber. The effect of these parameters on humidity inside the chambers itself could not be studied because of the complexity of the geometry of the experimental setup to be used for a time-dependent moisture transport simulation.

For an electronic enclosure with a single chamber, the internal humidity profiles due to condensation humidity control would be similar to that shown for cold chamber in figure 5.4a. The transient time for humidity control was in the order of few minutes as shown in the plot of cold chamber RH in figure 5.4a. The steady state RH values with a single chamber would depend on the size of the opening and the rate at which condensed water gets removed out of the enclosure. Higher size of the opening would cause higher RH due to ingress from the ambient similar to that shown for cold chamber RH in figure 5.8a. Non removal of condensed water would cause gradual increase of RH inside the enclosure. Simplest method to remove condensed water is to let the condensed drops slide off the cooling plate by gravity and out of the enclosure.

In many applications, electronics is integrated into the application itself for eg., a motor for pumping cold water in HVAC[13][14]. The motor control electronics is kept in a separate compartment as compared to the motor itself to protect from condensing conditions and liquid water. In such cases, a controlled opening could be made between the motor compartment and the electronics enclosure to permit humidity control to occur inside the electronic enclosure, thus protecting the electronics. The humidity profiles inside the motor compartment and electronic enclosure would be similar to that of the cold chamber and warm chamber discussed in this work.

The humidity control presented for the two-chamber setup can also be done in a switched manner by application of current pulses to the TEC[15][16]. This would help save energy spent in humidity control and also improve the coefficient of performance(COP) of the TEC.

There is a lack of literataure related to forced condensation based dehumidification in electronic applications. Tencer and Moss[17] discusses humidity control by heating, desiccants, coating and potting. Kim et. al[18] and Belov et. al.[19] investigated heating as a method for humidity control in electronics. Condensation based humidity control investigated in this work was able to dehumidify the air inside the warm chamber to less than RH of 70% for most of the sizes of the three openings. RH of 70% falls under safe humidity levels to prevent formation of monolayers of water leading to failures in electronics[17]. The humidity control method investigated in this work is also reliable than the desiccant based methods[10][11] due to lack of moving parts and low energy consumption. Condensation based methods are also better when compared to conformal coatings because a cleaning step can be avoided in the electronic manufacturing process. Also, condensation based humidity control does not face issues like conformal coatings which are also susceptible to cracking due to effect of ambient temperature and pressure[20].

5.3.8 Conclusion

The main conclusions from this work can be summarised below :

1. Condensation based humidity control was able to reduce the RH inside both chambers of the two chamber experimental setup to humidity levels less conducive for humidity related failures in electronics.

2. Effect of cooling plate temperature was to determine the saturated humidity in the chambers. Lower temperature on the cooling plate resulted in lower steady state RH in both cold and warm chambers.

3. Effect of warm chamber opening and connecting hole was to increase the volumetric flow thus resulting in lower transient times. Also, larger warm chamber opening and connecting size resulted in higher steady state RH in warm chamber due to higher ingress from the ambient.

4. Size of cold chamber opening had a dominant effect on the volumetric flow rate from warm to cold chamber. Larger cold chamber openings resulted in lower steady state RH and lower transient times in warm chamber due to larger humidity control flow into the cold chamber.

5. Larger condensing surface area and smaller cold chamber volumes caused a higher flow rate of humid air from warm to cold chamber. For constant values of diameter for the three openings, larger condensing surface area and smaller cold chamber volumes would result in lower steady state RH and transient times in the warm chamber.

By suitable sizing of the opening sizes, cold chamber volume, cooling plate temperature and surface area desired RH and transient times can be achieved for humidity control in electronic enclosures using the two-chamber approach investigated.

5.4 Acknowledgement

This research was conducted as part of the IN SPE project funded by Innovation Fund Denmark and CELCORR(www.celcorr.com). The authors would like to acknowledge the funding and help received from the consortium partners.

Bibliography

[1] D. Minzari, M. S. Jellesen, P. Moller and R. Ambat, " On the electrochemical migration of tin in electronics," Corrosion science, Vol. 53, Issue 10, pp. 3366–3379, 2011.

[2] H. Conseil-Gudla, Z. Staliulionis, M. S. Jellesen, M. Jabbari, J. H. Hattel, R. Ambat, " Humidity build-up in electronic enclosures exposed to constant conditions," IEEE transactions on components packaging and manufacturing technology, vol.7, Issue 3, pp. 412–423, 2017.

[3] H. Conseil, V. C. Gudla, M. S. Jellesen, R. Ambat, Humidity build-up in a typical electronic enclosure exposed to cycling conditions and effect on corrosion reliability, IEEE Transactions on Components, Packaging and Manufacturing Technology, vol. 6, Issue 9, pp. 1379–1388, 2016.

[4] M. Tencer, "Deposition of aerosol ("hygroscopic dust") on electronics – Mechanism and risk," Microelectronics reliability, vol. 48, Issue 8, pp. 584–593, 2008.

[5] V. Verdingovas, M. S. Jellesen, R. Ambat, "Solder Flux Residues and Humidity-Related Failures in Electronics: Relative Effects of Weak Organic Acids used in No-Clean Flux Systems," Journal of electronic materials, vol. 44, Issue 4, pp. 1116–1127, 2015.

[6] IPC-HDBK-830,"Guidelines for design, selection and application of conformal coatings", 2002.

[7] S. Zhan, M. H. Azarian, M. Pecht, "Surface Insulation Resistance of Conformally Coated Printed Circuit Boards Processed with No-Clean Flux", IEEE Transactions on Electronics Packaging Manufacturing, vol. 29, no. 3, pp. 217–223, 2006.

[8] K. Otsuka, Y. Takeo, H. Ishida, "The mechanisms that provide corrosion protection for silicone gel encapsulated chips," IEEE Transactions on Components Hybrids and Manufacturing Technology , Vol. 10, Issue 4, pp.666–671, 1987.

[9] H. Conseil, M. S. Jellesen and R. Ambat, " Contamination profile on typical printed circuit board assemblies vs soldering process," Soldering and Surface Mount Technology, Vol. 26, Issue 4, pp. 194–202 2014.

[10] M. M. Rafique, P. Gandhidasan, H. M. S. Bahaidarah, " Liquid desiccant materials and dehumidifiers – A review," Renewable and Sustainable Energy Reviews, Vol. 56, pp. 179–195, 2016.

[11] M. Sultan, I. I. El-Sharkawy, T. Miyazaki, B. B. Saha, S. Koyama, " An overview of solid desiccant dehumidification and air conditioning systems," Renewable and Sustainable Energy Reviews, Vol. 46, pp. 16–29, 2015.

[12] J. G. Vian, D. Astrain, M. Dominguez, Numerical modelling and a design of a thermoelectric dehumidifier, Applied Thermal Engineering, vol. 22, Issue 4, pp. 407–422, 2002.

[13] grundfos.com, 'UPM3 OEM circulator pump for HVAC systems', Available: https://www.grundfos.com/products/find-product/upm3.html#brochures. [Accessed: 19-July-2018]

[14] wilo.com, 'Wilo-Stratos PICO', Available:http://productfinder.wilo.com/com/en/c00000016000391ce00020023/product.html#tab=3. [Accessed: 19-July-2018]

[15] M. Ma, J. Yu, J. Chen, An investigation on thermoelectric coolers operated with continuous current pulses , Energy conversion and management, vol. 98, pp. 275–281, 2015.

[16] G. J. Snyder, J. P. Fleurial, T. Caillat, Supercooling of Peltier cooler using a current pulse , Journal of applied physics, vol. 92, Issue 3, pp. 1564–1569, 2002.

[17] M. Tencer, J-S. Moss, "Humidity Management of Outdoor Electronic Equipment: Methods Pitfalls and Recommendations", IEEE Trans. Components and Packaging Tech., vol. 25, no. 1, pp. 66-72, 2002.

[18] C. S. Kim, J. G. Lee, J. H. Cho, D. Y. Kim, T. B. Seo, "Experimental study of humidity control methods in a light-emitting diode (LED) lighting device", Journal of Mechanical Science and Technology, vol. 29, no. 6, pp. 2501–2508, June 2015.

[19] I. Belov, M. Lindgren, J. Ryden, Z. Alavizadeh, P. Leisner, "CFD assisted design evaluation and experimental verification of a logic controlled local PCB heater for humidity management in electronics enclosure", 11th International Thermal, Mechanical and Multi-Physics Simulation, and Experiments in Microelectronics and Microsystems (EuroSimE), April 2010.

[20] C. Emersic, R, Lowndes, I. Cotton, S. Rowland, R. Freer, "The effects of pressure and temperature on partial discharge degradation of silicone conformal coatings", IEEE Trans. Dielectr. Electr. Insul, vol. 24, no. 5, pp. 2986-2994, November 2017.

Chapter 6

Humidity transfer from warm to cold

Aim of this work is to study effect of humidity transfer from warm to cold on humidity profiles inside an enclosure. The parameters intended to be studied are warm temperature, cold temperature and connecting hole size. Two connected double-walled glass chambers were used as enclosures for the study. The study showed that the humidity profiles inside the warm chamber depended on the warm temperature, cold temperature the temperature differential and the connecting hole size.

6.1 Materials and methods

The experimental setup consists of two double-walled glass chambers connected to each other. The two chambers are cylindrical in shape with a length of 50mm and 100mm in diameter. The two chambers are dissimilar at the connecting side with the warm chamber side being able to be inserted into the cold chamber, making a sealed ground glass joint. Figure 6.1 shows the two glass chambers.

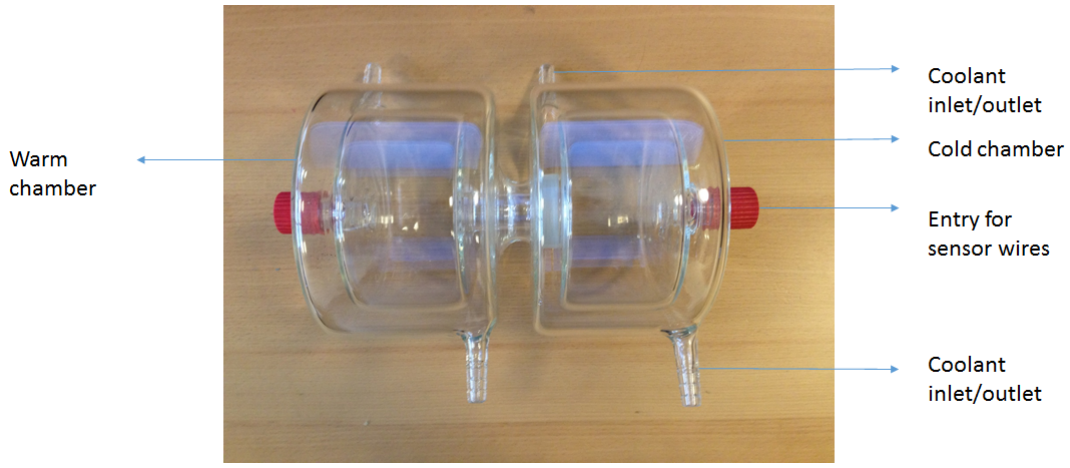

Figure 6.1: Glass enclosures used as warm and cold chambers for the experiment

The warm chamber and cold chambers are circulated with warm and cold water respectively to keep them at uniform temperatures using water thermostats. A temperature and humidity sensor is situated at the centre of both chambers. The

temperature sensor is of type PT1000 and humidity sensor is HIH-4021 from Honeywell. Figure 6.2 shows a block diagram of the experimental setup.

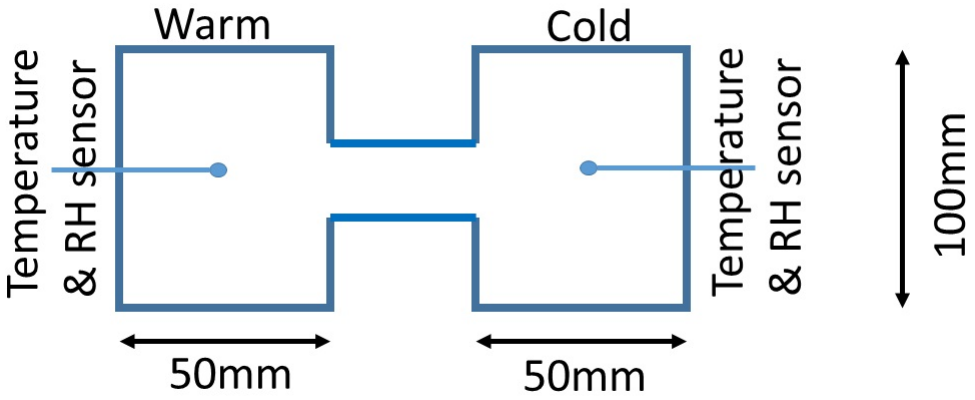

Figure 6.2: Block diagram of the experimental setup with glass echambers

Warm and cold water was circulated in the warm and cold chambers respectively. When the temperatures in both chambers stabilise, $100\mu L$ of water at the same temperature of the warm chamber is introduced into the warm chamber through an opening. The resulting humidity profiles in the warm and cold chambers are recorded using a Keithley 2700 data acquisition system. The cold chamber had condensed water inside during the entire duration of the experiment. Figure 6.3 shows the experimental setup.

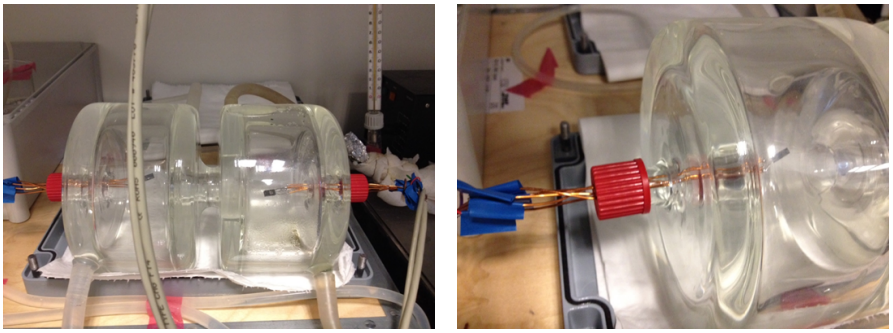

(a) (b)

Figure 6.3: Experimental setup with glass chambers

The experiments were conducted for warm chamber circulated water temperatures of 30^oC, 35^oC and 40^oC. The cold chamber circulated water temperatures were varied between 5^oC, 10^oC and 15^oC. The default size of the connecting hole between the chambers in the experimental setup is 16mm diameter. This was varied by attaching thin plates of desired opening size between the chambers. The plate was made of polyurethane foam of thickness 1.6mm and covered with aluminium foil. Figure 6.4 shows a picture of the plates with hole sizes of 3mm, 6mm and 9mm.

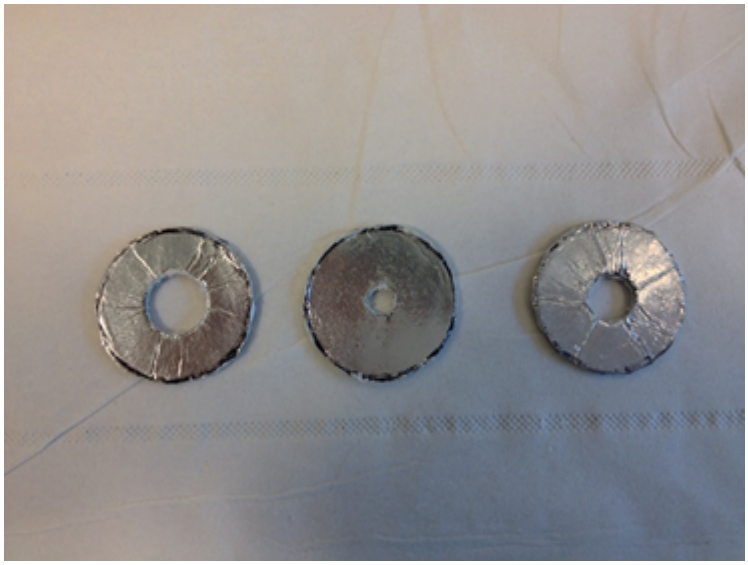

Figure 6.4: Plates of different opening sizes used to control connecting hole size

6.2 Results

6.2.1 Humidity profiles in the chambers

Figures 6.5a and 6.5b show the RH and AH profiles in the warm and cold chambers for warm chamber circulated water temperature of 30^oC and cold chamber circulated water temperature of 10^oC. When water is introduced, RH in the warm chamber increases due to evaporation. The RH remains at 100% until all the water has been vapourised. Time zero denotes the instant when the RH inside the warm chamber starts falling from 100% RH. It was observed from figure 6.5a that the initial and final steady state RH in the warm chamber after the introduction of water are the same at 31.6%. This showed that all the water that was introduced into the warm chamber was completely transferred into the cold chamber. This experiment showed the feasibility of using humidity transfer from warm to cold to control humidity in an enclosure. The RH measured by the cold chamber RH sensor during the entire duration was of the experiment was 79.4% and not 100%, since it was in the middle of the cold chamber away from the condensing walls.

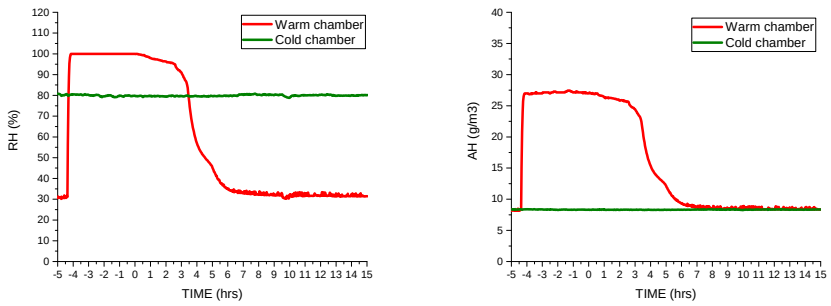

(a) RH profile in the chambers (b) AH profile in the chambers

Figure 6.5: Humidity profiles in the warm and cold chambers during the experiment

6.2.2 Effect of chamber temperatures

Figure 6.6 show the effect of cold chamber temperature on the humidity and transient times inside warm chamber for cold chamber circulated water temperatures of 5^oC, 10^oC and 15^oC. The warm chamber was circulated with water at 30^oC. The steady state RH in the warm chamber was 25.43% for 5^oC where as, it was 45.23% for 15^oC. When the cold chamber temperature decreases, saturated AH of air in the condensing cold chamber also decreases. This causes higher transport of humidity from warm to cold chamber and hence, lower steady state RH in warm chamber. Transient time increased from 4.54 hrs to 9.48 hrs for a change in cold chamber circulated water temperature from 5^oC to 15^oC. The transient time was also observed to increase for higher cold chamber temperatures due to lower convective flow between the chambers. So, by choosing suitable cold chamber temperature, the required steady state RH in the waarm chamber and transient time can be achieved.

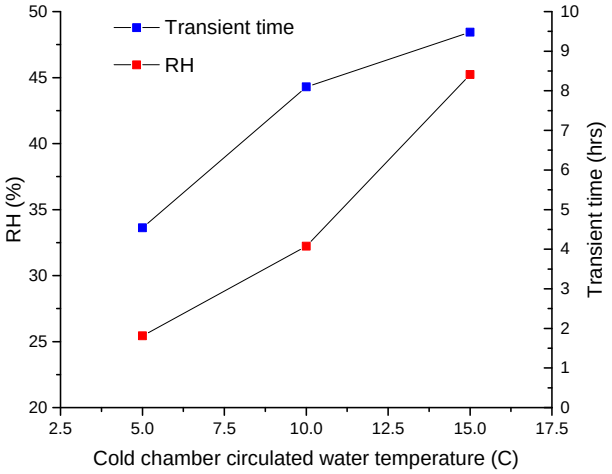

Figure 6.6: Effect of cold chamber temperature on steady state RH and transient times inside warm chamber

Figure 6.7 show the effect of warm chamber temperature on the humidity and transient times inside warm chamber for warm chamber circulated water temperatures of 30^oC, 35^oC and 40^oC. The steady state RH in warm chamber was 32.46% and 21% for 30^oC and 40^oC of warm chamber circulated water temperature. This decrease in RH was due to the increase temperature inside the warm chamber as the steady state AH was the same in both cases. The transient time also showed a decrease from 8.1 hrs to 6.7 hrs for circulated warm water temperature increase from 30^oC and 40^oC due to higher flow between the chambers with larger differential temperatures. The increase in the warm chamber temperature from 30^oC and 40^oC was able to achieve an RH change of only 11% compared to almost 20% for variation in cold chamber temperature. Also the change in transient time was also lower compared to that shown in figure 6.6.

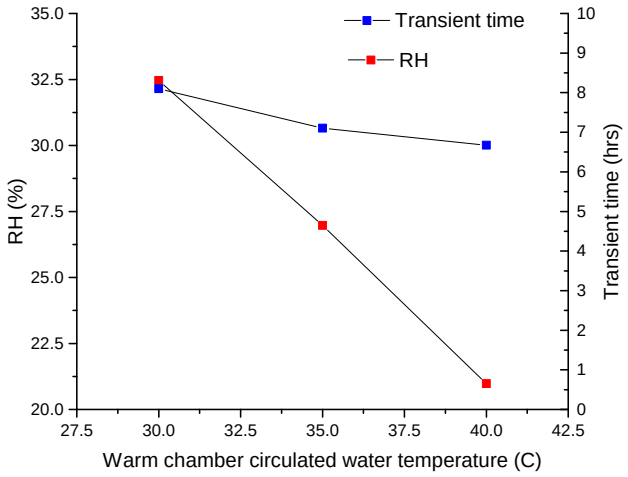

Figure 6.7: Effect of warm chamber temperature on steady state RH and transient times inside warm chamber

6.2.3 Effect of connecting hole size

Figure 6.8 shows the effect of connecting hole size on the transient time in warm chamber. The two transport mechanisms of humidity from warm to cold chamber are natural convection and diffusion. It was observed that the transient time decreases from 31.1hrs to 5.7hrs with corresponding increase in connecting hole diameter from 6mm to 16mm. This was because of the increase in natural convection flow between the chambers with higher hole size. For smaller values of the connecting hole, diffusion becomes the more dominant transport phenomena compared to convection. The convective flow rate also reduces with smaller hole sizes resulting in longer transient times.

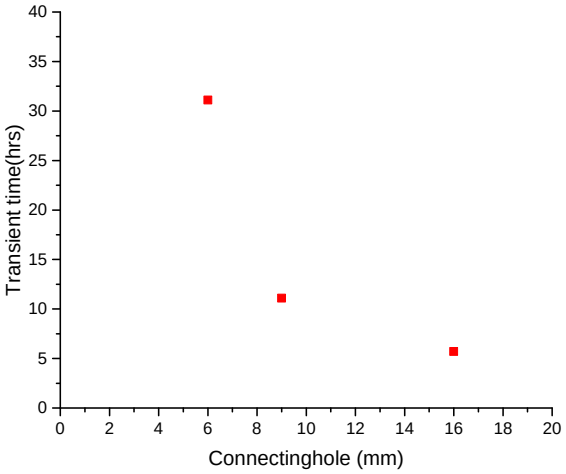

Figure 6.8: Effect of connecting hole size on transient time

6.3 Conclusion

- Liquid water introduced into the warm chamber was completely transported to the cold chamber as deduced from the same values of initial and final steady state RH in warm chamber. This showed the feasibility of using humidity transfer from warm to cold for humidity control.
- Lower temperature in the cold chamber caused lower steady state RH in warm chamber due to lower values of AH at lower temperatures in the cold chamber. Higher temperature in warm chamber also caused lower steady state RH in warm chamber. Lower warm and cold chamber temperatures also caused lower transient times due to increased flow between the chambers.
- Larger connecting holes led to lower transient times due to higher flow between the two chambers.

Chapter 7

Humidity accumulation and condensation in electronic enclosures

Abstract

The aim of this work is to study the climatic profiles of humidity and temperature inside an electronic enclosure with an internal parallel printed circuit board assembly (PCBA) structure subjected to cycling ambient temperature. An aluminium enclosure with controlled opening was used for the study. The enclosure had an internal structure of three parallel aluminium plates to replicate an electronic control unit (ECU) with parallel arrangement of PCBs. Heating was applied to one of the plates to simulate power dissipation by electronic components. The experiments were conducted for different conditions of power dissipation, inter-plate separation, heat capacity of plate and controlled-opening size on the enclosure. Humidity and temperature profiles inside the enclosure were studied using relative humidity (RH) and temperature sensors respectively, placed on the three plates. Condensation on the plates were analysed by calculating the dew-point temperatures on the plates. Effect of enclosure humidity build-up on PCBA was studied by monitoring impedance of surface insulation resistance (SIR) patterns placed on the three plates. Results of the study are used to draw implications for electronic devices due to above mentioned parameters.

Keywords: Humidity, Temperature, Electronic enclosure, Condensation, Reliability.

Submitted as: **S. Joshy**, R. Ambat, "Humidity accumulation and condensation in electronic enclosures", in Microelectronics Reliability, 2018.

7.1 Introduction

Application of electronics in harsh climatic conditions has made failures caused by high humidity more common. The main humidity related failures in electronics include unacceptable levels of leakage currents, electrochemical migration (ECM), conductive anodic filament (CAF), and short circuits due to condensation of water [1][2][3][4]. Humid environment result in the formation of a microscopic thin layer of water on the surface of PCBAs and components [5]. Presence of hygroscopic ionic residues left over from PCBA manufacturing process[6] and hygroscopic dust from atmosphere[7] enhance the thickness of this water layer by deliquescence. When the RH increases beyond the deliquescence RH (DRH) of these hygroscopic residues, a thicker and conductive water layer is formed causing significant leakage currents, SIR reduction and ECM[8]. The values of DRH for weak organic acids (WOA) used in no-clean solder fluxes used for PCBA manufacturing can be found in the literature[9].

Under constant conditions of temperature, humidity accumulates inside electronic enclosures by diffusion through the openings and walls of the enclosure[10]. High humidity can also result from the release of water vapour absorbed in the walls of the enclosure[10]. Conseil et al.[16] has shown that cycling conditions of ambient temperature can lead to humidity accumulation in the enclosure and condensation on the PCBA. Humidity accumulation and condensation was also observed to occur due to cycling power dissipation in the device[16]. Heat capacity and enclosure opening size accelerate the humidity accumulation and condensation process[16]. There is literature related to analysis of temperature and heat transfer for electronics[11][12][13][14] but, very few on combined humidity, temperature and its effect on reliability of electronics[10][15]. This work aims to study power dissipation and packaging related parameters like inter-plate separation, heat capacity, opening size on humidity profiles and reliability in an electronic enclosure with parallel PCBAs under cycling conditions of ambient temperature and power dissipation.

A parallel arrangement of PCBAs is commonly adopted in ECUs for reasons of modularity in design, reducing conducted electromagnetic interference (EMI) etc. The separation between the parallel PCBAs is determined by the overall size of the ECU and the board-to-board connectors used between the PCBAs. Power dissipation leading to temperature rise of devices in ECUs is mainly caused by metal-oxide semiconductor field-effect transistors (MOSFETs), insulated-gate bipolar transistors (IGBTs), inductors, transformers, power resistors and electrolytic capacitors. Power dissipation lead to temperature rise and convection between the air inside the enclosure and the ambient. High heat-capacity components like inductors, transformers, electrolytic capacitors etc and heat-sinks inside an ECU can lead to delay in local temperature rise (when the system is off and under a natural temperature variation) causing optimal surfaces for condensation and high humidity[16]. Openings on electronic enclosures can be controlled openings like drain holes for condensed water, holes for forced air cooling etc. or unintended openings like space between adjacent cables on an unsealed signal connector, cuts on cable insulation etc.

Conseil et. al.[16] has studied humidity accumulation in electronic enclosures and reliability using an aluminium enclosure. The current work builds up on that by studying a parallel plate structure simulating parallel PCBAs. The experiments

in this work used an aluminium enclosure with an internal arrangement of three parallel aluminium plates. One of the plates replicated a power-PCB with significant power dissipating components where as, the other two plates simulated control/logic PCBs with relatively no power dissipation. The enclosure was placed in an environmental chamber and the experiments were conducted for different conditions of power dissipation, inter-plate separation, heat capacity of plate and opening-size in the enclosure. Climate profile inside the enclosure as represented by measured RH, temperature and condensing times on the plates was observed to vary with the afore-mentioned parameters. Effect of enclosure humidity build-up on reliability of PCBA was investigated by placing a contaminated SIR pattern on the plate and measuring the impedance changes.

7.2 Materials and methods

An aluminium enclosure of dimensions 263mm x 162mm x 91mm was used for the experiments. Thickness of the wall of the enclosure was 4mm. The IP protection rating of the enclosures were IP 66/67/68. A circular opening was made on one wall of the enclosure to simulate controlled openings. The enclosure had three aluminium plates of dimensions 180mm x 90mm x 1.5mm placed inside at a separation of 20mm equidistant to each other and the walls of the enclosure. The experimental setup including the location of controlled openings and internal structure is shown in figure 7.1.

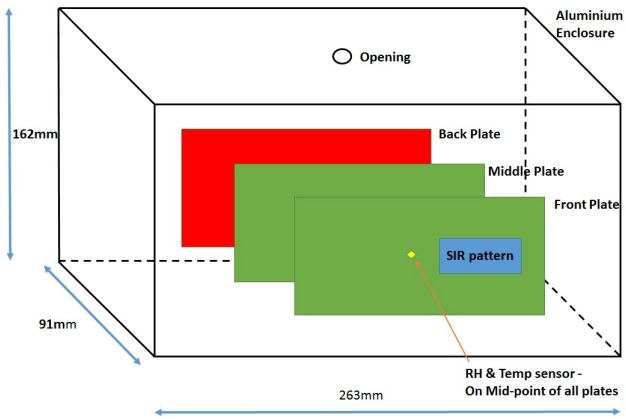

Figure 7.1: Schematic representation of the experimental setup with enclosure and parallel PCBA structure.

A temperature and RH sensor each were placed at the mid-points of surface of the three plates. Temperature sensors measured the temperature at the mid-point of the surface of the plates. The temperature sensor used was of PT1000 type with dimensions 1mm x 3mm with a thermal response time of 0.1s. The RH sensor was HIH-4021 manufactured by Honeywell. The data from the sensors were logged using a Keithley 2700 data acquisition system.

The back-plate in figure 7.1 was centrally pasted with an etched foil silicone heater of dimensions 150mm x 90mm to simulate a PCBA with power dissipating components. The heater was pasted on the side of the back plate facing the wall. An EAPS 16000 programmable power supply was used to power the heater. An ESPEC

SH-641 climatic chamber was used to simulate the ambient climatic profiles. The initial conditions before start of the experiment was 40^{o}C and 35% RH. For the duration of the experiment, the ambient RH is maintained constant at 99%. The ambient temperature is cycled with 40^{o}C for 1 hr and 15^{o}C for 1.5 hrs time. The heater is turned on when the ambient temperature is 40^{o}C and off when the ambient temperature is 15^{o}C. This simulates an ECU turning on during the day time, similar to a microinverter used for photovoltaic applications. Figure 7.2 shows the ambient climate profile measured inside the climatic chamber and the heater turn-on timings.

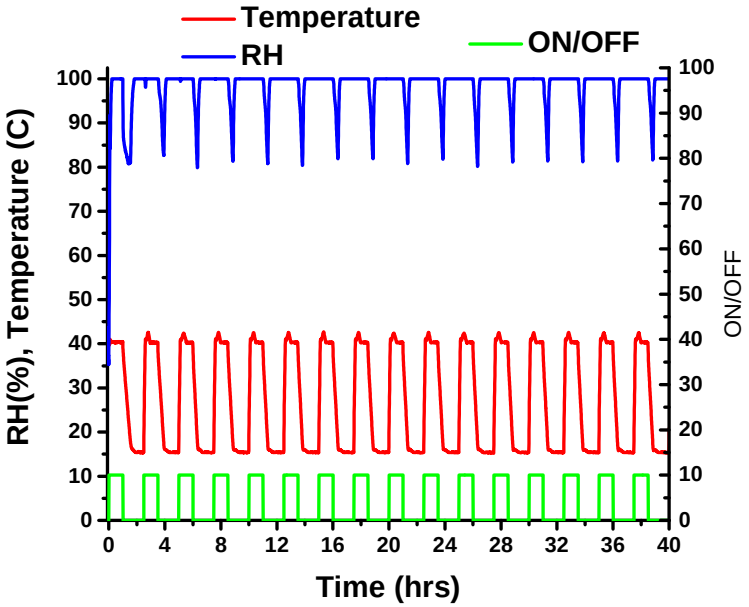

Figure 7.2: Climate profile measured by RH and temperature sensors inside the climatic chamber with internal heating ON/OFF timings.

Susceptibility to humidity related failures at different plates inside the enclosure was simulated by placing a contaminated SIR pattern. The SIR PCBs were placed near the centre of each of the three plates. The SIR PCBAs were made according to IPC 4101/21. The size of the SIR pattern was 25mm x 13mm and the pitch distance was 0.3mm. The thickness of the SIR PCB was 1.6mm. The SIR pattern consists of 21 pairs of intermeshing metal PCB tracks. Further details of the SIR pattern can be found in the literature [9]. The SIR PCBAs were contaminated with 15.6$\mu g/cm^2$ of sodium chloride (NaCl). When exposed to humid conditions a thin layer of water form on the surface of SIR PCBA. The thickness of the water layer depends on the local RH around the PCBA. Beyond deliquescence RH (DRH) of NaCl the water layer thickness increases rapidly, decreasing the value of impedance measured. The impedance of the contaminated SIR patterns were monitored at a fixed frequency of 20kHz using a Biologic VSP series potentiostat.

The effect of power dissipation was studied by varying the heat dissipated by the silicone heater on the back plate. The separation between the back plate and middle plate is adjusted to study the effect of inter PCB separation. The front and back plates were at fixed positions of 20mm to enclosure wall when the middle plate was moved to study effect of separation. Effect of heat capacity on humidity profiles was studied by using aluminium plates of different thicknesses for the middle plate. A 1.5 mm plate corresponded to a heat capacity of 59.7J/K where as for 3mm

and 5mm plates the heat capacity was 117.9J/K and 199J/K respectively. Lastly, enclosures with different hole diameters were used to study the effect of opening size on humidity accumulation. The different values of the parameters used in this investigation and their combination in each experiment are shown in table 7.1.

Table 7.1: Parameter values used in the experiment

Exp.no.	Experiment	Power dissipation(W)	Separation(mm)	Heat capacity(J/K)	Opening diameter(mm)
1	Power disipation	0	20	59.7	2
2	Power disipation	2.5	20	59.7	2
3	Power disipation	14.5	20	59.7	2
4	Separation	14.5	5	59.7	2
5	Separation	14.5	20	59.7	2
6	Separation	14.5	35	59.7	2
7	Heat capacity	14.5	5	59.7	2
8	Heat capacity	14.5	5	117.9	2
9	Heat capacity	14.5	5	199	2
10	Opening size	14.5	20	59.7	2mm dia tube 50mm long
11	Opening size	14.5	20	59.7	10

7.3 Results

Figure 7.3a shows the RH measured by the RH sensors on each of the three plates when the power dissipation is 14.5W, separation between the plates is 20mm, thickness of all three plates is 1.5mm and the enclosure opening diameter is 2mm. The RH values decrease during internal heating time and increase during the low-temperature phase when the internal heating is also off. Figure 7.3a shows that except the back plate the other two RH sensors experience 100% RH after initial few cycles during the low-temperature phase. Figure 7.3b shows the temperature on the plates and the enclosure during one cycle. Temperature increases on the plates and enclosure due to internal heating and ambient temperature rise from 15^{o}C to 40^{o}C. Temperature on the plates decrease when heating is off and the ambient cools from 40^{o}C to 15^{o}C.

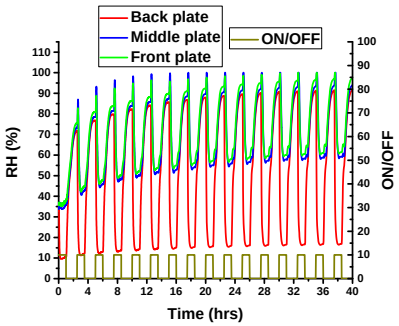

(a) RH profile for the three plates

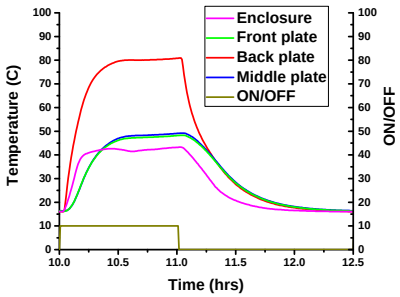

(b) Temperatures profile on the plates

Figure 7.3: Measured RH and temperature profiles on the plates with respect to internal heating timings.

Internal heating in the enclosure sets up natural convection between the volume inside the enclosure and the relatively cooler (40^{o}C) chamber conditions. Since the initial AH inside the enclosure of 17.85 g/cm^3 is lower than the ambient AH of 51 g/cm^3 when the ambient temperature is 40^{o}C, humidity accumulation occurs. When the power dissipation is turned-off and the ambient temperature decreases to 15^{o}C, the ambient AH of 12.8 g/cm^3 is lower compared to the enclosure AH and mass transfer of water vapour from enclosure volume to ambient occurs. However, residual humidity is trapped in the enclosure in the form of condensed and adsorbed water by the end of the low-temperature cycle. This process of humidity accumulation by natural convection and humidity trapping results in a cycle-by-cycle accumulation of AH inside the enclosure as shown in figure 7.4 for the front plate.

Absolute humidity was calculated according to the formula :

$$AH = \frac{2.16 \times (RH/100) \times 288.68 \times (1.098 + T/100)^{8.02}}{273 + T}$$

where 'T' is the temperature in degree celsius and RH is the relative humidity as percent.

Figure 7.5 shows the variation in impedance of SIR patterns on the three plates. It was observed that the impedance on the middle and front plates decreased during the low-temperature phase when internal heating was off. These impedances were

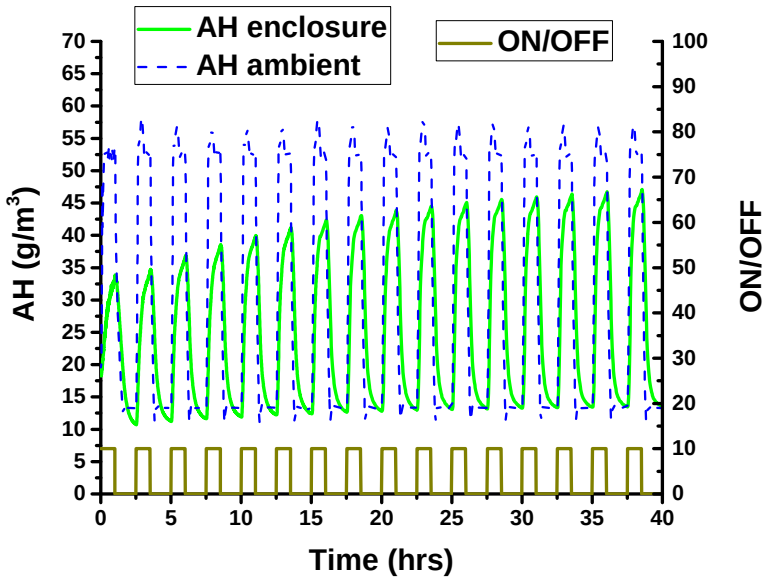

Figure 7.4: Plot of cycle-by-cycle humidity accumulation inside the enclosure with respect to chamber AH and internal heating

also observed to decrease over the duration of the experiment. The impedance on the back plate remained steady during the entire duration of the experiment.

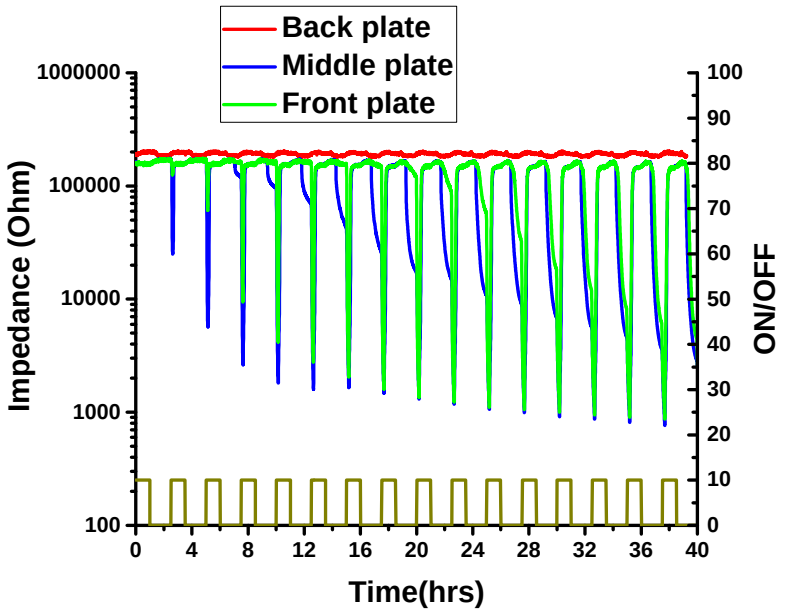

Figure 7.5: Impedance variation of SIR patterns on the three plates over the duration of the experiment

Humidity accumulation was analysed for the back plate by plots of peak value of RH reached in the final cycle with respect to the parameter analysed. For middle and front plates the time taken for onset of condensation was plotted w.r.t the parameter analysed. Condensation was detected when the measured temperature of the plate was equal to the calculated dew-point temperature of the plate. Dew-point

temperature was calculated using the Magnus formula[17] as :

$$T_{dew} = \frac{a \cdot ln(RH/100) + \frac{b \cdot T}{a+T}]}{b - [ln(RH/100) + \frac{b \cdot T}{a+T}]}$$

where 'a' is 243.12, 'b' is 17.62, 'RH' is the relative humidity in percent and 'T' is the temperature in celsius. Condensation was observed on middle and front plates when ambient temperature rises and internal heating was turned on for the back plate. This was observed in figure 7.3a as abrupt spikes in RH of middle and front plates during internal heating turn on time. This was also observed as spikes in impedance for middle and front plates in figure 7.5 during heating turn-on time. This condition existed for a short time until the power dissipation on the back plate started heating up the other two plates by convective heat transfer. Condensation was observed to occur first on the middle plate than the front plate. Condensation also occurred on the middle plate longer than the front plate.

From figure 7.3b, the temperatures on the plates were observed to attain near steady state in each cycle during the heating phase. These temperature values measured on the plates towards the end of the heating phase was plotted for each parameter.

In the following sections, effect of the parameters on reliability is investigated at the different plates inside the enclosure by a plot of impedance minima in each cycle over the duration of the experiment. Higher values of RH in the vicinity of SIR patterns caused deliquescence and later condensation resulting in a thicker layer of water on the SIR pattern which was observed as low impedance in the impedance measurements. The following subsections show the effect of the parameters on humidity profiles and reliability in electronic enclosures.

7.3.1 Effect of Power dissipation

Figure 7.6a shows the peak values of RH attained in the final temperature cycle of the experiment on the back plate. The RH on the middle and front plates increased with progressive temperature cycles and saturated at 100%. The lower values of RH on the back plate was due to the presence of power dissipation. With no internal heating, the peak value of RH on the back plate in the final cycle was 100%. This decreased to 97.77% and 91.84% when the power dissipations were 2.5W and 14.5W respectively.

The steady state temperatures on each plate and the outside surface of the enclosure for different power dissipations are shown in figure 7.6b. The temperature on the back plate increased from 40.2^{o}C at no power disipation to 50.4^{o}C at 2.5W and 80.4^{o}C at 14.5W. The temperatures on the middle and front plates were almost similar, varying from 40.2^{o}C for no power to 42^{o}C for 2.5W and 49^{o}C for 14.5W. But this increase in temperatures on the middle and front plates could not prevent condensation from occurring.

Figure 7.7 shows the time to onset of condensation for the different values of power dissipation on middle and front plates. Condensation did not occur on the back plate for power dissipation of 2.5W and 14.5W, occurring only with no internal heating. For the middle plate the time to condensation increased with higher values of power dissipation. For the middle plate, the time to condensation was 7.6 hrs for both 0W and 2.5W and 17.6 hrs for 14.5W. For the front plate which was most

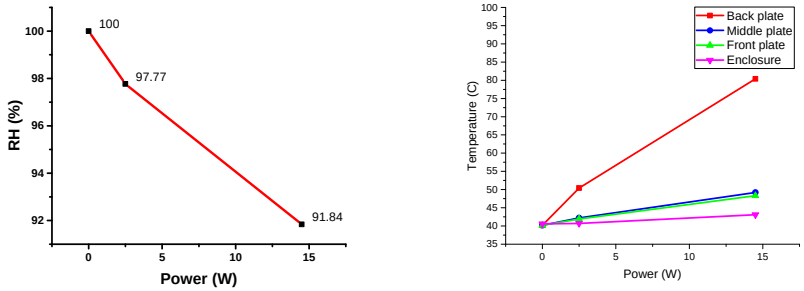

(a) RH variation with power dissipation on back plate

(b) Steady state temperatures on the plates

Figure 7.6: Effect of power dissipation on RH and temperatures on the plates

furthest from the source of power dissipation, the time to condensation was 15.1 hrs for 0W, 12.6 hrs for 2.5W and 22.6 hrs with 14.5W. The slight decrease in time to condensation for front plate from 0W to 2.5W in figure 7.7 could be due to the error introduced into the data due to the finite accuracy limits of RH and temperature senors. It was also observed that condensation occurs first on the middle plate and then on the front plate which was further away from power dissipating back plate.

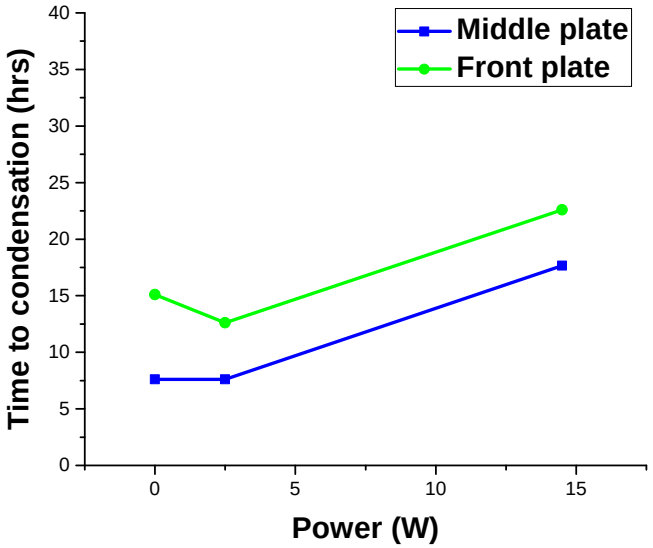

Figure 7.7: Plot of time to condensation on middle and front plates

Figure 7.8a shows the variation in impedance on the back plate for the different values of power dissipation. Impedance on back plate decreases for both no power dissipation and 2.5W. The impedance decreased to 182Ω and 2500Ω during the final cycle for 0W and 2.5W respectively. The impedance remained constant at 188kΩ for 14.5W. The decrease in impedance on the middle and front plates was seen to be similar, both decreasing to 182Ω, 196Ω and 800Ω for power dissipations of 0W, 2.5W and 14.5W respectively. It was also observed that the final impedance values on the back plate was higher than the middle and front plates for 2.5W due to the presence of internal heating.

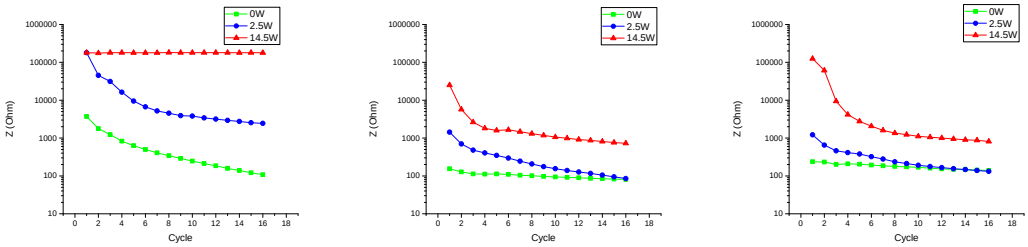

(a) Plot of impedance of SIR pattern on back plate

(b) Plot of impedance of SIR pattern on middle plate

(c) Plot of impedance of SIR pattern on front plate

Figure 7.8: Effect of power dissipation on impedance minima in each cycle of the experiment

7.3.2 Effect of separation

Figure 7.9a shows the peak value of RH in the final cycle on the back plate for different separations between the heated back plate and the middle plate. The final peak values of RH on middle and front plates were 100%. The variation in RH on the back plate was 5% for a change in separation with the middle plate from 5mm to 35mm.

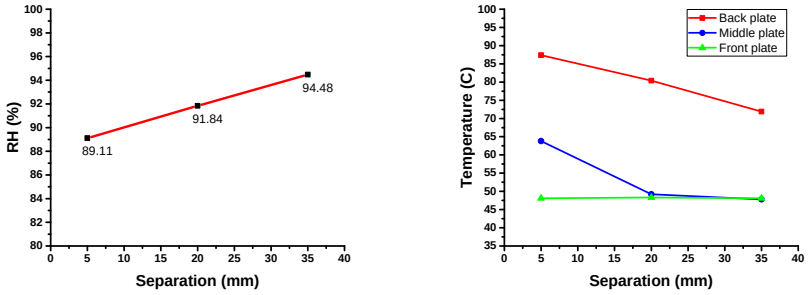

(a) RH variation with separation on back plate

(b) Steady state temperatures on the plates

Figure 7.9: Effect of separation on RH and temperatures on the plates

It was seen from figure 7.9b that temperatures on back and middle plates decreased as the separation between them increased. The peak temperature on the

back plate decreased from 87^{o}C to 72^{o}C when the separation with the middle plate increased from 5mm to 35mm. The middle plate showed decrease in temperature from 63.8^{o}C to 47.7^{o}C when the separation with back plate increased from 5mm to 35mm.

Condensation occurred on the front and middle plates, but not on the back plate due to 14.5W of power dissipation. Condensation was observed to happen on the front and middle plates for all three values of separation. Figure 7.10a shows the time to condensation on the middle plate. The time to condensation decreased on the middle plate as it was moved further away from the heated back plate. The time decreased from $\sim$ 25hrs for a separation of 5mm to $\sim$ 18hrs with 20mm. Condensation happened sooner at $\sim$ 8hrs with 35mm separation.

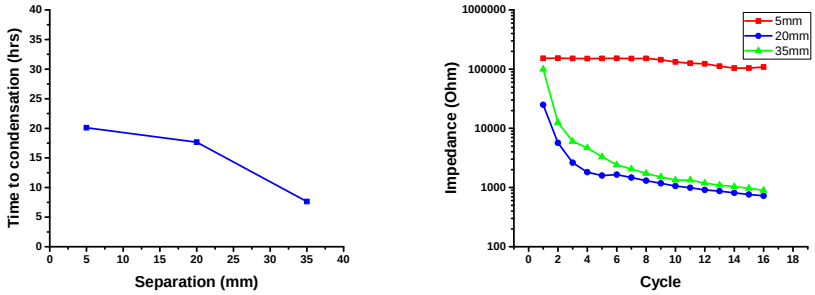

(a) Plot of time to condensation on middle plate

(b) Plot of impedance of SIR pattern on middle plate

Figure 7.10: Effect of separation on time to condensation and impedance minima in each cycle on middle plate

Figure 7.10b shows the variation in impedance on the movable middle plate for different values of separation from the heated back plate. The graph shows that impedance on the middle plates degrades for separations of 20mm and 35mm compared to minimal variation for 5mm from back plate. Even for separation of 5mm the impedance showed a slow decrease over consecutive cycles from 152kΩ to 108kΩ. The impedance on the middle plate showed impedance values similar for both 20mm and 35mm. The value of impedance in the final cycle of the experiment for both separations was 900Ω. No effect was found on the impedance of the front plate due to variation in distance between the back and middle plates.

7.3.3 Effect of heat capacity

To study the effects of heat capacity, the middle plate is kept closer to the heated back plate at a separation of 5mm to enhance its effect on residual heat absorption. Aluminium plates of different thicknesses were used to simulate different heat capacities for the middle plate in the experiment as shown in table 7.1. For different heat capacities of the middle plate the rate of rise and fall of temperatures on the plates change as shown in the work by Conseil et. al.[16]. Figure 7.11a shows the temperature profile on the middle plate for different values of heat capacity over a cycle. It was observed that the higher heat capacity took longer time to heat up and longer time to cool down. Figures 7.11b and 7.11c show the time constants

for temperature rise and fall respectively on the middle plate for the values of heat capacities studied.

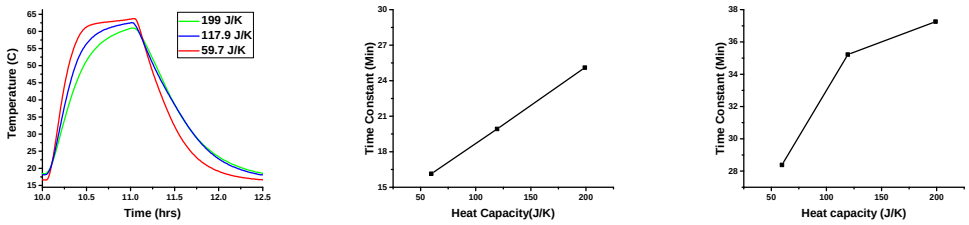

(a) Temperature profile on middle plate for various heat capacities

(b) Time constant during heat accumulation

(c) Time constant during heat release

Figure 7.11: Time constant during heating and cooling for middle plate

The plot of time constants during heating shows a linear increase w.r.t heat capacity from $\sim$ 16 mins to $\sim$ 25 mins. The time constant during cooling time was similar for both 5mm and 3mm middle plate with values $\sim$ 35 mins and $\sim$ 37 mins respectively. The 1.5mm middle plate showed a lower time constant of $\sim$ 28 mins.

The difference in time constants for temperature rise and fall on the middle plate influenced the RH on the heated back plate. Figure 7.12 shows the RH on the back plate in the final cycle for different values of heat capacities of the middle plate. For middle and front plates the RH saturates at 100% in the final cycle. The difference in final RH on the back plate was 4% between the higher and lower heat capacity middle plates.

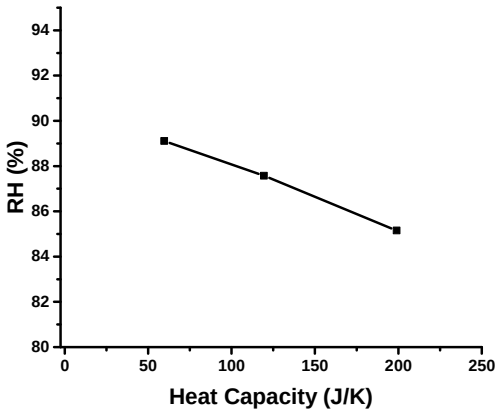

Figure 7.12: Effect of variation in heat capacity of middle plate to RH on back plate in the final cycle

Figure 7.13 shows the time to onset of condensation on the middle and front plates for different heat capacities of the middle plate. It was observed that condensation occurs for both plates at almost similar instants for 1.5mm and 3mm middle plate. For a 5mm middle plate condensation occurred much later in time of ~ 37 hrs. The time to condensation remained constant for the front plate which was further away from the middle plate, showing no effect of heat capacity towards condensation on front plate.

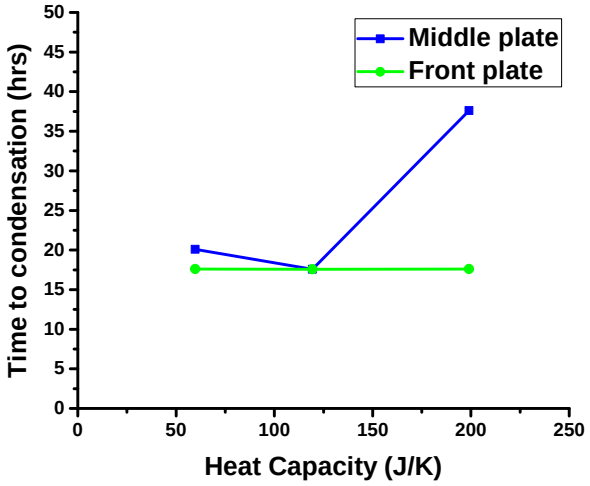

Figure 7.13: Effect of heat capacity of middle plate on time to condensation for middle and front plates

Figures 7.14a and 7.14b show the degradation in impedance on the middle and front plates respectively for different values of heat capacities of the middle plate. As observed from figure 7.14a higher heat capacity corresponded to lower values of impedance. The lowest impedance reached for 5mm thick middle plate was 1291Ω where as for 3mm and 1.5mm plates it was 19kΩ and 108kΩ respectively. For the front plate it was observed that the impedance was slightly higher with higher heat capacity middle plate with a value of 1100Ω compared to 300Ω and 600Ω for 3mm and 1.5mm middle plates respectively.

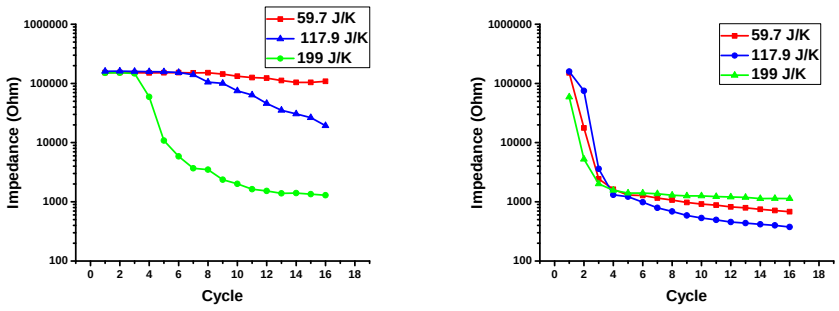

(a) Impedance variation on middle plate

(b) Impedance variation on front plate

Figure 7.14: Effect of heat capacity on the humidity build up and on the reliability

7.3.4 Opening size

For experiments with enclosures of 10mm opening and 2mm diameter tube of 50mm length, RH on the back plate and the temperatures on the plates were not influenced by the size of the opening. The peak temperature on the back plate was 83.6^oC and peak RH in the last cycle was 93% on the back plate.

Figure 7.15 shows the time to onset of condensation on the condensing middle and front plates. It can be observed that condensation occurred earlier with a bigger opening size. For the middle plate condensation occurred at 30hrs with 50mm tube and 12.6hrs with 10mm diameter hole.

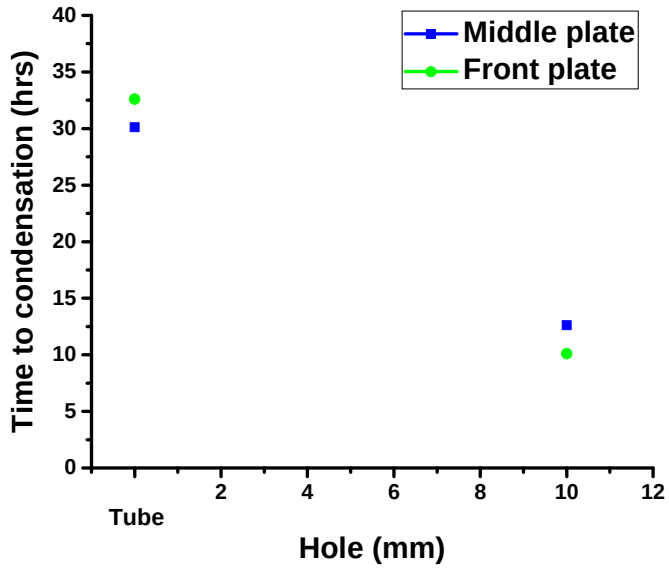

Figure 7.15: Effect of opening size on time to condensation on middle and front plates

Figures 7.16a and 7.16b show the impedance variation on middle and front plates for different opening sizes studied. For the middle plate in figure 7.16a the impedance corresponding to 50mm long tube was higher than that for 10mm diameter opening. The impedance curve for 50mm long tube settled at 3kΩ where as for the enclosure with 10mm diameter opening, the impedance settled at 1125Ω. For the case of front plate the trend is similar with the tube shaped opening showing higher impedance than the other two opening sizes.

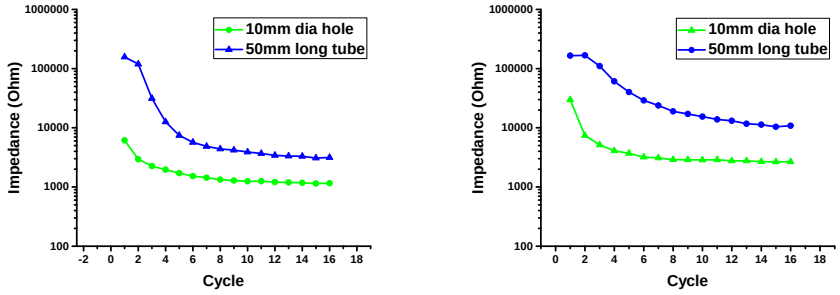

(a) Impedance variation on middle plate

(b) Impedance variation on front plate

Figure 7.16: Effect of opening size on impedance minima in each cycle for the middle plate

7.4 Discussion

Humidity accumulation was observed to occur inside the electronic enclosure due to cycling ambient temperature and internal heating. Internal heating was found to be the dominant factor affecting RH and impedance degradation on the back plate. Larger values of separation, higher heat capacity and enclosure opening size were found to cause higher impedance degradation and hence, higher susceptibility to humidity related failures on the middle plate.

Figures 7.3a and 7.3b showed typical humidity and temperature profiles in the enclosure. As shown in figure 7.4 humidity accumulation was observed inside the enclosure due to natural convection between the enclosure and ambient. Condensation was observed to occur on the middle and front plates during internal heating turn-on times as shown in figure 7.3a. Typical ECUs use polymers as part of electronic components and also as enclosure material [10] which can act as humidity buffers. The humidity absorbed is released back into the air inside the enclosure when heating starts, which would condense on the cooler control/logic PCB of the ECU. This process of condensation is shown to occur using hygrothermal modelling by Bayerer et. al., assuming only diffusion mode of mass transport [18]. Another source of humidity released during heating is water vapour adsorbed on walls of enclosure and PCBA. Condensation occurred for longer durations on the middle plate than the cooler front plates. This was because during heating turn-on time absorbed/adsorbed humidity is released more from the vicinity of the heated back plate and condenses first on the middle plate as it is nearest cooler surface encountered. Impedance was observed to decrease on the condensing middle and front plates due to humidity accumulation inside the enclosure over successive temperature cycles.

RH on the heated back plate decreased with higher power dissipation on it as seen from figure 7.6a. In the final cycle of the experiment the RH near the back plate was still above 90% for power dissipation of 14.5W. PCBA manufactured with DL-Malic acid and glutaric acid based no-clean solder fluxes experience considerable leakage currents when RH is above the respective DRH[8][9]. For a PCBA which has used DL-Malic or glutaric acid based no-clean solder fluxes for component assembly would not encounter leakage currents and ECM on the back plate for a power dissipation of 14.5W even though the DRH for DL-Malic acid and glutaric acids are lower than

90% because of the effect of heating. As observed from figure 7.8a, this shows a way to improve reliability on the three plates by heating. From figure 7.8a it can also be observed that impedance gradually decreased for a power dissipation of 2.5W, showing that this level of internal heating was not enough to improve reliability on the back plate. To prevent humidity related reliability degradation on the back plate a threshold power dissipation between 2.5W and 14.5W is required even though condensation was avoided by internal heating of 2.5W. Spending 14.5W to improve reliability would result in inefficient humidity control. The type of heating used in this work was convective heating. Hence, more efficient methods of heating like radiant heating or preferential condensation could be used to decrease humidity and attain required reliability. For the middle and front plates impedance decreased over successive cycles even for 14.5W internal heating on the back plate as observed from figures 7.8b and 7.8c. But, power dissipation delayed the onset of condensation on middle and front plates as seen from figure 7.7. It was also observed that power dissipation was the dominant parameter that determined the peak RH on the back plate, with the other parameters studied like separation, heat capacity and opening size having only minimal and no effect respectively.

With increase in separation between the heated back plate and middle plate, a decrease in temperature was observed on the back and middle plates. This was due to an increase in convection heat transfer from the plates due to increased separation. This decrease in temperature contributed to a corresponding increase in RH on the back plate as shown in figure 7.9a. When separation of the middle plate w.r.t heated back plate was increased, time to onset of condensation on the middle plate decreased as seen from figure 7.10a due to lower surface temperatures. The impedance curves for the middle plate showed improvement in reliability only for a separation of 5mm from the heated back plate while, for 20mm and 35mm separation the impedance decreased over successive cycles as seen from figure 7.10b. This implies that there is a critical value of separation of the middle plate from the heated back plate beyond which impedance degrades for a particular power dissipation. Therefore, a critical electronic component or control/logic PCB could be protected from humidity failures by suitable positioning it w.r.t a power dissipating component.

Higher heat capacity on the middle plate delayed the rise and fall of temperature on it as observed from figure 7.11. According to figure 7.13 higher heat capacity of 5mm middle plate (199J/K) prolonged the onset of condensation. Even though time to onset of condensation was prolonged as shown in figure 7.13, the impedance and reliability was lower for a higher heat capacity middle plate as observed from figure 7.14a. This was because of the low swing in peak to peak values of RH near the higher heat capacity middle plate due to sluggish rise and fall of temperature. This implies that electronic circuits situated on high heat capacity components like heat sinks would experience reliability issues especially if low DRH WOA based solder fluxes were used in PCBA manufacturing[16]. The high heat capacity middle plate also provided slight improvement in reliability for the front plate even though 35mm away as seen from figure 7.14b. This was because the higher heat capacity middle plate stored more heat energy during heating phase and released it during low temperature phase to keep the front plate comparatively warmer. In this particular case the heat capacity of aluminium middle plate was not enough to store enough thermal energy to prevent further impedance degradation on the front plate. The study on effect of heat capacity suggests utilising it as a passive humidity control technique by using

high heat capacity/low form-factor phase-change material modules.

The effect of higher opening size was observed to hasten onset of condensation and degrade impedance. This can be explained by the fact that bigger opening sizes allow higher flow due to natural convection between the enclosure and the ambient. This resulted in faster accumulation of humidity in the enclosure with 10mm opening size. Faster accumulation of humidity inside an electronic enclosure with larger opening size was also demonstrated by conseil et. al.[16]. The resistance of the 50mm tube to humidity transfer is higher than that of the 10mm diameter opening. Hence, condensation occurred in the enclosure with the 50mm tube much later in time. Also, slower accumulation of humidity inside the enclosure with the tube as opening caused higher impedance on the SIR pattern compared to 10mm diameter opening. So, smaller opening sizes should be preferred on electronic enclosures to reduce effect of reliability degradation to humidity related failures. Controlled openings are provided in electronic enclosures as drain holes, forced convection holes, pressure equalization etc. Drain holes need to be minimum 3mm in diameter to prevent water drops blocking the hole due to surface tension. Pressure equalisation hole of a particular diameter could be replaced with a tube of same diameter such that the resistance to humidity transfer is increased leading to longer time to condensation and lower degradation in impedance.

This work has investigated the dependence of power dissipation and other geometric parameters on humidity accumulation and reliability in an electronic enclosure. The current work can also be interpreted as a study of using intermittant internal heating for humidity control. Heating as humidity control method has been investigated in literature before[19][20]. But as shown in this work, convective heating might not be feasible in all situations in electronics due to its low efficiency. More efficient heating methods like radiant heating needs to be explored. Radiant heating is already being used in building space heating applications[21][22]. Use of heat capacity to keep components warm and improve reliability has been demonstrated in figure 7.14b. Phase-change materials could be used for this purpose because they have very high heat capacity and small size. Phase-change materials could be used in an electronic enclosure to absorb a part of the power dissipated by electronic components and then used to keep critical circuits warm during off-time of the device. Phase-change materials have been shown to improve the thermal performance of electronics in literature[23][24]. For a particular power dissipation inside an electronic enclosure, by choosing proper values for the enclosure packaging related parameters studied here and proper choice of humidity control techniques reliability of electronics to humidity related failures can be improved.

7.5 Conclusion

Humidity accumulation, condensation and reliability degradation due to cycling ambient temperature and internal heating was studied. The humidity profiles on back plate and time to onset of condensation was investigated on the middle and front plates. Reliability due to humidity failures was studied by impedance degradation of contaminated SIR patterns. The following conclusions can be derived from this work :

- Cycling ambient temperature and internal heating caused a cycle by cycle

humidity accumulation inside the electronic enclosure. Condensation occurred on the cooler middle and front plates during the internal heating turn on time due to release of absorbed and adsorbed water vapour. Reliability as denoted by impedance of SIR patterns decreased over the duration of the experiment.

- Internal heating improved reliability on the heated plate for an internal power dissipation of 14.5W but, not on the middle and front plates. This shows that internal heating can be a method to improve reliability inside an electronic enclosure. Also, the higher amount of energy needed for this while using convective heating shows that more efficient heating methods like radiant heating would be more feasible for use in electronic enclosures.

- For a separation of 5mm from the heated back plate, impedance on the middle plate remained steady . This shows that reliability of a component or circuit on the can be improved by suitably placing it with respect to a power dissipating source inside an electronic enclosure.

- For higher heat capacity middle plate, impedance of the degraded over successive temperature cycles. This shows that circuits placed on high heat capacity components can experience degradation in reliability due to humidity. Presence of high heat capacity components can also cause a slight improvement in reliability for circuits in its vicinity due to release of stored thermal energy.

- Enclosures with smaller openings having higher resistance to convective flows like tubes experience lower drop in impedance over successive temperature cycles. So, Smaller opening sizes for enclosures should be preferred for better reliability to humidity related failures.

7.6 Acknowledgement

This research was conducted as part of the IN SPE project funded by Innovation Fund Denmark and CELCORR(www.celcorr.com). The authors would like to acknowledge the funding and help received from the consortium partners.

Bibliography

[1] R. Hienonen, R. Lahtinen, Corrosion and climatic effects in electronics, VTT Publications, 2000.

[2] D. Minzari, "Investigation of electronic corrosion mechanisms," Ph.D dissertation, Technical University of Denmark, Kgs. Lyngby, 2010.

[3] B. Rudra, M. Pecht, D. Jennings, "Assessing time-to-failure due to conductive filament formation in multi-layer organic laminates", IEEE Transactions on Components, Packaging and Manufacturing Technology : part B, vol. 17, no. 3, pp. 269–276, Aug. 1994.

[4] C. Schimpf, K. Feldmann, C. Matzner, A. Steinke, "Failure of electronic devices due to condensation", Microsystem Technologies, Vol. 15, Issue 1, pp. 123–127, 2009.

[5] M. Tencer, Moisture Ingress into Nonhermetic Enclosures and Packages.A Quasi-Steady State Model for Diffusion and Attenuation of Ambient Humidity Variations, Electronic components and technology conference, pp. 196–209, 1994.

[6] H. Conseil, M. S. Jellesen, R. Ambat, "Contamination profile on typical printed circuit board assemblies vs soldering process", Soldering and Surface Mount Technology, Issue 4, Vol. 26, pp. 194–202, 2014.

[7] R. B. Comizzoli, C. A. Jankoski, G. A. Peins, L. A. Psota-Kelty, D. J. Siconolfi, J. D. Sinclair, "Reliability of electronics in harsh environments: Electrical leakage and corrosion caused by hygroscopic pollutant particles", Elec trochemical society proceedings, Issue 29, Vol. 99, pp. 186–193, 1999

[8] V. Verdingovas, M. S. Jellesen and R. Ambat, "Relative effect of solder flux chemistry on the humidity related failures in electronics," Soldering and Surface Mount Technology, Vol. 27, Issue 4, pp. 146–156, 2015.

[9] V. Verdingovas, M. S. Jellesen, R. Ambat, " Solder Flux Residues and Humidity-Related Failures in Electronics: Relative Effects of Weak Organic Acids Used in No-Clean Flux Systems," Journal of electronic materials, vol.44, Issue 4, pp. 1116–1127, 2015.

[10] H. Conseil-Gudla, Z. Staliulionis, M. S. Jellesen, M. Jabbari, J. H. Hattel, R. Ambat, " Humidity build-up in electronic enclosures exposed to constant conditions," IEEE transactions on components packaging and manufacturing technology, vol.7, Issue 3, pp. 412–423, 2017.

[11] C. Sintamarean, F. Blaabjerg, H. Wang, Y. Yang, "Real Field Mission Profile Oriented Design of a SiC-Based PV-Inverter application", IEEE Transactions on Industry Applications, Vol. 50, Issue 6, pp. 4082–4089, 2014.

[12] T. Lee, B. Chambers, M. Mahalingam, "Application of CFD Technology to Electronic Thermal Management", IEEE Transactions on Components Packaging and Manufacturing Technology, vol. 18, No. 3,1995.

[13] A. Ortega, B. Lall, J. Chicci, M. Aghazadeh, "Heat transfer in a low aspect ratio horizontal enclosure for laptop computer application", Proc. of Ninth SEMI-THERM, pp. 42-49, 1993.

[14] B.S. Lall, A. Ortega, H. Kabir, "Thermal design rules for electronic components on conducting boards in passively cooled enclosures", Thermal Phenomena in Electronic Systems 1994. I-THERM IV. Concurrent Engineering and Thermal Phenomena. InterSociety Conference on, pp. 50-61, 1994.

[15] S. Joshy, M. S. Jellesen, R. Ambat, "Effect of interior geometry on local climate inside an electronic device enclosure", 16th IEEE Intersociety Conference on Thermal and Thermomechanical Phenomena in Electronic Systems (ITherm), pp. 779–783, 2017

[16] H. Conseil, V. C. Gudla, M. S. Jellesen, R. Ambat, Humidity build-up in a typical electronic enclosure exposed to cycling conditions and effect on corrosion reliability, IEEE Transactions on Components, Packaging and Manufacturing Technology, vol. 6, Issue 9, pp. 1379–1388, 2016.

[17] Sensirion, Application Note Dew-point calculation, pp.1-3, Available : http://irtfweb.ifa.hawaii.edu/~tcs3/tcs3/Misc/Dewpoint_Calculation_Humidity_Sensor_E.pdf [Accessed : 03-April-2019]

[18] R. Bayerer, M. Lassmann, S. Kremp, "Transient Hygrothermal-Response of Power Modules in Inverters - The Basis for Mission Profiling under Climate and Power Loading", IEEE Transactions on Power Electronics, vol. 31, Issue. 1, pp. 613-620, 2016.

[19] M. Tencer, J. S. Moss, "Humidity Management of Outdoor Electronic Equipment: Methods, Pitfalls, and Recommendations," IEEE Trans. Components and Packaging Tech., Vol. 25, No. 1 (2002), pp. 66-72.

[20] I. Belov, M. Lindgren, J. Ryden, Z. Alavizadeh, P. Leisner, "CFD assisted design evaluation and experimental verification of a logic controlled local PCB heater for humidity management in electronics enclosure," International Thermal, Mechanical and Multi-Physics Simulation, and Experiments in Microelectronics and Microsystems (EuroSimE), 2010.

[21] D. Anastaselos, I. Theodoridou, A. M.Papadopoulos, M. Hegger, "Integrated evaluation of radiative heating systems for residential buildings", Energy, vol. 36, no. 7, pp. 4207-4215, 2011.

[22] M. Bojic, D. Cvetkovic, M. Miletic, J. Malesevic, H. Boyer, "Energy, cost, and CO2 emission comparison between radiant wall panel systems and radiator systems", Energy and Buildings, vol. 54, pp. 496-502, 2012.

[23] M. J. Vesligaj, C. H. Amon, "Transient thermal management of temperature fluctuations during time varying workloads on portable electronics", IEEE Transaction on Components and Packaging Technology, vol. 22, no. 4, pp. 541-550, 1999.

[24] E. M. Alawadhi, C. H. Amon, "PCM thermal control unit for portable electronic devices: experimental and numerical studies", IEEE transaction on component and packaging technologies, vol. 26, no. 1, pp. 116-125, 2003.

Chapter 8

Humidity profile inside electronic enclosures with retained water

This work studies the effect of enclosure hole size and inter PCB spacing on temperature and humidity inside an electronic enclosure under constant heating conditions and in the presence of retained liquid water. Liquid water can be present in electronic enclosures due to rain, during servicing of the product, condensation inside the enclosure etc. The enclosure has three parallel aluminium plates which simulates PCBA in an electronic unit. Humidity and temperature profiles under constant heating was studied by applying a slow ramp of internal power dissipation on one of the plates. The humidity and temperature profiles were found to depend on PCB spacing and enclosure hole size.

8.1 Materials and methods

The experimental setup consisted of an aluminium enclosure with parallel arrangement of aluminium plates simulating PCBs. The enclosure size was 263mm x 162mm x 91mm and the aluminium plates were 180mm x 90mm x 1.5mm. The plates had RH and temperature sensors placed on their mid-points. The plates also had SIR patterns contaminated with $15.6\mu g/cm^2$ placed on them. A Biologic VSP series instrument was used to monitor the impedance at a fixed frequency of 20KHz. One of the plates - back plate has a mat heater pasted on it. The back plate is 10mm from the enclosure wall. The middle plate is varied in separation from 7.5mm, 11.25mm and 15mm from the back plate. The front plate is 60mm from the back plate. 100ml of liquid water was added in the enclosure to simulate retained water. When humidity saturates inside the enclosure, the voltage applied to the resistive mat heater was varied at a slow rate of 20mV/2min so that, at any instant the RH and temperature measured by the sensors would be steady state values for the heating power at that instant. The experiment was conducted under conditions of 24C and 50% RH. Figure 8.1 shows the experimental setup.

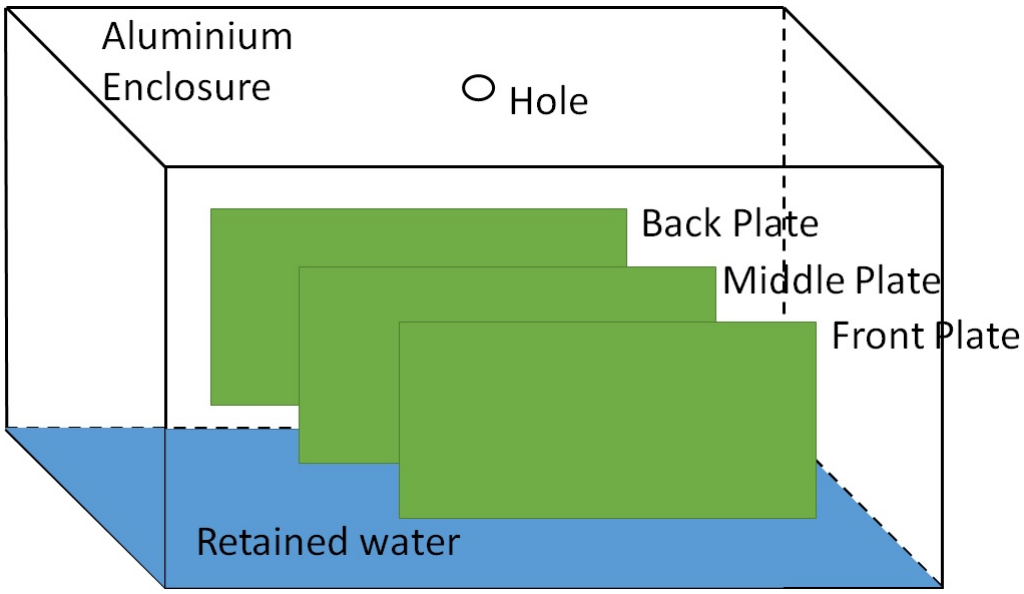

Figure 8.1: Schematic diagram of enclosure with parallel plates and retained water

8.2 Results

8.2.1 Effect of PCB separation

Figure 8.2a shows the variation in RH and temperature measured on the middle plate for different separations when the back plate was at 50^oC. The temperature decreased on the middle plate from 41.2^oC at 7.5mm separation to 38.6^oC at 15mm. This decrease in temperature was due to better heat removal by convection from the back plate with larger separation from the middle plate. The decrease in temperature caused a corresponding increase in RH from 58.8% to 87.2%. Figure 8.2b shows the impedance change on the middle plate during the course of the experiment. It was observed that impedance showed minimal drop in value with lower separation of 7.5mm compared to larger separations of the middle plate and back plate. This was due to lower RH and higher temperature on middle plate with 7.5mm separation as seen from figure 8.2a.

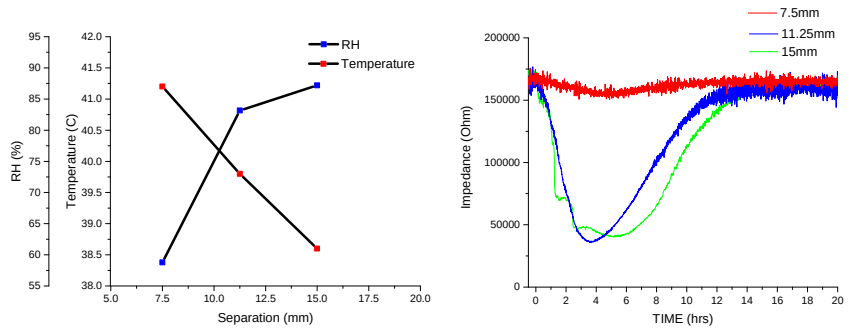

(a) (b)

Figure 8.2: a) RH and temperature variation for different separations b) Impedance degradation on middle plate for different separations from the heated plate

8.2.2 Effect of hole size

Figure 8.3 shows the effect of enclosure hole size on RH and temperature on the middle plate when the back plate was at 50^oC. The temperature on the middle plate was similar at 39.8^oC for hole sizes of 2mm and 10mm. For the enclosure without any holes, the temperature measured on the middle plate was 41.2^oC. The RH measured on the middle plate increased from 77.6% for no hole to 82.5% for a 10mm hole.

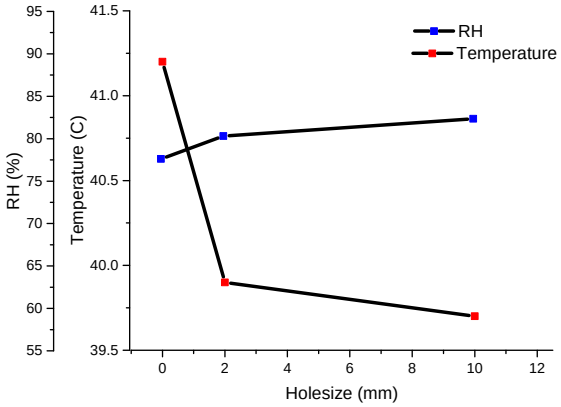

Figure 8.3: Effect of hole size on RH and temperature on the middle plate for different enclosure hole sizes

8.3 Conclusion

- A smaller separation between the back plate and middle plate resulted in higher temperature and lower RH on the middle plate. The lower separation also helped prevent degradation of impedance on the SIR pattern, showing improvement in reliability to humidity related failures.
- A bigger hole size contributed to lower RH on the middle plate due to slight decrease in temperature with increasing hole size.

Chapter 9

Circuit analysis to predict humidity related failures in electronics - Methodology and recommendations

Abstract

Aim of this paper is to demonstrate the use of circuit analysis to predict humidity robustness of an electronic circuit design. There is a lack of design tools which can predict failures due to humidity, especially the effect of humidity on electrical functionality of circuits. This work provides a methodology for utilising circuit simulation tools to detect humidity related faults associated with a circuit design by using experimentally determined leakage current data or surface insulation resistance using test pattern or model circuits. Simulation of circuits were performed with the experimentally determined SIR value as a parasitic resistance across two nodes of the circuit. Commonly used circuits such as a differential amplifier and a non-inverting comparator were analysed by this methodology. Based on the analysis, circuits with higher humidity robustness have been suggested as examples to demonstrate the effectiveness of this methodology. Finally, the correlation between the properties of the water layer on SIR pattern and actual components was done, which further demonstrates the applicability of the methodology.

Keywords: Electronic circuit, Humidity, Contamination, Surface insulation resistance, Leak current.

Published as: **S. Joshy**, V. Verdingovas, M. S. Jellesen, R. Ambat, "Circuit analysis to predict humidity related failures in electronics - Methodology and recommendations", Microelectronics Reliability, Vol. 93, pp. 81-88, Feb. 2019

9.1 Introduction

Electronic devices are used nowadays in variety of climatic conditions. Some of the applications are in controlled indoor climate, but others are exposed to harsh conditions like humid offshore locations, hot engine compartments of automobiles, atmospheres with corrosive gases etc. Application of electronics in harsh climates have shown failure modes due to high temperature[1][2], high humidity[3][4], gaseous corrosion[5][6], atmospheric contamination[7][8][9], and their combination. The failures due to humidity are aggravated by the recent drive towards miniaturisation and low-power consumption. Currently, robustness of electronic products to humidity is incorporated in the industry using prior knowledge of failures. There is a lack of simulation and analysis tools which can predict the effect of humidity and contamination on the electrical functionality of the circuit.

High humidity can accumulate inside electronic enclosures under both constant and cycling conditions of ambient temperature[10][11]. High humidity can also result from release of adsorbed and absorbed water from the walls of the enclosure[10]. Various mechanisms of humidity ingress into electronic enclosures is summarised by Jacobsen et.al.[14]. Presence of water vapour in the air can lead to formation of thin layer of water on a surface. The average number of monolayers of gas adsorbed on a surface is described by Brunauer-Emmett-Teller (BET) theory[12]. Thickness of the water layer increases with increasing humidity and becomes visible under condensing conditions. Thick water layer containing dissolved ions on a Printed circuit board assembly(PCBA) leads to significant increase in leakage currents and failure modes such as electrochemical migration (ECM)[15][16][17][18].

A thicker layer of water could form on a PCBA surface even under non-condensing conditions in the presence of hygroscopic contamination. The PCBA manufacturing and component assembly process adds hygroscopic residues to the PCBA surface. Even no-clean solder fluxes used for component assembly leaves behind hygroscopic and ionic weak-organic acids (WOA) on the PCBA surface capable of causing significant leakage currents[19][20]. Commercially available solder flux systems commonly use WOAs as the activator component of the flux. WOAs like DL-malic acid present on PCBA can cause ECM failures even at RH of 80%[21][22].

The properties of water layer formed on a PCBA can be studied electrically by monitoring the leakage current or impedance of an SIR pattern[23][24]. The value of leak current could be monitored for different climatic conditions of RH and PCBA-surface contamination levels. This empirical data represents the behaviour of the water layer on a PCBA under different conditions of RH and WOA concentrations. Using this experimentally determined leakage-current data, the effect of formation of the water-layer and its electrical interference on the PCBA functionality can be modelled as a parasitic resistance[25]. This parasitic resistance could be included in analysis of a circuit using standard circuit simulation tools to predict the effect of humidity and contamination on its functionality.

Circuit analysis to determine the effect of humidity and contamination on functionality of electronic circuits has been demonstrated in our earlier publications[25][26]. This paper has analysed more generic circuits using the above methodology and showed how the circuit modifications in such cases could improve the humidity robustness. The paper also evaluated the validity of using the leakage-current data from standard SIR patterns for this analysis. The circuits analysed in this paper for

demonstration are a differential amplifier and a non-inverting comparator. Leakage current data from SIR patterns contaminated with adipic acid and DL-malic acid, representing two extreme type no-clean solder flux residues from the point of view of aggressiveness are used for the analysis. Adipic acid is less corrosive because it has lower solubility in water and higher deliquescence RH (DRH) whereas, DL-Malic acid is highly soluble and has a lower DRH which makes it more corrosive. Sensitivity of both the differential amplifier and non-inverting comparator are compared for conditions in which the PCBA is made using adipic or DL-malic acid based no-clean flux and residues are remaining on the surface. Alternate circuit designs which are more tolerant to humidity-related failures are suggested which include an instrumentation amplifier and an inverting comparator. Also shown are design modifications like splitting of bigger resistances to multiple smaller resistances to make the circuits more robust to humidity. The experimentally determined data from SIR pattern is compared with that of land patterns of actual components with package dimensions 0402, 0603 and 0805 to demonstrate the validity of using data from standard SIR patterns. PCBAs contaminated with succinic and glutaric acids are used for this comparison. Data from the actual components agree with the data from SIR pattern for both WOAs within an order of magnitude of leakage current.

9.2 Extraction of SIR data for circuit analysis from humidity experiments

The experimental data which describes the properties of water layer on PCBA comes from our earlier work[21]. The SIR patterns used were FR-4 PCBAs of size 13mmx25mm and pitch size of 0.3mm. The surface concentrations of WOAs on the SIR pattern used for the studies were $25\mu g/cm^2$, $50\mu g/cm^2$ and $75\mu g/cm^2$. Leakage current measurements were done with the SIR patterns placed in an ESPEC PL-3KPH climatic chamber at different levels of humidity and applied d.c voltage. Further details of the experiment design, methods and materials can be found else where[21][25].

The leakage current data from the experiments were converted to equivalent SIR for applied voltage of 5V. The SIR data thus obtained for adipic and DL-malic acids at various humidity levels are shown in tables 9.1 and 9.2.

As seen from the data, SIR values drop with increasing values of RH and WOA surface concentrations for both adipic and DL-malic acid. The SIR drops drastically beyond the DRH of the WOA which is around 80% for DL-malic acid and 98% for adipic acid. The decrease in resistance is more pronounced for SIR patterns contaminated with DL-malic acid as expected due to its higher solubility in water compared to adipic acid. The data in tables 9.1 and 9.2 are used for analysis of circuits in this paper.

To correlate the leakage current data from SIR pattern with that on actual components, leakage current measurements were done on land patterns of surface-mount components placed on a test PCBA described elsewhere[27]. The WOAs used for this test were succinic acid and glutaric acid. The test PCBA contains land patterns for surface mount component sizes of 0402, 0603, 0805 and an SIR pattern on the same PCBA. The test PCBA was contaminated with WOA at the surface with a concentration of $100\mu g/cm^2$. The test PCBA was placed in the ESPEC PL-3KPH

Table 9.1: SIR data for different values of RH and concentration of adipic acid at 25^oC and d.c electrical input

RH	SIR(MΩ) $25\mu g/cm^2$	SIR(MΩ) $50\mu g/cm^2$	SIR(MΩ) $75\mu g/cm^2$
60	5209.29	3090.5	2789.48
70	4945.24	2157.70	1665.36
80	2865.82	1204.58	922.45
90	504.23	494.56	449.64
95	209.69	263.49	293.21
98	157.32	133.65	194.91
99	102.78	45.73	23.79

Table 9.2: SIR data for different values of RH and concentration of DL-Malic acid at 25^oC and d.c electrical input

RH	SIR(MΩ) $25\mu g/cm^2$	SIR(MΩ) $50\mu g/cm^2$	SIR(MΩ) $75\mu g/cm^2$
60	2902.40	1634.53	602.40
70	2587.40	303.69	39.93
80	2071.03	21.12	3.18
90	781.92	1.58	0.42
95	151.02	0.65	0.32
98	30.83	0.55	0.32
99	6.62	0.52	0.28

environment chamber with required potential bias and subjected to different humidity profile as required. The leakage current across the component land-patterns and SIR pattern on the test PCBA were measured using a VSP Biologic potentiostat. The following section describes the comparison of leakage current data from SIR and components.

9.3 Comparison of leak-current level from SIR and component testing

Leakage currents were measured across surface-mount land-patterns of sizes 0402, 0603 and 0805 at a contamination surface concentration of $100\mu g/cm^2$. Figures 1 and 2 show how the SIR values compare to resistances across actual components for succinic and glutaric acid respectively as contamination. Succinic acid and adipic acid has similar DRH of around 98%. Glutaric acid has a lower DRH of around 83%, near to that of Malic acid. Its solubility is also similar to that of DL-Malic acid of around 1400g/L of water at 25^oC[21].

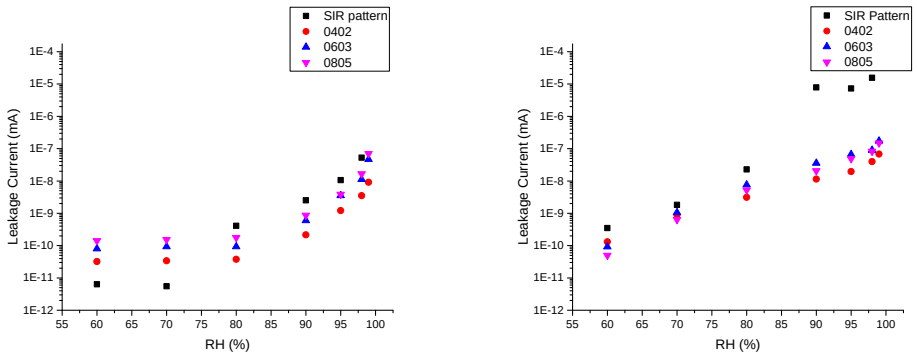

(a) (b)

Figure 9.1: Comparison of leakage-current from SIR and actual components for a) Succinic acid b) Glutaric acid as contamination at 25^oC and d.c electrical input.

For succinic acid it was seen that the leakage-current values for the SIR and land-patterns are within an order of magnitude of each other in the full range of RH as shown in figure 9.1a. For glutaric acid, the leakage-current values for SIR pattern and land-patterns are also within an order of magnitude of each other until the DRH of glutaric acid of 83-89%. Beyond the DRH of glutaric acid, the SIR pattern showed higher leakage current. For RH higher than DRH, the resistance of SIR pattern was two orders of magnitude lower compared to land-patterns as shown by figure 9.1b. So, the method of using resistance of water layer from SIR values for analysis with electronic circuits is a valid approximation for succinic acid in the entire range of RH upto 100%. For Glutaric acid, the approximation is valid until DRH beyond which the accuracy of the SIR data degrades.

9.4 Analysis of humidity robustness of circuits using electrochemical data

Two types of circuits are used for analysis in this work: (i) a differential amplifier and (ii) a non-inverting comparator. The differential amplifier is a common circuit block used in analog electronics to amplify sensed pressure, strain, electric current etc. The circuit produces an output voltage which is a constant times the difference of the voltages at the two input terminals given by:

$$Vout = G \cdot (Vin_+ - Vin_-) \tag{9.1}$$

where, 'G' is the differential-gain of the amplifier.
The gain 'G' is also given in terms of the resistances as

$$G = R1/R2 \tag{9.2}$$

if R1 = R4 and R2 = R3. Figure 9.2a shows the schematic of a differential amplifier of gain 10.

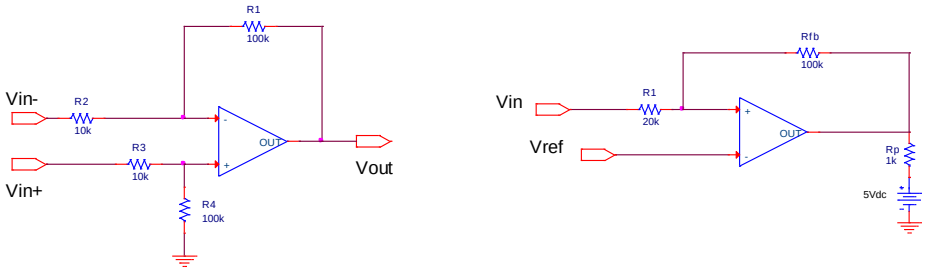

(a) (b)

Figure 9.2: Circuits analysed for humidity robustness a) differential amplifier b) non-inverting comparator.

A non-inverting comparator is used to detect a specific level on a sensed signal like temperature, pressure, current, voltage etc. Figure 9.2b shows the schematic of a non-inverting comparator. It is commonly used in power electronic circuits to detect over-current and over-temperature conditions. The output of the comparator could be used to disable the high-current flow in the circuit, thus protecting the device. The non-inverting comparator has two main properties - the upper tripping point (UTP) and lower tripping point (LTP). When input is above the UTP, output of the comparator is a logic-high and when below LTP, the output is a logic-low. The LTP and UTP of the non-inverting comparator in figure 9.2b is 2V and 3V, respectively.

According to the methodology used in this paper, the water layer was modelled as a resistance across two nodes of the circuit with properties defined by the SIR data from humidity experiments. Applying this methodology to the circuit of differential amplifier of figure 9.2a with water layer assumed to form across R1, the equivalent circuit for analysing humidity robustness becomes the one shown in figure 9.3.

When the RH of the ambient climate in which the circuit operates changes properties of the water on the PCB also changes according to the experimental data from humidity experiments. So, the value of Rp in figure 9.3 is a variable

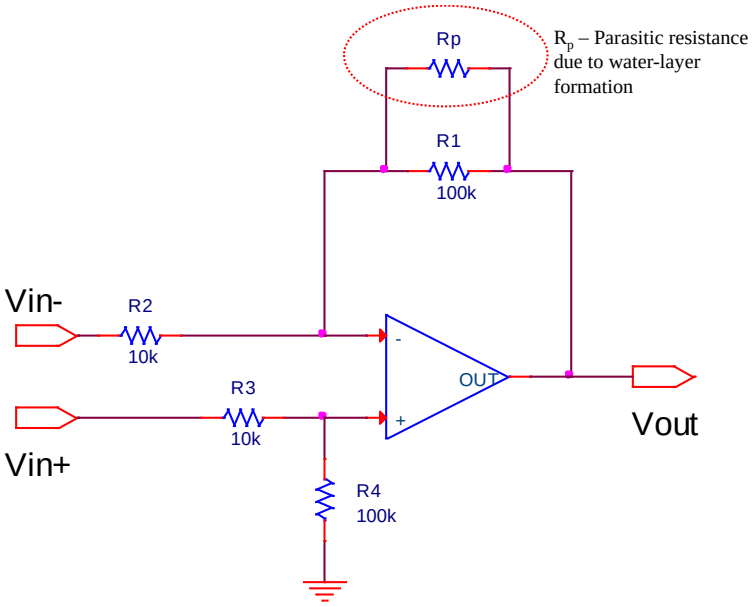

Figure 9.3: Model of water layer formation across resistor R1 of differential amplifier

with respect to ambient RH. Similar logic applies to the effect of contamination surface concentration on Rp. The following sub-sections discuss in detail the effect of humidity and contamination on the sensitivity of differential amplifier and non-inverting comparator circuits. Orcad Capture CIS was used in this work for circuit simulation.

To simulate the effects of humidity and contamination, a differential sine voltage of 0.1V and 1kHz a.c is applied across the terminals Vin+ and Vin- of the differential amplifier circuit shown in figure 9.2a. The nominal output of the circuit in figure 9.3 for the above mentioned input is a sine wave of 1V in amplitude, corresponding to the gain of 10. When water layer forms across a resistance, the net resistance of the parallel combination with the parasitic resistance Rp due to the water layer is lower than the individual resistances. So, if water layer forms across R1 or R4 the effect would be to reduce the gain 'G' according to equation 9.2. But if the water layer is across R2 or R3 the gain would increase.

To study effect of humidity and contamination on a non-inverting comparator, the water layer is assumed to form on resistors Rfb and R1 of figure 9.2b. A 5V peak-to-peak amplitude sine wave of 1kHz frequency and 2.5V d.c offset is applied as the input.

9.4.1 Humidity robustness of differential amplifier circuit

The effect of humidity and contamination on the functionality of differential amplifier is simulated assuming water layer formation across the terminals of one component only at a time. With this assumption the differential amplifier circuit is simulated for humidity and contamination effects on resistors R1 and R2. Figures 9.4a and 9.4b show the variation in differential gain for different climatic conditions of RH and DL-Malic acid for the components R1 and R2 in the circuit of figure 9.2a.

It is seen from figures 9.4a and 9.4b that the absolute value of error in gain increases with increasing RH. For DL-Malic acid, which represents residue from an

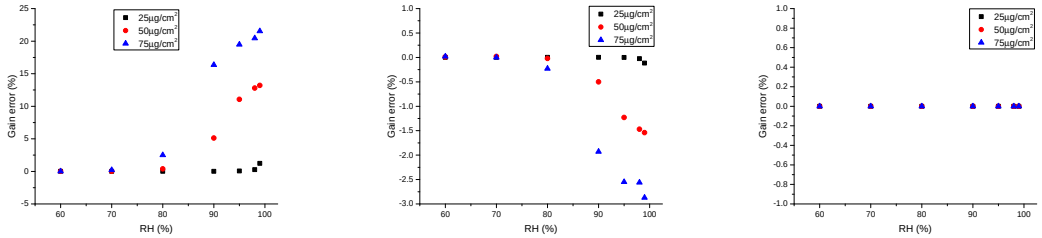

(a) (b) (c)

Figure 9.4: Variation in 'G' for effect of a) DL-Malic as residue on R1 b)DL-Malic as residue on R2 and c) adipic acid as residue on R1 with 0.1V, 1kHz sine wave electrical input and 25^{o}C.

aggressive no-clean flux system, the error increased drastically beyond 80%, which is the DRH for DL-Malic acid. The error in the gain was only 2.5% below 80% RH and 75$\mu g/cm^2$ WOA surface concentration. The error increased steadily for RH above 80% which is the DRH of DL-Malic acid. The error reached 25% for 99% RH at 75$\mu g/cm^2$ of DL-Malic acid. The sudden increase in error above DRH is because of a thicker water layer formation due to deliquescence[21]. For surface concentration of 50$\mu g/cm^2$ the trend in gain error with RH was similar to that for 75$\mu g/cm^2$. For 25$\mu g/cm^2$ the error in gain was found to be negligible showing that the reduction in SIR is not significant for interfering with the circuit.

The error in gain with adipic acid as contamination as shown in 9.4c was negligible compared to that of DL-Malic acid. This shows that circuits manufactured with adipic acid based no-clean solder fluxes expected to perform more reliably compared to DL-Malic acid based solder fluxes in humid climatic conditions.

The other resistances in the circuit of figure 3 did not cause as much error as that of R1. This is because the sensitivity of gain is dependent on the resistances, in this particular case of the differential amplifier R1 being the most sensitive.

9.4.2 Humidity robustness of Non-inverting comparator circuit

Figures 9.5a and 9.5b shows the effect of humidity on LTP and UTP due to water layer formation on resistor Rfb, when DL-Malic acid is used as contamination. Figures 9.6a and 9.6b shows the effect of humidity on LTP and UTP due to water layer formation on resistor R1, when malic acid is used as flux.

Analysis of the comparator also shows that the absolute value of error increases with increasing RH and surface contamination concentration. The highest error in LTP and UTP are obtained when DL-Malic acid was used as contamination. The highest error in LTP is 10% when 'Rfb' gets affected by humidity and DL-Malic acid concentration was 75$\mu g/cm^2$. The maximum error in UTP for Rfb under similar conditions was 6%. When R1 gets affected by humidity and contamination, the highest error in LTP was 2% and UTP was 1.2% both for 75$\mu g/cm^2$ of DL-Malic acid. For 50$\mu g/cm^2$ and 25$\mu g/cm^2$ of DL-Malic acid, the error is lower compared to 75$\mu g/cm^2$. The error increases with RH for all three values of surface concentrations. The error in LTP and UTP for both resistors with adipic acid as contamination was negligible as shown in figures 9.7 and 9.8.

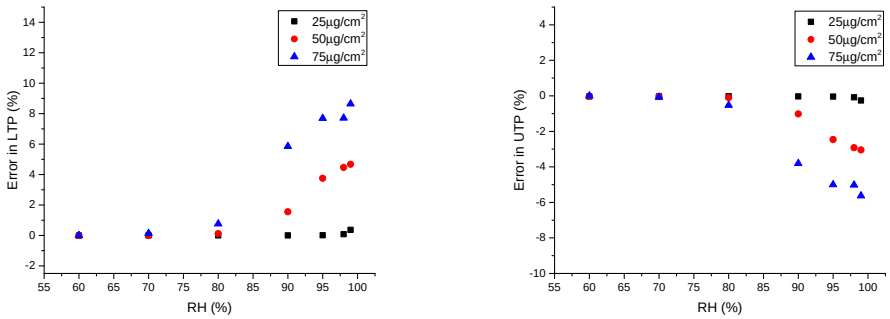

(a) (b)

Figure 9.5: Effect of humidity and malic acid on Rfb - a) variation in LTP b) variation in UTP for 1kHz sine wave electrical input and 25^{o}C

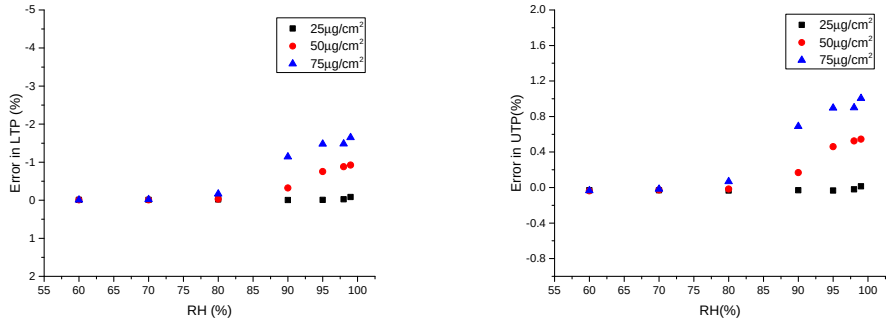

(a) (b)

Figure 9.6: Effect of humidity and malic acid on R1 - a) variation in LTP b) variation in UTP for 1kHz sine wave electrical input and 25^{o}C

9.4.3 Effect of contamination type on humidity robustness

An implication of the analysis of differential amplifier and non-inverting comparator with adipic and DL-Malic acids as contamination is that PCBs assembled with solder fluxes where adipic acid is the main constituent WOA would not cause severe failures due to humidity. On the other hand, solder fluxes with DL-Malic acid as WOA would cause upto a 25% error in gain for the differential amplifier when the humidity is above 80% RH. Even though the acceptability of error in circuit performance characteristics like gain depends on the application, a 25% error in gain would be unacceptable in any application.

From the analysis of the two above circuits, adipic acid performs better compared to DL-Malic acid in presence of humidity. This is because of the high deliquescence RH of adipic acid 99% and also its low solubility of 15g/kg in water[21]. Whereas DL-Malic acid exhibits a low DRH of 80% and higher solubility of 1400g/kg of water[21]. High DRH of the WOA used in solder flux provides greater margin to formation of a thick water layer due to deliquescence. Also, lower solubility translates to lower conductivity of the water layer or higher values of 'Rp' in the equivalent circuit as shown in figure 9.3, which is favourable from a humidity related reliability perspective. So by choosing the proper WOA based solder-flux in the

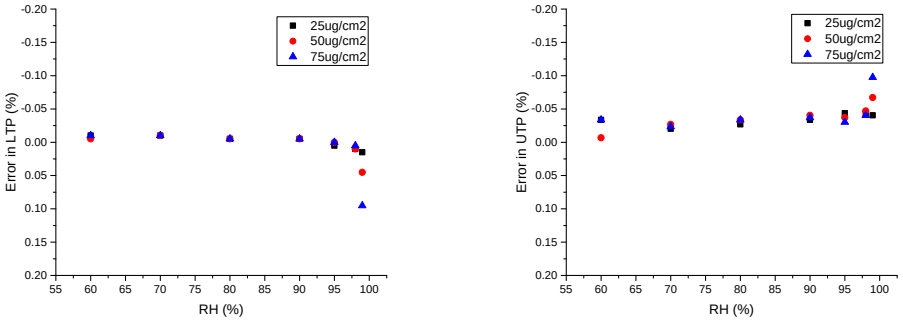

(a) (b)

Figure 9.7: Effect of humidity and adipic acid on Rfb - a) variation in LTP b) variation in UTP for 1kHz sine wave electrical input and 25^{o}C

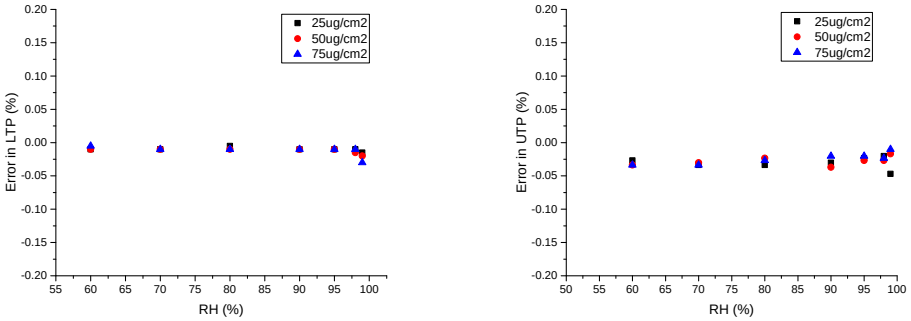

(a) (b)

Figure 9.8: Effect of humidity and adipic acid on R1 - a) variation in LTP b) variation in UTP for 1kHz sine wave electrical input and 25^{o}C

component assembly process the effects of humidity could be minimised to a great extent.

The methodology demonstrated in this paper to simulate humidity and contamination related effects on electronics used leakage-current data where a single WOA was the surface contamination. But, commercially available solder fluxes have multiple WOAs as activators. Solder fluxes also contain vehicle, solvent and additive components[28] which may have an effect on the formation of water layer on PCBs. More research can be done to study the correlation between data from single and multiple WOA and also the data from actual commercially available solder fluxes. The leakage-current/SIR data could be implemented as a library in circuit simulators to simulate the effects of humidity and contamination.

Another way to minimise the effects of humidity and contamination is to incorporate modifications in the cirucit design itself so that the circuit becomes more fault-tolerant. The following section demonstrate based on the above analysis, how one could improve the humidity robustness by modification of circuits.

9.5 Improvements to circuit reliability due to humidity

An instrumentation amplifier is a modified version of the differential amplifier with better characteristics like higher input impedance and lower output impedance. Figure 9.9a shows an instrumentation amplifier of gain 10 designed with opamps. The gain 'G' of the instrumentation amplifier in figure 9.9a is given by:

$$G = (R2/R1) \cdot (1 + 2 \cdot R6/R5) \tag{9.3}$$

The instrumentation amplifier uses more components compared to a differential amplifier with the advantage of better input and output impedances.

Similar to a non-inverting comparator, an inverting comparator is also used to detect a specific level on a sensed signal like temperature, pressure current, voltage etc. But unlike the non-inverting comparator, for an inverting comparator, output of the comparator is a logic-low when input is above the UTP and a logic-high when below LTP. Figure 9.10a shows an inverting comparator configuration.

The following subsections compares the functionalities of instrumentation amplifier with the differential amplier and inverting with non-inverting comparator. Also analysed is the effect of splitting a high-value resistor into multiple resistances and related humidity responses.

9.5.1 Instrumentation amplifier vs differential amplifier

To relate the performances of differential and instrumentation amplifiers in the presence of humidity and contamination, the errors in gain of both the circuits were compared when humidity and contamination affects the resistances R1 and R6 of differential and instrumentaion amplifiers respectively. The simulated contamination was DL-Malic acid at a surface concentration of 75ug/cm^2. The same 0.1V, 1kHz sine signal applied for differential amplifier is used as the input also for this circuit. Figure 9.9b shows the comparison of the two circuits, which indicate that the error in gain was similar for both the amplifiers until 80% RH which is the deliquescent RH for malic acid. For RH greater than 80%, instrumentation amplifier shows much less error in gain compared to the differential amplifier. The maximum error shown by instrumentation amplifier was only 6% whereas for differential amplifier this was near to 25%. This shows that an instrumentation amplifier has higher reliability to humidity and hygroscopic contamination compared to differential amplifier. The instrumentation uses lower value components compared to the differential amplifier to achieve the same value of gain. Effect of humidity on a smaller value resistor is less compared to that of a bigger value resistor due to the formation of parallel equivalent of Rp with the resistor concerned. Also, since the gain determining parameters are distributed among higher number of resistances for an instrumentation amplifier probability of water film formation on all the resistors at the same time also decreases. Lower value resistances combined with the topology results in better robustness of instrumentation amplifier compared to the differential amplifier.

But, this improvement in reliability would come at an expense of higher component count. The instrumentation amplifier uses 3 opamps and 7 resistors whereas a differential amplifier uses only 1 opamp and 4 resistors. Hence, the choice to

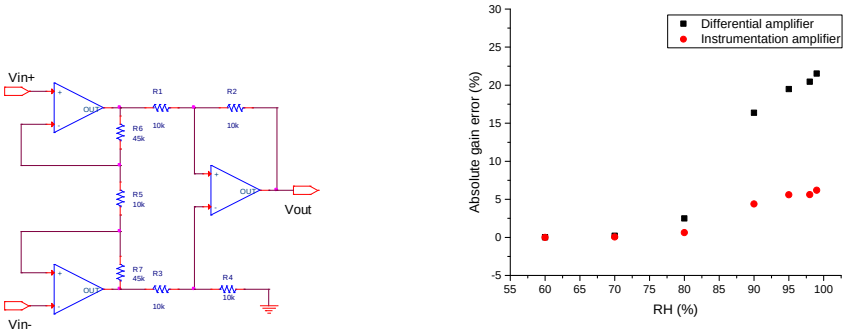

(a) (b)

Figure 9.9: Comparison of differential and instrumentation amplifiers for effect of humidity - a) Schematic of Instrumentaion amplifier b) Variation in gains of differential and instrumentation amplifiers with 0.1V, 1kHz sine wave electrical input and 25^{o}C

use either a differential or instrumentation amplifier would be based on a trade-off between the degradation in circuit performance and PCB space usage.

9.5.2 Inverting comparator vs Non-inverting comparator circuit

When the non-inverting comparator of figure 9.2b is used for detecting over-currents for circuit protection applications, the 10% error in LTP during humidity exposure is definitely not acceptable and suitable solutions need to be found to lower the vulnerability of the circuit to humidity-related effects. The inverting comparator could be a suitable alternative to the non-inverting comparator. A comparison is done between the non-inverting type of comparator to the inverting type of comparator. An inverting comparator is designed with the same threshold values as that of the non-inverting comparator. Figure 9.10b compares both the circuits for their LTP when DL-Malic acid at $75\mu g/cm^2$ is used as the contamination affecting resistor Rfb in both circuits. Negligible difference was noticed in the effect of humidity and contamination on UTP of both comparator configurations.

Figure 9.10b showed that inverting comparator performs slightly better with lower error in LTP of 6% compared to 10% for non-inverting comparator. The error in UTP was similar for both circuits. This improvement in performance with an inverting comparator could be beneficial depending on the application. Since same value components were used for both inverting and non-inverting comparators, the higher robustness of the inverting configuration is solely due to the difference in the circuit topology.

9.5.3 Higher humidity robustness by splitting high resistances

From the analysis of the differential amplifier, it was seen that the most sensitive component was R1. Therefore one solution for improving humditiy robustness is to reduce the sensitivity of the resister for parasitic water film formation acting

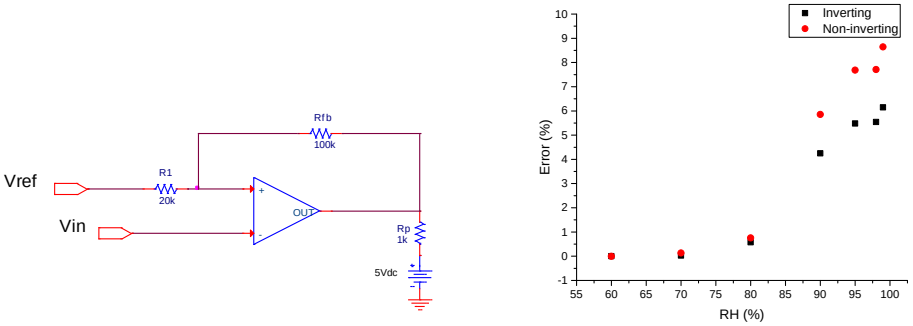

(a) (b)

Figure 9.10: a) Inverting comparator b) Comparison of LTP for inverting and non-inverting comparators for 1kHz sine wave electrical input and 25^{o}C

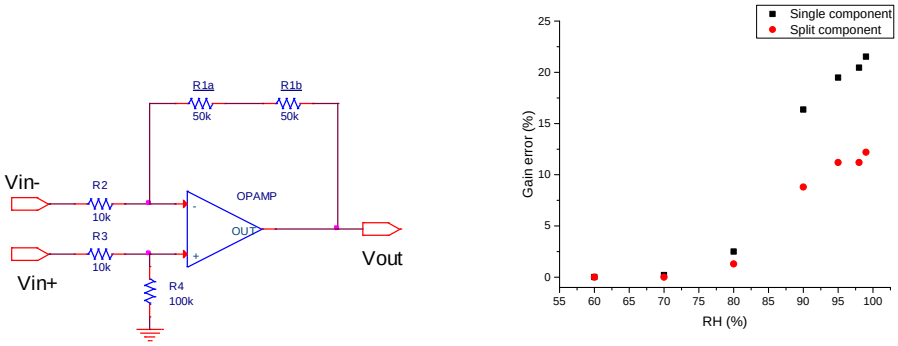

(a) (b)

Figure 9.11: a) Schematic of differential amplifier with split components b) comparison of error in gain with single and split components with 0.1V, 1kHz sine wave electrical input and 25^{o}C.

as parallel resistor. This can be done by splitting the component R1 to multiple components of lower resistance. This will effectively serve two purposes: (i) reduce the sensitivity of each resistor and (ii) making it difficult to form water film on all resistors at the same time. When a resistor is split into multiple resistances the parasitic resistance due water layer Rp forms across each of the individual resistances. Assuming the same value for Rp across all the split resistances the net resistances of the network is higher than that with a single high resistance. Figure 9.11a shows the schematic of a differential amplifier with R1 split into two 50K resistances. Figure 9.11b compares the error in gain with single and split resistances for 75$\mu g/cm^2$ of DL-Malic acid as contamination.

The highest error in the differential amplifier with split components was 14% compared to 25% with single resistance for R1. Further improvements in humidity robustness can be achieved by splitting resistor further in this case or on any circuit when there is a critical component. The acceptability of the decrease in error and the number of components to which a resistance is split into is a trade-off that should be decided during the design-phase of the circuit.

9.6 Summary

This work has demonstrated simulation of robustness degradation of electronic circuits due to humidity and surface contamination using experimental leakage-current data. The leakage-current data extracted was for two WOAs which are used as activators in the no-clean flux systems namely - adipic and DL-Malic acid on a standard SIR pattern. The reliability of the circuits analysed decreased with increasing RH and decreased rapidly beyond DRH of the WOA used in the solder flux. The reliability of electronic circuits to humidity and contamination can be significantly improved by the right choice of solder flux and the circuit configuration. A simulation of the effect of using various solder fluxes on circuits can be done in the design phase of the product itself by using the methodology presented here. The simulation can help in choosing the right solder flux and make suitable circuit modifications to improve reliability. If the reliability target cannot be met by the above, then accumulation of high humidity itself should be prevented by humidity control techniques or by use of conformal coatings. The methodology demonstrated in this work can be incorporated into circuit simulation software packages to predict reliability of electronic circuits towards humidity and contamination in the design phase of the product itself.

9.7 Acknowledgement

This research was conducted as part of the IN SPE project funded by Innovation Fund Denmark and CELCORR(www.celcorr.com). The authors would like to acknowledge the funding and help received from the consortium partners.

Bibliography

[1] V. Smet, F. Forest, J. Huselstein, F. Richardeau, Z. Khatir, S. Lefebvre, M. Berkani, "Ageing and failure modes of IGBT modules in high temperature power cycling", IEEE Trans. Ind. Elec., vol. 58, no. 10, pp. 4931-4941, October 2011.

[2] R. M. Nelms et al. "200C operation of a 500 W dc-dc converter utilizing power MOSFETs," IEEE Trans. Industry Applications, Vol. 33, No. 5, pp. 1267-1272, Sept./Oct. 1997.

[3] S. J. Krumbein, "Metallic Electromigration Phenomena", IEEE CHMT, pp. 5, March 1988.

[4] R. Hienonen, R. Lahtinen, Corrosion and climatic effects in electronics, VTT Publications, 2000.

[5] C. Hillman, J. Arnold, S. Binfield, and J. Seppi, "Silver and Sulfur: Case Studies, Physics, and Possible Solutions," SMTA International Conference, 2007.

[6] D. Minzari, M. S. Jellesen, P. Moller and R. Ambat, "Morphological study of silver corrosion in highly aggressive sulfur environments," Engineering failure analysis, vol. 18, Issue 8, pp. 2126 – 2136, 2011.

[7] M. Tencer, "Deposition of aerosol ("hygroscopic dust") on electronics – Mechanism and risk," Microelectronics reliability, vol. 48, Issue 8, pp. 584–593, 2008.

[8] R. B. Comizzoli, R. P. Frankenthal, P. C. Milner, J. D. Sinclair,"Corrosion of Electronic Materials and Devices", Science, Vol. 234, no. 4774 , pp. 340-345, 1986

[9] J. D. Sinclair, L. A. Psota-Kelty, C. J. Weschler and H. C. Shields, " Deposition of Airborne Sulfate, Nitrate, and Chloride Salts as It Relates to Corrosion of Electronics," Journal of electrochemical society, Vol. 137, Issue 4, pp. 1200–1206, 1990.

[10] H. Conseil-Gudla, Z. Staliulionis, M. S. Jellesen, M. Jabbari, J. H. Hattel, R. Ambat, " Humidity build-up in electronic enclosures exposed to constant conditions," IEEE transactions on components packaging and manufacturing technology, vol.7, Issue 3, pp. 412–423, 2017.

[11] H. Conseil, V. C. Gudla, M. S. Jellesen, R. Ambat, Humidity build-up in a typical electronic enclosure exposed to cycling conditions and effect on corrosion reliability, IEEE Transactions on Components, Packaging and Manufacturing Technology, vol. 6, Issue 9, pp. 1379–1388, 2016.

[12] A. W. Adamson, A. P. Gast, Physical chemistry of surfaces, John wiley and sons Inc., 1997.

[13] M. Tencer, Moisture Ingress into Nonhermetic Enclosures and Packages.A Quasi-Steady State Model for Diffusion and Attenuation of Ambient Humidity Variations, Electronic components and technology conference, pp. 196–209, 1994.

[14] J. B. Jacobsen, J. P. Krog, A. H. Holm, L. Rimestad, A. Riis, Climate-Protective Packaging Using Basic Physics to Solve Climatic Challenges for Electronics in Demanding Applications, IEEE Industrial Electronics Magazine, vol. 8, Issue 3, pp. 51–59, 2014.

[15] D. Minzari, M. S. Jellesen, P. Moller and R. Ambat, " On the electrochemical migration of tin in electronics," Corrosion science, Vol. 53, Issue 10, pp. 3366–3379, 2011.

[16] H. Conseil, M. S. Jellesen and R. Ambat, " Printed Circuit Board Surface Finish and Effects of Chloride Contamination, Electric Field, and Humidity on Corrosion Reliability," Journal of electronic materials, Vol. 46, Issue 2, pp. 817–825, 2017.

[17] B.I. Noh, S.B. Jung, "Characteristics of environmental factor for electrochemical migration on printed circuit board", Journal of Materials Science: Materials in Electronics, Vol. 19, Issue 10, pp. 952-–956, 2008.

[18] D.Q. Yu, W. Jillek, E. Schmitt, "Electrochemical migration of lead free solder joints", Journal of Materials Science: Materials in Electronics, Vol. 17, Issue 3, pp 229-–241, 2006.

[19] D. Pauls, "Residues in printed wiring boards and assemblies," Circuit World, vol. 27, no. 1, pp. 32–41, Oct. 2000.

[20] H. Conseil, M. S. Jellesen and R. Ambat, " Contamination profile of Printed Circuit Board Assemblies in relation to soldering types and conformal coating," Proceedings of Eurocorr 2014, 2014.

[21] V. Verdingovas, M. S. Jellesen and R. Ambat, "Solder Flux Residues and Humidity-Related Failures in Electronics: Relative Effects of Weak Organic Acids Used in No-Clean Flux Systems," Journal of Electronic Materials, Vol. 44, Issue 4, pp. 1116–1127, 2015.

[22] S. Zhan, M. H. Azarian, M. Pecht, "Surface Insulation Resistance of Conformally Coated Printed Circuit Boards Processed with No-Clean Flux", IEEE Transactions on Electronics Packaging Manufacturing, vol. 29, no. 3, pp. 217-223, July 2006.

[23] L. C. Zou; C. Hunt, "Characterization of the Conduction Mechanisms in Adsorbed Electrolyte Layers on Electronic Boards Using AC Impedance," Journal of the Electrochemical Society, Vol. 156, Issue 1, pp. C8–C15, 2009.

[24] V. Verdingovas, M. S. Jellesen and R. Ambat, "Relative effect of solder flux chemistry on the humidity related failures in electronics," Soldering and Surface Mount Technology, Vol. 27, Issue 4, pp. 146–156, 2015.

[25] V. Verdingovas, S. Joshy, M. S. Jellesen, R. Ambat, "Analysis of surface insulation resistance related failures in electronics by circuit simulation," Circuit World, Vol. 43, Issue 2, pp. 45–55, 2017.

[26] S. Joshy, V. Verdingovas, M. Jellesen, R. Ambat, "Simulation of electronic circuit sensitivity towards humidity using electrochemical data on water layer", proceeding in 17th Electronics Packaging Technology Conference (EPTC), pp. 1-5, 2015.

[27] V. Verdingovas, M. S. Jellesen, R Ambat, "Impact of NaC1 Contamination and Climatic Conditions on the Reliability of Printed Circuit Board Assemblies", IEEE Transactions on Device and Materials Reliability, vol. 14, no. 1, pp. 42-51, 2014.

[28] M.S. Jellesen, D. Minzari, U. Rathinavelu, P. Moller, R. Ambat, " Corrosion failure due to flux residues in an electronic add-on device", Engineering failure analysis", Vol. 17, Issue 6, pp. 1263-1272, 2010.

Chapter 10

Overall discussion

This chapter contains an overall discussion of the investigations presented in the papers. The results have shown possibility to control humidity and prevent humidity failures inside electronic enclosures by preferential condensation and internal heating methods. The results have also shown the main enclosure packaging related factors and their contribution to humidity accumulation and humidity profiles in electronic enclosures. The circuit simulation methodology was used to predict humidity related failures in electronic circuits and was also used to find more reliable circuit topologies.

Study of humidity transfer from warm to cold showed that high humidity inside an electronic enclosure can be lowered by mass transfer to a condensing surface, hence showing the feasibility of using forced condensation for humidity control. The condensing surface required to bring about humidity transfer and hence humidity control can be realised by using thermoelectric coolers (TEC). A condensing surface could also exist in an enclosure due to the nature of the application, for example a pump used to circulate cold water. The surfaces of the pump in contact with cold water could be condensing in nature and when interfaced with the enclosure of the pump control electronics through suitable opening, could control any high humidity in the electronic enclosure. The main parameters that influenced mass transfer to the condensing surface were warm temperature, cold surface temperature, connecting hole between the warm and cold sections and enclosure openings which control humidity ingress from ambient. The effect of enclosure openings on humidity control was investigated in chapter five. Lower humidity was achieved in the warm chamber by having a lower size for the warm chamber opening which limits the ingress of humidity from ambient into the warm chamber. But, the adverse effect of using a smaller warm chamber opening was the slower transient response of the humidity control mechanism. In a humidity control application using TECs to create a condensing surface, the cold surface temperature depends on the current through the TEC. A higher current would correspond to lower cold surface temperatures and hence, lower RH. But, this would increase the power consumed for humidity control, which is critical especially for battery powered applications. The values of the different opening sizes and cold surface temperature should be selected based on maximum acceptable RH in the warm chamber, preferred transient response times and also on the knowledge of the ambient climatic conditions.

Humidity accumulation was observed in an electronic enclosure with parallel plates subjected to cycling ambient temperature and internal heating leading to

impedance degradation and susceptibility to failures. Power dissipating PCBAs and circuits in their near vicinity would be relatively safe from humidity related failures due to their higher surface temperatures from the heat dissipated. Components placed on high heat capacity components like heat sinks would experience humidity related failures as demonstrated. So, critical components should be placed farther away from high heat capacity components to ensure their reliability. Another way to improve reliability of PCBA in electronic enclosures would be to use controlled openings with higher resistance to flows like tubes instead of holes. As compared to humidity control by forced condensation, internal heating was able to prevent reliability degradation only on specific surfaces of PCBA and not in the entire enclosure. This is because forced condensation is an absolute humidity control method, where the absolute amount of humidity in the air is controlled where as, heating is a relative humidity control method where the RH near critical surfaces are controlled to prevent condensation.

The simulation methodology using SIR data was used to analyse reliability of commonly used electronic circuits like a differential amplifier, instrumentation amplifier, non-inverting and inverting comparators to humidity and contamination. The simulations were used to identify sensitive components in the circuit and also to select more reliable circuit topologies. This improvement in reliability could happen at the expense of more number of components and hence, larger PCB area. The simulation methodology can be used as a tool in the design and analysis phase of product development to choose reliable circuit topologies and to compare and select suitable solder flux for component assembly.

Chapter 11

Overall conclusion

1. Humidity transfer occurred from warm chamber to cold chamber. The main factors that influenced the humidity transfer were temperature of the warm chamber, cold chamber temperature and connecting hole size.

2. Humidity control by forced condensation was demonstrated using a two-chamber set-up. Forced condensation reduced the RH inside both chambers of the set-up. This showed a humidity control method for an electronic enclosure capable of exchanging humidity to a condensing surface.

3. Humidity control by forced condensation was found to be influenced by cold surface temperature and enclosure opening sizes. Lower cold surface temperature caused lower RH in both chambers. Effect of larger warm chamber opening and connecting hole sizes were to increase the steady state RH inside the warm chamber where as, a larger cold chamber opening sizes led lower RH values.

4. Cycling ambient temperature and internal heat dissipation was shown to cause humidity accumulation inside electronic enclosures. Internal heating resulted in release of adsorbed water vapour which condensed on cooler surfaces, increasing the susceptibility to humidity related failures on those surfaces.

5. Humidity control by internal heating was demonstrated in an enclosure with simulated parallel PCBs. Reliability improvement due to the heating was found to be feasible only on directly heated PCBA surfaces and PCBA placed in close proximity to the heat source.

6. Circuits located near high heat capacity components would experience impedance degradation and humidity related failures due to higher time constants for temperature, leading to low peak to peak temperatures and RH in their vicinity.

7. Larger enclosure opening size caused higher impedance degradation and susceptiblity to humidity related failures. Enclosure openings like tubes have higher resistance to flow leading to slower accumulation of humidity inside the enclosure, and hence should be preferred as controlled openings on electronic enclosures.

8. The simulation methodology using SIR data was used to analyse common electronic circuits. Components in the circuits causing higher error in presence

of humidity and contamination were identified using the simulation methodology. Circuits with better reliability to humidity were suggested. Also, effect of different WOAs on circuit performance in the presence of humidity was analysed.

Suggestions for future work

Condensation based humidity control could be implemented in an electronic enclosure using thermoelectric coolers(TEC) to study both continuous and pulsed operations. Energy required to be spent for humidity control by condensation could also be investigated.

High heat capacity components could be used to store heat dissipated by electronic components during operation and later used to keep critical components warm can be explored. Experiments can be conducted to investigate the feasibility of using phase change materials to store a part of the generated heat, which can be used later to keep the PCBA warm during the off time of the heater. Use of Resistor-capacitor(RC) networks to model accumulation of humidity inside electronic enclosures both by diffusion and convection could be investigated as an alternative to computationally intensive CFD models.

The methodology to predict humidity related failures can be implemented as part of a circuit simulation tool to analyse reliability of circuits under conditions of humidity and contamination. This would also help to compare different flux systems and choose the most reliable flux system to be used in component assembly.

This PhD work was motivated by the need to improve the reliability of electronics to humidity related failures by understanding humidity build-up inside electronic enclosures and study suitable humidity control techniques. In the industry, reliability to humidity related failures is taken care with experience generated over many years of product development. This work aims to contribute to the scientific understanding of humidity build-up and humidity control inside electronic enclosures. This work has studied the effect of enclosure packaging level parameters on humidity build-up under conditions of cycling ambient temperature. Enclosure humidity profiles under constant ambient conditions and condensed water was also studied. Humidity control techniques based on heating and preferential condensation were investigated. Humidity transfer from warm to cold regions inside an enclosure were studied with hermetically sealed glass enclosures. A methodology based on electronic circuit analysis to predict humidity related failures and evaluate different electronic circuits in the presence of humidity and contamination was also studied.

DTU Mechanical Engineering
Section of Materials and Surface Engineering
Technical University of Denmark

Produktionstorvet, Bld. 425
DK-2800 Kgs. Lyngby
Denmark

Tlf.: +45 4525 2205
Fax: +45 4525 1961

www.mek.dtu.dk

October 2018

ISBN: 978-87-7475-553-1